EFFECT OF MINOR IMPURITIES ON THE ELECTRICAL PROPERTIES OF SE AND SE CONTAINING GLASSES

by

M.A.C. ASSUNÇÃO

A thesis submitted to the University of Warwick

for admission to the degree of

Doctor of Philosophy

DEPARTMENT OF PHYSICS, DECEMBER 1985

In memory of Professor P.W. McMillan

Aos meus pais

ABSTRACT

A number of selenium glasses doped with halogens (Cl, Br, I), in the range of few p.p.m. up to 4 at %, were prepared in an oxygen-free atmosphere by melt quenching.

D.C. conductivity as a function of the temperature was measured and for the higher impurity concentration samples the measurement of the thermoelectric power, D.C. photoconductivity, electron spin resonance and optical absorption coefficient was also undertaken. Other supporting experiments included infrared spectrometry, differential scanning calorimetry, energy dispersive analysis of X-Rays and field effect. X-Ray diffraction was used to check the lack of long-range order in each sample.

A general review of amorphous semiconductors is included with particular reference to their electronic and optical properties and the importance of defect states.

Results demonstrate the large effect of halogens on conductivity and that the conduction remains p-type with no observable E.S.R. signal. Data obtained are compared with those available in the literature and discussed within the framework of the CFO-Mott theory. Tentative interpretation of the results is made via a "dangling bonds model" assuming a single particle acceptor level.

Additional complementary studies of a number of chalcogenide glasses doped with Br are also included. The effect of several other additives (Ag, Cu, Tl, Na, Sb, Al, Bi) on the D.C. conductivity and other properties of vitreous selenium is briefly investigated.

CONTENTS

CHAPTER III (continued) — PAGE NUMBER

LIST OF FIGURES

FOLLOWING
PAGE NUMBER:

FOLLOWING
PAGE NUMBER:

LIST OF TABLES

ACKNOWLEDGEMENTS

I would like to acknowledge the considerable influence of the late Professor P.W. McMillan on the definition and materialization of this project. His constant understanding and scientific and philosophical insights were of invaluable help.

I am indebted to Dr. Diane Holland not only for her helpful discussion of the results and careful reading of the manuscript but also for her continued interest and encouragement. I should also like to thank Professor A.J. Forty for his assistance.

A large number of Warwick University Physics Department staff provided experimental advice and everyday assistance, as well as great sympathy and kindness and I thank them all accordingly. Special thanks are due to Dr. R. Maddison, Mr. R. Buckle, Mr. R. Lamb and Mr. P. Beecraft and to my fellow post-graduates. My thanks go also to Mrs. Carmel Parrott who carefully typed the manuscript.

I wish to record my gratitude to Drs. R. Todhunter, R. Kosłowski and R. Pettifer and the late Mrs. Patricia Lewis whose friendship and cheerfulness were most important.

The group "Materiais não cristalinos" at University of Aveiro helped in both experimental matters and discussion of some topics. Professor S.K. Mendiratta and Miss Conceição Carvalho deserve, in particular, a special mention.

I should like to thank Universidade de Aveiro, INIC and INVOTAN for their funding of the work.

Finally, my deepest thanks to Professors J. and M.H. Andrade e Silva for their trust and Matilde for her love and infinite patience.

MEMORANDUM

This dissertation is submitted to the University of Warwick in support of my application for admission to the degree of Doctor of Philosophy. It contains an account of my own work performed principally at the School of Physics, University of Warwick, in the period May 1980 to August 1983 under the general supervision of Professor P.W. McMillan. No part of it has been used previously in a degree thesis submitted to this or any other University. The work described herein is the result of my own independent research except where specifically acknowledged in the text.

M.A.C. ASSUNCAO

CHAPTER I - INTRODUCTION

1.1 Non-crystalline semiconductors: some definitions

For the past twenty years a considerable effort in both fundamental and applied research has been dedicated to a novel group of solid state materials generally designated as non-crystalline semiconductors. The word semiconductor is not restricted here to that, commonly applied in the crystalline case, of an electronic conductor with a resistivity value intermediate between that characterizing good conductors and insulators; but, in a more general way, it is applied to any electronic conductor whose resistivity is strongly dependent on temperature, that is, governed by an activation energy or energies. These are associated with a gap of mobilities rather than with an energy band gap as in crystals. Such a definition allows that pure selenium glass, for example, having a resistivity greater that 10^{14} Ohm.cm can be considered semiconducting whereas in the usual sense it will be classified as an insulator.

It is also necessary to clearly state the meaning of various terms that are often used synonymously for non-crystalline. These include the words amorphous, glassy and vitreous which in some scientific areas are assigned to different materials. Glassy and vitreous are synonymous and specify a solid (usually prepared by quenching from the melt) and exhibiting a glass transition temperature. The term amorphous indicates non-crystallinity, i.e. lacking long-range order. This term includes glasses and also other materials, often prepared by techniques other than melt-quenching, which do not show the glass transition. However, given the scope of this work and the need to avoid being repetitive, the adjective amorphous is throughout used as equivalent to glassy, vitreous and non-crystalline whenever terminological misunderstanding is unlikely.

The name non-crystalline semiconductors includes covalent solids (tetrahedral amorphous films, tetrahedral glasses, non-oxide chalcogenide glasses, etc.), oxide glasses (mixed valence semiconductors) and dielectric films (Fritzsche 1974) . Some organic polymers also exhibit electronic conduction.

Chalcogenide glasses, with which this work deals, are known also as lone-pair semiconductors and are based on one or more of the elements sulfur, selenium and tellurium. All these three elements can be produced in the amorphous state on their own and they also readily form glasses (cross-linked networks) combining with one or more of several elements belonging to the III-A, IV-A and V-A groups. Chalcogenide glasses generally do not exhibit an electron paramagnetic resonance signal and are characterized by a relatively well defined optical absorption edge, an efficient photoconductivity and other properties typical of a gap free of states. Other experiments, however, point to the existence of a "pinned" Fermi energy. The attempts to solve the apparent inconsistency gave rise to models based on two electron states and in which the lone-pair electrons play an important role. Such models are discussed in chapter II.

1.2 Brief historical survey

Early developments in the production and use of glass concerned just a particular form of it, the oxide glasses, and did not involve more than empirical knowledge. It is not possible to speak about glass science prior to the twentieth century. In 1926 Goldschmidt suggested a criterion for glass formation based on the ratio between the anion and cation radii. However, if a date has to be referred to as a turning point that is probably 1932, when Zachariasen published his famous paper entitled "The atomic arrangement in glass" on the structure of covalently bonded non-crystalline solids.

The beginning of the study of amorphous semiconductors dates only from the 1950's, previous to which only selenium and As_2Se_3 were known as glasses. It was the Russian school of Leninegrad with Kolomiets, Goryunova et al. and Ovshinsky, all working on chalcogenides, Spear with drift mobility experiments in a-Se and Fritzsche with work on impurity conduction that brought out experimental evidence fundamental for the subsequent development of theoretical concepts on amorphous semiconductors. A review of this early work was made, amongst others, by Owen (1967) and Kolomiets (1964).

Landmarks in the understanding of non-crystalline solids were the classical paper "Absence of diffusion in certain random lattices" by Anderson (1958), introducing the concept of localization, and the formulation of the Ioffe and Regel (1960) rule focussing on the semiconducting similarities between glasses and crystals as long as their short range order resembles each other. In the late 1960's Tauc et al. (1966) published important work on optical absorption and Mott (1969) and Cohen et al. (1969) put forward the ideas of localized tail states and mobility edges which came to constitute the basic features of the often called Mott-CFO model. A year earlier Ovshinsky (1968) had published a paper on switching and memory devices which initiated extensive interest in the subject.

In 1970 Davis and Mott brought a contribution to the understanding of the observed difficulty of doping amorphous semiconductors by suggesting that the Fermi level could be pinned by defects. The possibility of polaron formation in amorphous solids was meanwhile suggested by Emin et al. (1972). In 1975 an important breakthrough was achieved by Spear and Le Comber who successfully doped (p-type and n-type) glow-discharge amorphous hydrogenated silicon. Still in the same year the paradox verified in chalcogenides and referred in 1.1 was solved by the Street

and Mott model. This uses the concept of two electron states as a consequence of a negative correlation energy, an idea put forward by Anderson (1975). In the following year Kastner et al. reformulated the idea identifying the gap states as valence alternative pairs.

The theory of electrons in non-crystalline semiconductors is still in its infancy; however considerable progress has been made in the understanding and prediction of the effect of disorder upon band structure, and thus on the electrical and optical properties, and was recognised by the award of the 1977 Physics Nobel prize to Sir N.F. Mott and P.W. Anderson who shared it with J.H. VanVleck.

A lot of other interesting experiments and theoretical ideas whose importance may be only later appreciated have, since then, been put forward. The reviews by Mott (1978) and Fritzsche(1983) are excellent presentations of "The origin of some ideas on non-crystalline materials" to cite the title of the former paper. The latter provides also some insight on more recent developments.

1.3 Applications of non-crystalline semiconductors

The announcement of new applications of non-crystalline materials makes regular headlines in the news. The technological interest of amorphous solids is based essentially on two important characteristics: they are easily prepared in large areas or volumes; and they are generally isotropic whereas crystals are not.

The field of applications of non-crystalline semiconductors is still small although the prospects of becoming industrially important are increased every day. The use of such chalcogenide glasses as selenium or As_2Se_3 in xerography, due to their photoconduction properties and ability to develop an electrostatic image, is widespread. Semiconducting

chalcogenides have additional applications as a consequence of a number of other properties besides semiconducting behaviour. In particular, chalcogenide glasses are generally very good infrared transmitters when compared to oxide glasses and can, to a certain extent, be tailored, by judicious choice of the composition, to have the desired properties. Other applications comprise: computer-memory elements based on the electrical pulse induced switching phenomenon (Te_{80} Ge_{20} glass, for example); 3-terminal analog devices and other electronic elements; secondary electron emission based devices; photography and holography; etc.

Another use of amorphous semiconductors being developed is their utilization as solar cells. These incorporate a-Si:H from which the Dundee team successfully formed the first p-n junction so demonstrating that devices could actually be fabricated.

The above list of applications is undoubtedly far from being exhaustive. A wake of both fundamental and applied research on non-crystalline materials is now on its way. From the first International Conference on Liquid and Amorphous Semiconductors in 1965 to the one held in 1983 there was an enormous increase in attendance. The same happened in other specialized areas. It is therefore expected that a large number of technologically important materials will be developed in parallel with the improvement in scientific insight. A review on glass applications has been published, among many others, by MacKenzie (1977) and contains a number of important references. Interesting also is the paper by Kreidl (1977) on future applications of glasses.

1.4 The project and the choice of experiments

It was not until the end of the nineteen sixties that the possibility of influencing the electrical properties of chalcogenide glass was first reported. Until then there was the conviction that amorphous semi-

conductors could not be doped (Kolomiets 1964) . Initially it was theoretically suggested that impurities should not affect conductivity for two possible reasons: either the non-crystalline solid comprised a large density of gap states that capture the electrons from any eventual impurity donors - which could be the case of amorphous silicon - or else, the rearrangement of atoms surrounding the impurity atom will cause all the electrons to be stuck in bonds (cf. Mott and Davis 1979). This will be the case of chalcogenides.

However, Owen (1967) reported that 1 at% of silver impurity causes the D.C. conductivity of arsenic sulphide to increase by more than four orders of magnitude, together with a decrease in activation energy. Earlier Danilov (1965) had already observed a similar result, although less marked, in copper doped arsenic selenide. Lacourse et al. (1970) gave evidence of a more drastic effect of yet smaller concentration (few p.p.m.) of impurity upon the resistivity of pure vitreous selenium. The impurity was in this case oxygen. Since then large conductivity increases have been noticed in selenium glass doped with potassium and chlorine (Twaddell et al. 1972) , in arsenic selenide glass containing small additions of silver, indium or thallium or in arsenic sulphide glass with copper impurity (cf. Mott 1976) and even in multicomponent glasses as $Te_{48}As_{30}Ge_{10}Si_{10}$ containing 2% of manganese (Kumeda et al. 1978) . At the same time further addition of other elements such as As, Hg, Bi or Si to previously oxygen doped selenium glass seems to cancel the former effect (McMillan and Shutov 1977; Lacourse et al. 1970). In addition, information about impurity effects on drift mobility also became available (Schottmiller et al. 1970; Kolomiets and Lebedev 1966).

Such was the state of the art at the beginning of this project. If a paper has to be mentioned as having the greatest influence of

all, that was the report by Twaddell, Lacourse and MacKenzie (1972). The possibility of n-doping chalcogenide glasses, until then universally observed as being p-type materials, was to cause great interest. The production of a non-crystalline solid capable of being doped both n and p type had only recently been achieved in a different kind of material (Spear and Le Comber 1975).

That possibility conditioned therefore the selection of halogen elements as a first doping agent. Vitreous selenium was retained as the host material not only because some of the impurity effects had been observed in this material but also as a uni-component glass its relative simplicity should eventually make the interpretation of results less troublesome. Later it was decided that measurements on Te or S containing glasses (structurally not very different from Se) should be carried out. The bulk form was chosen as the properties of films may be dependent on preparation conditions such as substrate temperature and so results would be difficult to compare with those reported elsewhere.

Once the impossibility of producing halogen n-doped vitreous selenium was established and after the halogen-selenium systems had been physically studied to the best of the technical facilities and personal abilities concerned, the impurity effect of other elements was considered. Monovalent substitutes were chosen since they were expected to most strongly affect the defects concentrations held responsible for the pinning of the Fermi energy.

The main idea underlying the project conditioned, of course, the choice of experiments to be carried out. The measurement of the D.C. conductivity and the determination of the thermoelectric power were priorities. Drift mobility experiments were also an obvious thing to do. However, lack of time and the availability in the literature of data on

the glasses investigated precluded this. To investigate any change of the defects paramagnetic state, and thus obtain information about the impurity role, electron spin resonance measurements were also conducted.

A number of other supporting experiments was considered useful for various reasons. Infrared spectroscopy and differential thermal analysis could provide valuable structural information about the glasses. Optical absorption and photoconductivity were possible ways of estimating the materials optical gap. Electron microscopy and energy dispersive analysis of X-Rays would allow the verification of eventual inhomogeneities in the samples and a check on the composition, respectively. X-Rays diffraction was fundamental to guarantee the amorphousness of the samples.

1.5 Plan of the thesis

The writing of the thesis is organized in the following way. In addition to this short introduction, it comprises four main sections. In the second chapter a review of the basic ideas on non-crystalline semiconductors is presented. The third contains a description of the experimental techniques involved in the project, whilst in the fourth the results are presented and discussed. To finalise, the fifth chapter summarises the main conclusions.

CHAPTER II - REVIEW OF SOME IDEAS ON AMORPHOUS SEMI-CONDUCTORS

2.1 Introduction

In this chapter it is intended that a brief account be given of some properties of amorphous semiconductors with special emphasis on their electronic properties. The characterization of non-crystalline solids, although requiring new concepts, uses some parameters in common with crystal theory and, therefore, a parallel discussion of various aspects concerning the two solid forms is followed throughout.

As the properties of amorphous semiconductors are dependent upon their type of structure as well as on their thermal history, an indication of various structural models and methods of preparation is presented before dealing with the different models describing the electronic states and their conduction properties.

Section 2.6 refers to the role of defects and related impurities which have been assuming increasing importance in the study of amorphous materials and constitute the very heart of this thesis. This is followed by sections on optical properties and field effect.

2.2 Crystalline and non-crystalline solids

2.2.1 Glass formation

Crystals and glasses are solids that result from two rather different solidification processes. As a matter of fact a liquid may solidify either discontinuously to a crystalline solid or continuously to an amorphous one. This is shown in fig. 2A where the two possible volume versus temperature curves are represented. The path followed is determined by the cooling rate and so, if the temperature changes slowly enough a crystalline material will be formed. However, at sufficiently high

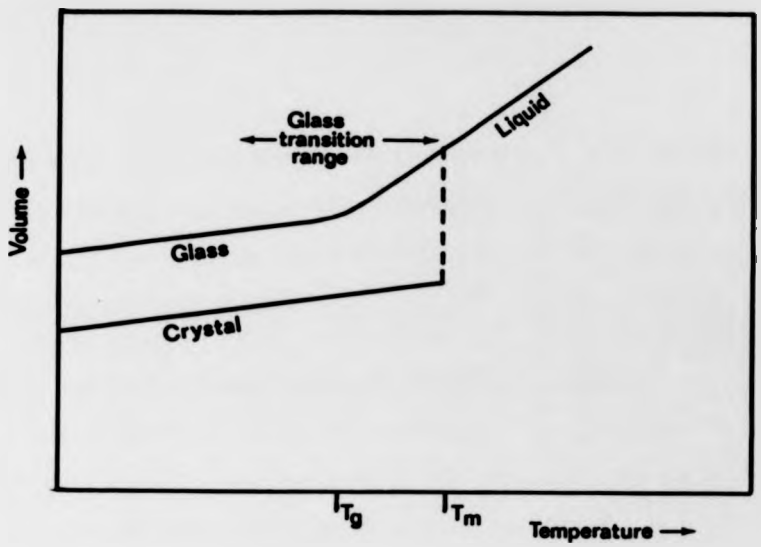

Fig. 2A - Volume-temperature dependence for a material condensating into a solid phase. The two general transformations from liquid to crystalline and vitreous states are represented.

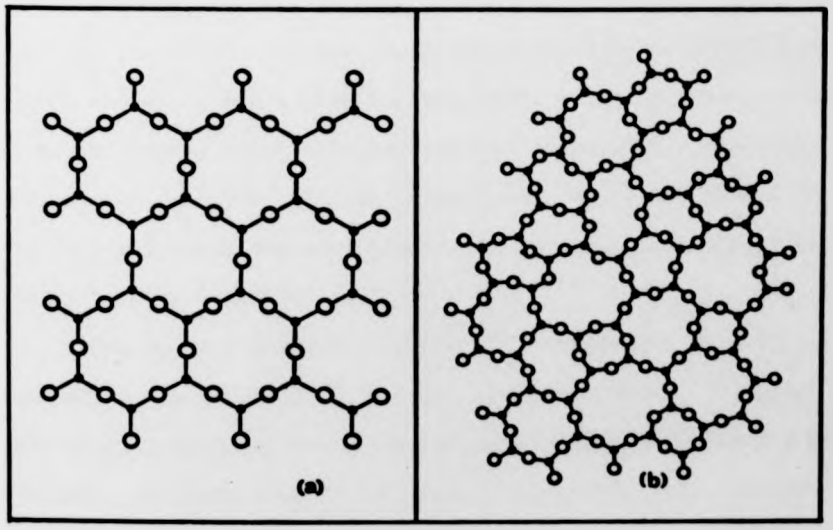

Fig. 2B - The Zachariasen's diagram for the two dimensional CRN of a R_2X_3 glass (b) is compared with the structure of the crystalline form (a) of the same material.

cooling rates the melting point is bypassed without volume discontinuity and a liquid-glass, apparently second-order transition, takes place. The temperature, Tg, around which the transition occurs is called the glass transition temperature.

2.2.2 Methods of preparation of amorphous solids

Glass forming ability is seemingly a universal property. This was expressed by Turnbull (1969) in a more elegant way: "The 'ideal' glass model predicts that all liquids would form glasses when sufficiently undercooled". For that reason the existing number of preparation methods of this type of material is quite a large one and almost every day new technological developments are introduced so that higher rates of cooling can be obtained and new amorphous solids produced.

In addition to the conventional (slow cooling) melt quenching method, with rates of cooling, dT/dt, in the range $10^{-4} - 10^{-1}$ °C.s^{-1} and the laser glazing method where $dT/dt = 10^{10} - 10^{12}$ °C.s^{-1} may be achieved, non-crystalline solids can also be prepared by splat-quenching and melt spinning which are also melt quenching processes, by vapour condensation techniques (glow discharge decomposition, thermal evaporation, chemical vapour deposition, electron and ion bombardment, etc.) and by gel desiccation to only allude to the most important (see for instance, Bagley 1974 ; Elliott 1984 ; Zallen 1983) .

With so many different methods of preparation available some materials can be obtained by more than one method. This does not mean necessarily that the two resulting products have the same properties. In point of fact, even if the same technique is used, materials with different characteristics can result if no careful control of all parameters is made. Materials can differ either on a macroscopic level

with distinct types and extension of inhomogeneities or microscopically via the introduction of structural defects. Such inhomogeneities and defects may in turn influence several properties of the substance and particularly its electric properties.

2.2.3 Structure of amorphous solids

As a result of a different formation process crystals and glasses are fundamentally distinct in their topology. In the crystalline state the atomic structure consists of a translationally periodic array, i.e. the atomic equilibrium positions show long-range order. By contrast in an amorphous material no long-range order persists and the array of atoms is strongly disordered. This does not mean, however, that the atoms are randomly arranged as the bonding properties of the constituent elements of the material imply a high degree of local correlation. Hence glasses have in common with crystals a high degree of short-range order, exhibited essentially in the existence of the same coordination number, and also in a separation between adjacent neighbours which is approximately constant throughout the glass and similar to the bond length of the corresponding crystal. The non-periodicity, characteristic of the amorphous state, appears essentially as a consequence of fluctuations in both the values of bond angles and dihedral angles, parameters that are normally constant in a crystal.

The basis of these ideas was first put forward by Zachariasen (1932) and its applicability extends to most covalently bonded amorphous solids. It constitutes the continuous random network (CRN) model and is illustrated in fig. 2B showing the original two-dimensional Zachariasen's diagram. The main features of an ideal CRN glass structure are therefore the absence of long-range order, a spread in bond angles (and in dihedral

angles also, in the tri-dimensional case) and the non-existence of dangling bonds, that is bonds for which covalent bonding requirements are not fulfilled. Zachariasen's rules are not applicable to glass-forming systems such as metals and others in which covalent bonding is not predominant. In particular, for some monoatomic glasses such as amorphous metals, random close packing models (dense random packing of spheres and random packing of trigonal prisms) have been proposed. The discussion of these and of alternative models to the CRN hypothesis (microcrystallites model- Goodman 1975 ; Wang and Merz 1976 -, etc.) is however outside the scope of this work.

Chalcogenide glasses and organic polymers deviate from the "ideal" situation of network continuity consisting, as they do, of interrupted chains. Nevertheless, and even if the structures of most of these glasses is not yet fully understood, it is generally accepted that they present a short-range order which is essentially the same as in the corresponding crystal. This is particularly true in the case of glassy selenium which is believed to be a molecular solid composed principally of long polymeric chains with a random coil structure interconnected by Van der Waals forces, but with some Se_8 rings probably also being present. Though there is some doubt, it is widely accepted that selenium atoms in amorphous Se are two-fold coordinated (excepting the chain ends) and present bond lengths and bond angles close to those in crystalline Se.

As a result of the structural characteristics of the amorphous state, the mathematical simplifications associated with periodicity such as Bloch functions, Brillouin zones and other concepts related to the idea that the wavevector, $\vec{k}$, is a good quantum number, and that are of such a great importance in crystal theory, are called into question.

If periodicity exists, the electron states can be described by waves, extending through the whole solid, of the type

$$\Psi(\vec{k},\vec{r}) = u(\vec{k},\vec{r}) \exp(i\vec{k}.\vec{r})$$

where $u(\vec{k},\vec{r})$ is a periodic function of the position $\vec{r}$ with the same periodicity as the crystal lattice. The consequences of this are that the permitted energies of the electrons constitute a band structure in the k-space, $E(\vec{k})$. However, if periodicity is not present, no reciprocal or k-space can be defined and $E(\vec{k})$ is not a good representation. Nevertheless as many basic electronic properties of a solid depend essentially on the bonding characteristics there is a concept from conventional solid state physics which remains useful. It concerns the electronic density of states per unit volume per unit energy interval which, if the short-range electronic interactions are dominant, is determined mostly by the type of bonding (Weaire and Thorpe 1971) . Such a concept has became a fundamental tool in the non-crystalline solid state theory.

2.3 Anderson localization

One of the consequences of the lack of long-range order is the existence of electron states which are localised. By localisation it is understood that the wave function is confined to a small region containing only a few atoms so that when moving away from that region the probability density $|\Psi|^2$ decays exponentially with distance. This is characteristic of the amorphous state although localised states do occur in crystalline materials where defects or impurities have been introduced. However, in crystals, localised states have an extrinsic character appearing as discrete energy levels (donors or acceptors) whereas in glasses they are intrinsic to the solid and form an energy band rather than a well defined energy line.

The first criterion for localization, that is for the disorder induced transition from extended to localised character, was proposed by Anderson (1958). Anderson's model considered that in an amorphous solid, instead of a unique potential well, typical of the crystalline state, there is a succession of potential wells whose depth changes randomly from site to site (fig 2C(b)) and applied a tight-binding, one-electron picture. It was then possible to establish that the criterion for the delocalization - localisation transition is contained in the relation $W > B$, where B is proportional to the overlap band width in the absence of disorder and W is the width of the random distribution of the wells depth. When the ratio W/B is large the wavefunctions suffer few perturbations from neighbours and it is then that localisation sets in. In particular if the ratio is large enough all of the states in the valence band may become localised. For smaller degrees of disorder there are nevertheless some states which are localised. It is hence possible to visualise the different cases that follow:

When the electrons energy, E, is high they are in Bloch states, i.e. the electrons are quasi-free and can move throughout the whole glass (fig. 2D(a)). However, as E approaches a certain value E_C, the random potential begins to strongly influence the electron behaviour and for E just above E_C the free path of the carriers is vastly reduced. Immediately below E_C the potential energy wins over the kinetic term and the electron becomes bound to a site, that is, localised (fig. 2D(d)). The value of E_C is, obviously, determined by the disorder parameter W/B.

2.4 Models for the density of states

The specific form of the distribution of energy states is, in a covalently bonded crystalline semiconductor, dependent on both the long

The first criterion for localization, that is for the disorder induced transition from extended to localised character, was proposed by Anderson (1958). Anderson's model considered that in an amorphous solid, instead of a unique potential well, typical of the crystalline state, there is a succession of potential wells whose depth changes randomly from site to site (fig 2C(b)) and applied a tight-binding, one-electron picture. It was then possible to establish that the criterion for the delocalization - localization transition is contained in the relation $W > B$, where B is proportional to the overlap band width in the absence of disorder and W is the width of the random distribution of the wells depth. When the ratio W/B is large the wavefunctions suffer few perturbations from neighbours and it is then that localization sets in. In particular if the ratio is large enough all of the states in the valence band may become localized. For smaller degrees of disorder there are nevertheless some states which are localized. It is hence possible to visualize the different cases that follow:

When the electrons energy, E, is high they are in Bloch states, i.e. the electrons are quasi-free and can move throughout the whole glass (fig. 2D(a)). However, as E approaches a certain value E_C, the random potential begins to strongly influence the electron behaviour and for E just above E_C the free path of the carriers is vastly reduced. Immediately below E_C the potential energy wins over the kinetic term and the electron becomes bound to a site, that is, localised (fig. 2D(d)). The value of E_C is, obviously, determined by the disorder parameter W/B.

2.4 Models for the density of states

The specific form of the distribution of energy states is, in a covalently bonded crystalline semiconductor, dependent on both the long

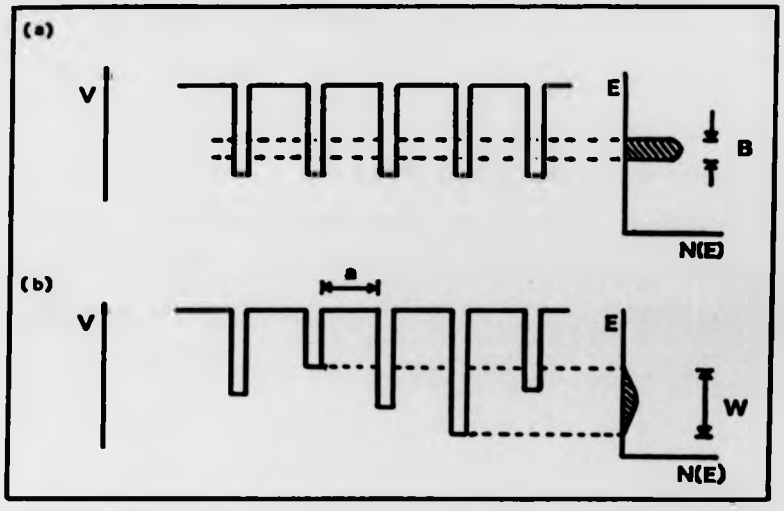

Fig. 2C - Representation of the potential distribution and expected density of states: (a) in a crystal; (b) in the Anderson model. When W exceeds B the Anderson transition takes place.

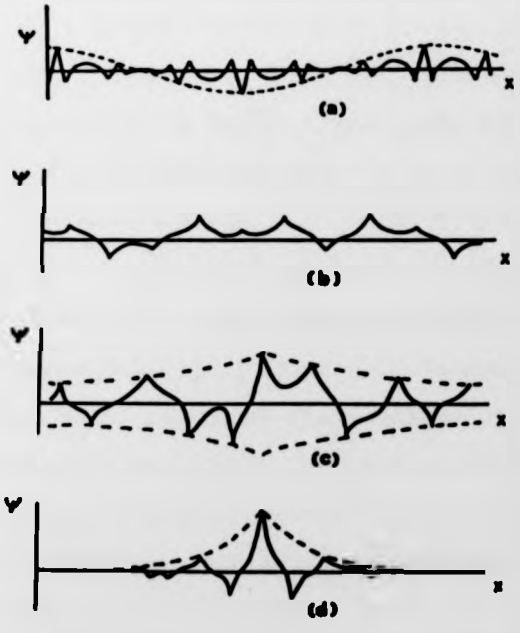

Fig. 2D - Illustration of the electron wavefunctions:
a) extended-state
b) state just non-localized ($E \gtrsim E_C$)
c) state just localized ($E \lesssim E_C$)
d) localized-state

(based on: a) Zallen 1983; b), c) and d) Mott and Davis 1979)

and short-range order of the crystal although the general form of that distribution is mainly determined by the latter. A typical density of states curve for a crystalline semiconductor is shown in fig. 2E. The main features are that, firstly, all the states are extended, secondly, the edges at both the valence band maximum and the conduction band minimum are sharp, therefore giving rise to a well defined energy gap; and lastly, the shape of the curve may present peaks.

When it comes to amorphous semiconductors the long range order is lost and that leads to the destruction of all sharp features and to the occurrence of localized states. At the same time the local order is essentially preserved except for a very small variation in the interatomic distances and slightly larger variation in the valence angles. That should be manifest as a general similarity of the valence and conduction bands of extended states with those of the corresponding crystalline form. This seems corroborated by the fact that amorphous semiconductors are transparent in the infrared region.

Based on Anderson's ideas, Mott (1969; 1970) suggested that localized states could not occupy every energy in the spectrum but would only form tails above and below the valence and conduction bands respectively. Mott assumed consequently that there would be well defined energies, E_V and E_C, in each band, separating the localized and extended regimes. Furthermore he noted that, at the boundary energies between the two types of states, there is a drop in carrier mobility of several orders of magnitude corresponding to the change in character of the wave function. A similar idea was proposed by Cohen (1970 a,b) who suggested that such a mobility drop, rather than being discontinuous, could take place in a gradual way so that just inside the extended bands the mean free path is of the order of the interatomic spacing. Thus the interval

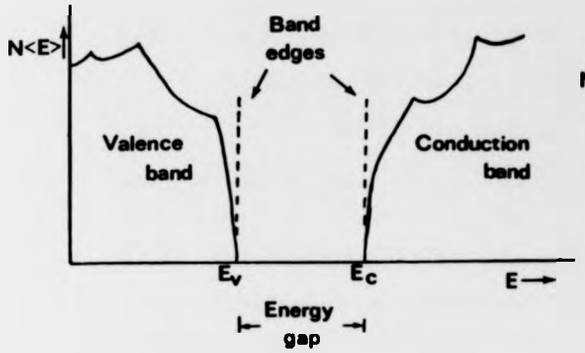

Fig. 2E - Electron density of states curve for a crystalline semiconductor.

Fig. 2F - Electron density of states curve for an "ideal" non crystalline solid showing tailing of localized states at band edges according to Mott's suggestion.

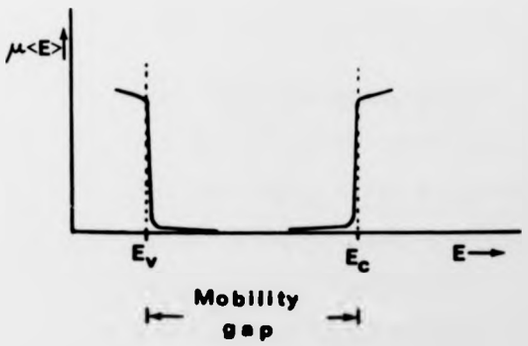

Fig. 2G - Sketch of the electron and hole mobility as a function of the electron energy showing a mobility gap.

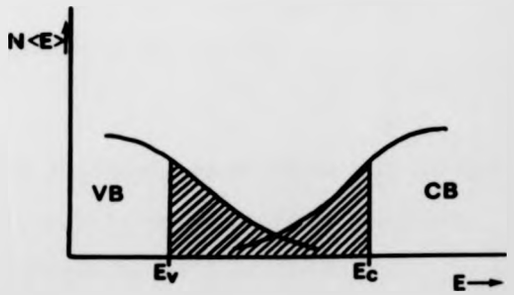

Fig. 2H - The CFO model showing tail overlap in the middle of the pseudo-energy gap.

between E_V and E_C, although being an energy pseudo-gap, defines a mobility gap with E_V and E_C being the so-called mobility edges.

These ideas, illustrated in fig. 2F and 2G, constitute the basic features of the models proposed for the band-structure of non-crystalline semiconductors which are now described in more detail.

2.4.1 The Cohen-Fritzsche-Ovshinsky model

The differences between the various models proposed concern mainly the form of the localized state distribution across the gap. In this model, known as the CFO model, Cohen et al. (1969) argued that in a semiconducting multicomponent glass, where to a topological disorder has to be added a compositional disorder, the extension of the localized tails at the conduction and valence band edges could become sufficiently large that they overlap, giving rise to a reasonably high density of states in the middle of the gap. That high degree of disorder will justify, at the same time, a smearing out of all particular features inside the gap. Such a model is represented in fig. 2H.

2.4.2 The Davis-Mott models

The CFO model, although relevant for some glasses other than alloys (for ex. a-Si), seems inappropriate for the case of vitreous materials characterized by sharp absorption edges as is the case for most chalcogenides. Davis and Mott (1970) suggested that the width of the localized tails in those materials should be narrow and, in an alternative model, introduced a distinction between the states placed near the band edges which are localized due to structural disorder, and other states in the gap, also localized but with origin in network defects and particularly dangling bonds. A single band near the middle of the gap was proposed in order to account for the pinning of

the Fermi level. A splitting of that band in two may also be possible. A representation of these models is shown in fig. 2I.

2.4.3 The Marshall-Owen and other models

Marshall and Owen (1972) proposed a model for As_2Se_3 showing exactly two bands, one of acceptors and other of donors states, as being responsible, by self-compensation, for the confinement near the gap centre of the Fermi level.

Experimental evidence available points to the existence, in some non-crystalline semiconductors, of several localized gap states of a rather sharp character. A band diagram such as in fig. 2J may then be more appropriate for these glasses.

A rather different view of the problem calling for the role of lattice distortion in the transport mechanism was brought in by Emin and co-workers (1972). Emin was able to explain experimental data of DC conductivity, thermopower and Hall effect in terms of a small polaron transport theory (see for example Nagels 1979).

2.5 Electrical transport

In this section the formulae governing some transport properties are discussed in the framework of the CFO-Mott and Davis theory.

2.5.1 DC conductivity

The conductivity, σ, of a semiconductor can be written in the form

$$\sigma = -e \int N(E).\ \mu(E)\ kT\ \frac{\partial f(E)}{\partial E}\ .\ dE \qquad (2.1)$$

where N(E) and $\mu(E)$ are, respectively, the density of states and mobility functions of the energy E. k is the Boltzmann constant, e the electron charge and T represents the absolute temperature.

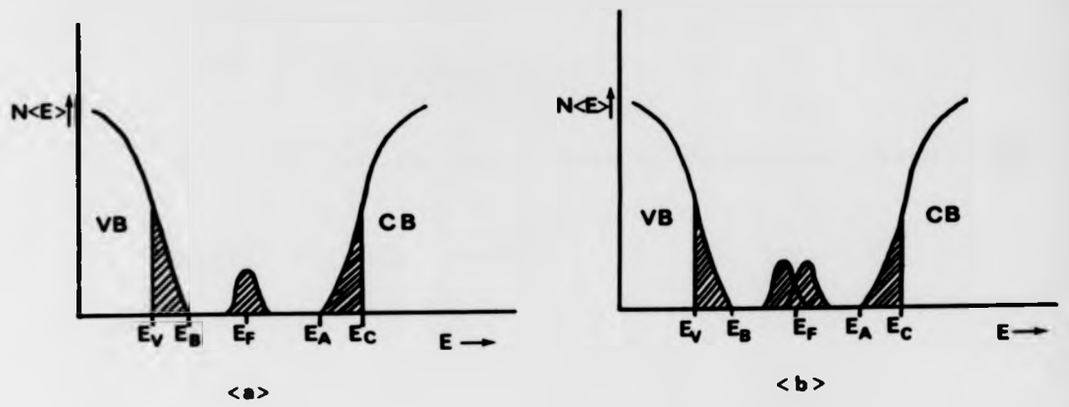

Fig. 2I - (a) Davis–Mott model proposing a band of compensated levels near the gap centre; (b) the centre band may be split into two bands.

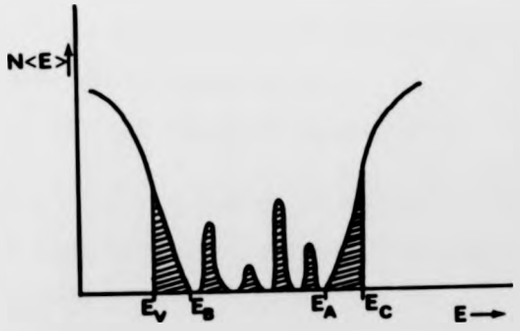

Fig. 2J - Density of states curve for a glass with defect states.

f(E) is the Fermi-Dirac distribution function,

$$f(E) = \frac{1}{1 + \exp\left[(E-E_F)/kT\right]}$$

in which E_F, the Fermi energy, is determined by the gap states distribution. Since

$$\frac{\partial f(E)}{\partial E} = -\frac{f(E)}{kT} \cdot (1-f(E))$$

equation (2.1) becomes

$$\sigma = e \int N(E) \cdot \mu(E)\, f(E) \cdot (1-f(E))\, dE \qquad (2.2)$$

The Davis-Mott model yieldsthree possible main mechanisms for electrical conduction:-

a) Extended state or band conduction - when $E > E_c$ ($E < E_v$ for holes) conduction takes place via Bloch states. As, according to Mott and Davis ideas, the Fermi level is close to the middle of the gap, the difference E_C-E_F is sufficiently large so that the Boltzmann distribution function

$$f_B(E) = \exp\left[-(E-E_F)/kT\right]$$

constitutes a good approximation for the determination of the states occupancy. So (2.1) can be rewritten as

$$\sigma = e \int N(E)\, \mu(E)\, \exp\left[-(E-E_F)/kT\right] dE \qquad (2.3)$$

Since there is a mobility gap the integration over all available energy states has a negligible contribution from the states located below E_C. Hence and successively,

$$\sigma = e \int_{E_C}^{+\infty} N(E)\, \mu(E) \cdot \exp\left[-(E-E_F)/kT\right] dE$$

and

$$\sigma = e \cdot N(E_C)\, \mu(E_C)\, kT \exp\left[(E_C-E_F)/kT\right] \qquad (2.4)$$

if a constant density of states and a constant mobility are assumed in the extended region.

This is, at least as far as mobility is concerned, a dubious

supposition since it is reasonable to expect an increase in the free path of the carriers when the energy moves away from E_C. However, due to the form of the distribution function and excepting the case of very high temperatures, it is principally the states just above E_C that contribute to the bulk of the conduction. Therefore, it is about the value of the mobility at E_C, $\mu(E_C)$, that most of the physical interest is centred.

Mott determined the "minimum metallic conductivity" that is the lowest value for conductivity in a non-activated process. At E_C this is of the order of 200-300 $\Omega^{-1}cm^{-1}$ (Mott and Davis 1979) . It was then possible, considering the density of states in the nearly free electron model, to estimate $\mu(E_C) \sim 10\ cm^2 V^{-1}s^{-1}$ at room temperature.

On the other hand Cohen (1970a) suggested that at $E \gtrsim E_C$ the electron motion is essentially by diffusion (Brownian like motion), with the electrons jumping from one atom to the neighbouring one. The free path is then similar to the interatomic distance, a, and applying the Einstein relation,

$$\mu = \frac{1}{6} \cdot \frac{e a^2}{kT} \upsilon \qquad (2.5)$$

(υ being the electronic frequency), a similar value of μ is obtained.

It must be noticed that both arguments lead to the same dependence of $\mu(E_C)$ vs.T, that is

$$\mu(E_C) \propto \frac{1}{kT} \qquad (2.6)$$

This cancels the temperature dependence of the pre-exponential factor of (2.4). The expression of σ can thus be written as

$$\sigma = \sigma_o \cdot \exp\left[-(E_C - E_F)/kT\right] \qquad (2.7)$$

with $\sigma_o = eN(E_C)\ kT\ \mu(E_C)$. As suggested by optical measurements the mobility gap diminishes when temperature increases. If a linear temperature dependence is assumed, that is,

$$E_C - E_F = \Delta E - \gamma T \qquad (2.8)$$

(2.4) becomes

$$\sigma = C_o \exp\left(-\Delta E/kT\right)$$

Where $C_o = \sigma_o \exp\left(\frac{\gamma}{k}\right)$. σ_o was estimated as lying between 10 and 10^3 $Ohm^{-1}.cm^{-1}$ (Mott and Davis 1979) . As the value of γ is, from optical measurements, situated approximately between 2×10^{-4} and 4×10^{-4} $eV.deg^{-1}$, the constant C_o must have values in the range 10^2-10^5 $Ohm^{-1}.cm^{-1}$.

b) <u>localized state conduction in the band tails</u> - When $E < E_C (E > E_V$ for holes), the wave functions are localized and so charge transport is impossible without thermal activation. Conduction in the band tails of localized states then takes place via thermally assisted tunnelling with the electrons hopping from one state to the nearest one after exchanging energy with a phonon. Hence the mobility is expected to contain an activation term affecting the expression (2.5) that is

$$\mu_{localized} = \frac{1}{6} . \upsilon \frac{ed^2}{kT} . \exp\left[-W/kT\right]$$

where υ is the hopping frequency and d the hopping distance. Assuming W of the order of kT and a typical phonon frequency, it is possible to estimate $\mu_{localized}$ as being close to 10^{-2} $cm^2V^{-1}s^{-1}$ at room temperature. This means a mobility change, when crossing E_C, of approximately three orders of magnitude as already indicated.

Supposing that in the tails the variation of the density of states is linear,

$$N(E) = \frac{N(E_C)}{E_C - E_A} (E - E_A) \qquad (2.9)$$

then integration (2.2) yields for the contribution to the conductivity from the tail states,

$$\sigma_{localized} = C_1 . \exp\left[-(E_A - E_F + W)/kT\right]$$

where

$$C_1 = \frac{1}{6} \cdot \upsilon\, e^2 d^2\, N(E_C) \frac{kT}{E_C - E_A} \left\{ 1 - \exp\left[\frac{E_A - E_C}{kT}\right]\left[1 + \frac{E_C - E_A}{kT}\right]\right\}$$

As the tail states are a direct consequence of the disorder potential their width should be similar to the width of the random distribution of the potential wells. It is then reasonable to assume $E_C - E_A \sim 0.1$ to 0.2 eV. This leads to a ratio, C_1/C_o, in the range 10^{-6} - 10^{-4} indicating a large drop in the pre-exponential factor of the conductivity curve when the transport mechanism changes from extended to localized.

In general the decrease in the density of states in the tail is rather sharp and so a linear dependence is probably a valid approximation. In the other cases where the density of states N(E) is some power of E an estimate of the value of C_1 may be somewhat difficult to make. A comparison with experimental values can yet be harder since the experimental intercepts of the ln σ vs. $1/T$ curves will be influenced by any variation with temperature of the difference $E_A - E_F$. Nevertheless due to both the low density of states in the tail and the very low carrier mobility, C_1 will be expected to be always several decades smaller than C_o.

c) <u>Localized states conduction near the Fermi level</u> - If there is a band of localized states near the Fermi energy, localized conduction will take place once more via phonon assisted hopping. Conductivity is therefore of the form

$$\sigma_F = C_2 \exp\left[-W_2/kT\right],$$

where W_2 is the activation term and C_2 depends on the hopping distance, phonon frequency, density of states at E_F and overlapping of the neighbouring localized wavefunctions. As the density of states at E_F

is probably smaller than that at the tail band and also the extent of their wave functions is very reduced, the constant C_2 is smaller than C_1. So this conduction mechanism is mainly of importance at low temperatures. However, as temperature decreases phonons become rare and of very low energy. In such a situation it can be energetically more favourable to hop beyond the nearest neighbour to find a final state closer in energy to the initial state. Mott (1969) showed that such a process, the so-called variable range hopping, implies a temperature dependence of the conductivity expressed by the relation

$$\sigma = C_3 \exp \left[\left(- T_{o/T} \right)^{\frac{1}{4}} \right]$$

A $T^{-\frac{1}{4}}$ dependence of ln σ has been widely observed in tetrahedrally bonded glasses (see for instance Mott and Davis 1979).

The relative importance of the different transport processes according to the region of temperatures considered can be summarized in fig 2K(a) bearing in mind eq. (2.1). Thus, for a large range of temperatures the ln σ versus $1/T$ curve is expected to reflect the different activation energies characteristic of the various mechanisms discussed (fig. 2K(b)).

2.5.2 Thermopower

The thermopower, S, is given by the expression

$$S = \frac{\Pi}{T}$$

where Π is the Peltier coefficient whose physical meaning is the energy transported by the carriers per unit charge. The energy is measured relatively to the Fermi energy and since the contribution of each electron is proportional to its contribution to the conductivity, the thermopower can be written in the form

$$S = - \frac{1}{eT} \int (E-E_F) \cdot \frac{\sigma(E)}{\sigma_{total}} \cdot dE$$

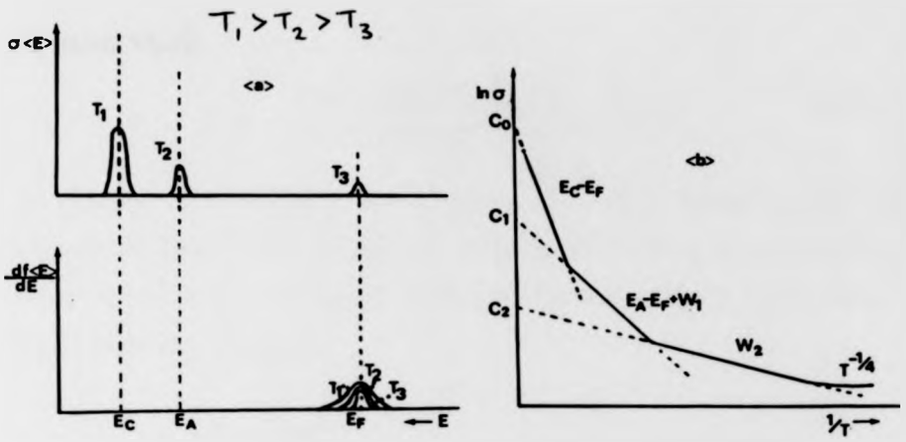

Fig. 2K – (a) Schematic representation of the influence of temperature on the type of conduction according to equation (2.1) and to the forms of $\frac{\partial f(E)}{\partial E}$, also represented, N(E) and μ(E) as illustrated in figures 2I(a) and 2G respectively; (b) illustration of the different activation energies and pre-exponential factors corresponding to the different conduction regimes expected over a large temperature range.

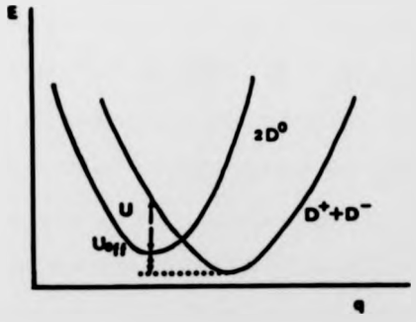

Fig. 2L – Configurational diagram for the formation of a D^+, D^- pair assuming that the electron pairing cost (Hubbard energy, U) is overcome by the gain due to configurational changes. The net result is therefore a negative correlation energy U_{eff}.

or using (2.1)

$$S = -\frac{k}{e} \cdot \frac{\int \mu(E)\, N(E) \cdot [(E-E_F)/kT] \frac{\partial f}{\partial E} \cdot dE}{\int \mu(E)\, N(E) \cdot \frac{\partial f}{\partial E} \cdot dE} \qquad (2.10)$$

In the case of conduction via extended states and assuming, once more, a constant density of states and a constant mobility over the whole band, equation (2.10) can be easily integrated using the Boltzmann approximation, yielding

$$S = -\frac{k}{e}\left(\frac{E_C - E_F}{kT} + A\right) \qquad (2.11)$$

The value of the constant $A(=1)$ is here a direct consequence of assuming $N(E)$ and $\mu(E)$ as constants.

If the mobility gap changes linearly with temperature, that is equation (2.8) is valid, then

$$S = -\frac{k}{e}\left(\frac{\Delta E}{kT} + \frac{\gamma}{k} + 1\right) \qquad (2.12)$$

Thus a plot of S against $1/T$ should show a similar activation energy to that of the curve $\ln \sigma$ versus $1/T$. Furthermore this plot would allow a determination of γ as long as the value of γ/k is great enough to render any error in the estimate of A insignificant.

For the case of conduction via localized states placed at the band tails and assuming that the activation energy for hopping W is not a function of temperature, the terms in the integration (2.10) containing W cancel. The activation energy for the thermopower is then smaller than the corresponding energy for D.C.conductivity, the difference being exactly W. In fact, if W is constant and a density of states of the form (2.9) or even with some power affecting the term $(E-E_A)$ is assumed, it is possible to show that the expression for the thermopower is still of the form of equation (2.11). Specifically,

$$S_{localized} = -\frac{k}{e}\left(\frac{E_A - E_F}{kT} + A'\right) \qquad (2.13)$$

where A' is temperature dependent.

2.6 The role of impurities: defect states and impurity states

It was mentioned before that topological defects are responsible for the appearance of gap states and so forth, in some respect, for the electrical properties of the glasses. Here it will be discussed how these native defects arise and how they are strictly related to the influence of impurities on the electrical properties of non-crystalline solids. A review of atomic defects in glasses is made e.g. by Robertson (1982).

In the early years of amorphous semiconductors physics it was experimentally observed that the conductivity of chalcogenide glasses was insensitive to changes in composition which could be as high as a few percent. This fact led to the suggestion that impurities would generally have no effect on the electrical properties of such glasses. As already referred in 1.4, the suggestion was based upon the idea that a glass structure could rearrange itself in a manner such that all available electrons were taken up in bonding. That is, impurities in a glass were expected to be coordinated in such a way that the requirement of covalent bonding would be fulfilled and thus no formation of either donor or acceptor states would occur. This is summarized by the "8-n rule" (see e.g. Zallen 1983), which specifies that the nearest neighbour coordination of an atom in a covalent glass, Z, is given by

$$Z = 8-n$$

where n is the number of s plus p electrons of the atom considered.

This gives quite a good picture of the short-range order in an ideal glass and certainly accounts for the observed behaviour in many covalent glasses. Nevertheless real glasses deviate from this ideal situation and in both tetrahedrally bonded amorphous semiconductors

and chalcogenide glasses, bonding defects exist. Bonding defects are namely dangling bonds where the normal coordination of the glass is undersatisfied, i.e. where an orbital is occupied by a single electron.

In amorphous silicon, for example, dangling bonds exist in the concentration of one per 10^3 atoms and are responsible for the large density of states inside the gap. This makes pure a-Si a variable range hopping conductor and technologically rather uninteresting. However, the elimination of those unsaturated ends by hydrogenating the silicon transforms the material in a standard semiconductor and enables it to be doped either n or p-type.

Vitreous selenium is a typical case in which dangling bonds arise. It constitutes a network glass of dimension one, containing chain ends which, obviously, deviate from the normal coordination $Z=2$. Since the number of atoms in a chain averages 10^5, the concentration of defects approaches 20 parts per million. However, and contrary to the case of a-Si, there is no E.S.R. signal suggesting that all electrons at the chain terminators must be paired. An explanation of this fact was first proposed by Street and Mott (1975) assuming that defects in a-Se can be occupied by zero, one or two electrons giving rise to three types of states, D^+, D^o and D^- respectively. It was also supposed that the total energy due to lattice plus electrons is smaller for the configuration containing D^+ and D^- (both defects without spin) than for the configuration where neutral ends D^o (with impaired spin) are present. That is to say that the potential energy gain due to the Coulombic repulsion at D^- is less than the decrease in lattice energy. The process

$$2D^o \longrightarrow D^+ + D^-$$

is so exothermic as illustrated by the configurational diagram of fig. 2L. Thus instead of the neutral one-fold coordinated chain ends (D^o centres)

the model assumes that one half of the dangling bonds becomes negatively charged although keeping the single coordination (D^- centres) whilst the other half becomes positively charged and 3-fold coordinated by strongly binding to an atom of a neighbouring chain via the lone pair of this atom (D^+ centres). This model, illustrated in fig. 2M, is not exclusive to chalcogenides but applies as well to other undercoordinated situations such as two-fold arsenic atoms.

Kastner, Adler and Fritzsche (1976) discussed the process of defect formation in terms of chemical bond arguments. These authors suggested that a large fraction of Se dangling bonds convert during the formation of the glass into pairs of different defects which they named Valence Alternation Pairs (VAP's). It was noticed that after the formation of a VAP the total number of bonding and lone pair electrons is the same as in a continuous random network (defect free ideal glass). Therefore, the energy to form a VAP should be quite low. In fact, considering the reaction for VAP formation in a simplified form,

$$2\,C_2^{\,o} + U_{LP} \longrightarrow C_3^{\,+} + C_1^{\,-}$$

where the upper and lower indexes stand for the charge and coordination states respectively, U_{LP} is essentially due to two energy contributions. A negative contribution which is the energy cost of transferring one electron between two initially neutral atoms to place it along its lone pair counterpart on the chain end and form C_1^-. And a positive one which derives from bringing one electron from a non-bonding situation (lone pair) to a bonding state to form C_3^+, thus lowering substantially its energy. In other words, whereas the energy needed to create two neutral ends from an ideal network is twice the energy of displacing one electron from a bonding to a lone pair state, the energy to form a VAP is simply the energy necessary to transfer an electron from one to another neutral

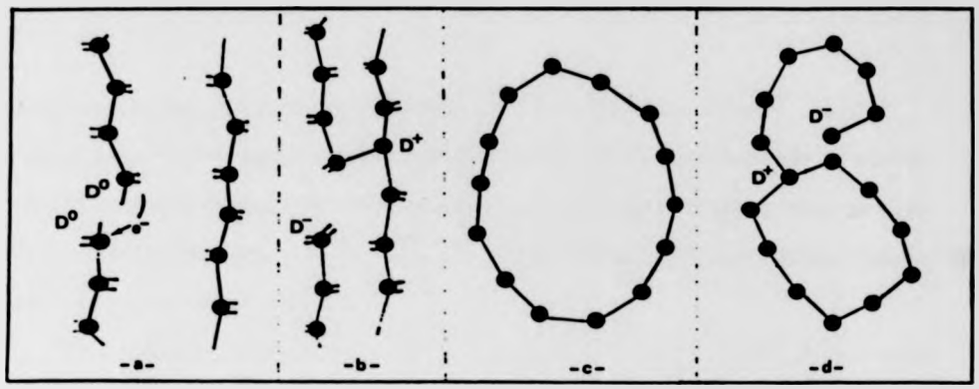

Fig. 2M - Schematic formation of charged defects (D^+, D^-) in vitreous selenium ((a) and (b)). When all the chain ends are transformed in charged centres the total number of bonds is the same as in the hypothetical ideal continuous network ((c) and (d)).

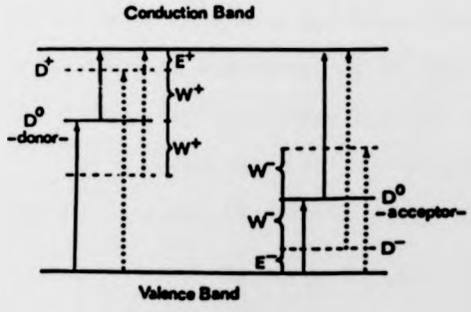

Fig. 2N - Energy levels arising from D^+ and D^- defects as in chalcogenide glasses. Solid arrows indicate thermal transitions. Other arrows represent optical absorption transitions.

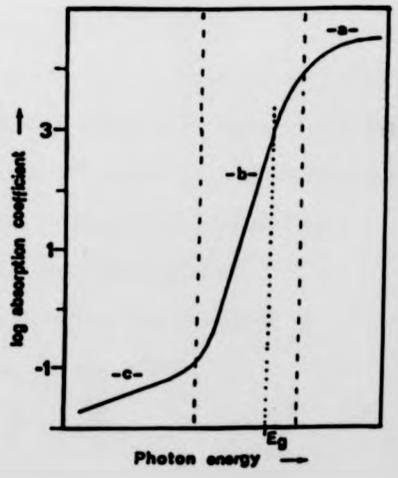

Fig. 2 O - Illustration of the optical absorption edge in amorphous semiconductors presenting three distinct regions.

atom, which is, plausibly, smaller. Hence, the net energy could possibly be negative, even if lattice stiffness is taken into account.

Therefore, though the two models use different ideas, they arrive at a similar result. C_3^+ and C_1^-, where C means chalcogenide, denote the same states as do D^+ and D^-.

The energy level scheme for the electronic states associated with the defects is shown in fig. 2N (Davis 1979). As the D^- centres contain, in addition to the lone pair, two more electrons that have a similar character, their energy must lie near the valence band (E^- above). These D^- levels can capture a hole and thus form D^o states placed at an upper energy given the distortion energy involved (W^-). The levels so formed can be considered as acceptors with W^-+E^- being exactly the thermal energy necessary to excite an electron from the valence band to the defect.

The D^+ centres are three fold coordinated and, so, if an extra electron is located on one of them it must stay in an anti-bonding state occupying therefore an energy close to the conduction band (E^+ below). This centre then acts as a donor. However, as the D^o level is formed there is a lowering of the energy of W^+ due to the electron-phonon interaction. The donor level therefore binds an electron with energy W^++E^+.

As a consequence of the presence of the defects the position of the Fermi level is determined by the equation (Davis 1979)

$$E_C - E_F = (W^+ + E^+ + E_g - W^- - E^-)/2$$

where E_g is the mobility gap, and so effectively pinned midway between the donor and acceptor levels. This in turn determines the electrical properties of the glass. However, if by the introduction of alien atoms, somehow, the balance between those defects is altered, the Fermi level changes as do the activation energy and eventually the transport

mechanism of the semiconductor, Hence it was shown (Mott 1976) that if only the D^- centres are destroyed the activation energy for p-type conduction will be reduced by one third. This might explain the behaviour of oxygen doped a-Se as discussed in chapter IV.

2.7 Other properties

2.7.1 Optical absorption edge

The absorption edge corresponds to electronic transitions from the maximum of the valence band to the minimum of the conduction band. It represents therefore a measure of the optical gap and therefore of the mobility gap.

In most non-crystalline semiconductors a plot of the absorption coefficient α as a function of the photon energy in the region of the absorption edge is in accordance with the schematic representation of fig. 20. It shows three characteristic parts: a high absorption region ($\alpha > 10^4 cm^{-1}$), a region of exponential dependence and a tail of weak absorption.

a) The power law absorption region. The high absorption region is most probably associated with transitions between extended states just beyond their respective mobility edges. The optical properties of both amorphous and crystal line semiconductors can, in general terms, be obtained from the one electron expression for the imaginary part, ϵ_2, of the dielectric constant. For interband absorption in non-crystalline semiconductors the following expression can be derived using the random phase approximation (see for ex. Tauc 1974)

$$\epsilon_2(\omega) \simeq 2\left(\frac{2\pi e}{\omega m}\right)^2 . a\, \hbar^2 \int_a^{\hbar\omega} N_V(-E)\, N_C(\hbar\omega - E)\, dE \qquad (2.14)$$

where a is the interatomic spacing, ω is the photon frequency and N_V and N_C are respectively the density of states in the valence (initial states)

and conduction (final states) bands. It is generally assumed that the forms of N_V and N_C just beyond the mobility edges are

$$N_V(E) \propto (E_V - E)^p \quad ; \quad N_C(E) \propto (E - E_C)^q$$

If the energy is measured from the valence band extreme, E_V, the integration of (2.14) by use of the binomial expression yields,

$$\epsilon_2(\omega) = \frac{\text{constant}}{\omega^2} \left[\hbar\omega - (E_C - E_V)\right]^{p+q-1} \qquad (2.15)$$

Since

$$\alpha(\omega) = \omega\, \epsilon_2(\omega)\, nc \qquad (2.16)$$

where n is the refractive index and c a known universal constant (2.15) becomes

$$\alpha(\omega) = \frac{\text{constant}}{\omega} \left[\hbar\omega - (E_C - E_V)\right]^{p+q+1}$$

If both band edges are parabolic, as in crystals, this reduces to

$$\omega \cdot \alpha(\omega) = \text{constant} \left[\hbar\omega - (E_C - E_V)\right]^2$$

which is the experimentally observed behaviour in many amorphous semiconductors. As localized to extended transitions are also allowed the experimental interpretation of the value $E_C - E_V$ should be made with care especially if the tail states density is high. In this case the measurable value of $E_C - E_V$ could be smaller than the mobility gap and approach in fact the energy between the edge of the valence band tail and the conduction band mobility edge.

b) <u>The exponential absorption region</u>. For absorption coefficients less than $\sim 10^4 cm^{-1}$ a variation of α with the photon energy of the form

$$\alpha(\omega) = \alpha_o \exp\left[\hbar\omega / E_t\right] \qquad (2.17)$$

is almost universal. E_t, the slope of $\ln\alpha$ vs. $\hbar\omega$ is practically temperature independent below the glass transition temperature, but

decreases with T for higher temperatures. At the same time, at room temperature, the observed values of E_t range in a narrow interval from 10 to 25 eV^{-1} (Connell 1979).

This form of the absorption edge occurs as well in some crystalline solids and is named an Urbach edge. An interpretation of this exponential behaviour for glassy semiconductors was made considering the fact, already discussed, that equation (2.14) is also valid for localized-delocalized transitions. The exponential behaviour will then simply mean that the tail band density of states has an exponential dependence on E of the form

$$N(E) = \text{constant.} \exp (E_t\ E)$$

This explanation is however unlikely, for the reason (already indicated) that most materials held a similar value for E_t. Other interpretations, some of which are based on interactions with internal electrical fields, have been suggested. Nevertheless the precise origin of this phenomenon seems as yet not to be understood fully.

c) The weak absorption region. This low absorption tail may be due to optical transitions, either between two localized states or between states of a different kind (localized $\rightleftharpoons$ extended). Light scattering cannot however be ruled out as a contributor to this observed tail.

2.7.2 Photoconductivity

Photoconductivity occurs when, by the effect of light, there is either an increase in the number of free carriers or a lowering of barriers existing eventually inside the material. The increase in free carrier concentration by absorption of appropriate electromagnetic radiation can take place for two reasons: the absorbed photon results in band to band promotion (intrinsic photoconductivity) or, otherwise, it is involved in a transition to or from an impurity or defect state

(extrinsic photoconductivity). The excess conductivity $\Delta\sigma$ is then given by

$$\Delta\sigma = e(\Delta n \mu_n + \Delta p \mu_p)$$

where Δn and Δp are the excesses in the charge carrier densities. Under steady-state conditions these excess densities equal the product of their rate of generation and their lifetime. The generation rate is obviously related to the quantum efficiency, that is, to the number of electron-hole pairs formed when a photon is absorbed.

The measurement of the photocurrent as a function of the energy of the incoming photon can thus provide information about both the approximated width of the pseudo-forbidden gap and the energy separation of the gap levels from the valence or conduction bands. However, as the optical absorption edge in non-crystalline semiconductors is not sharp and there is a dependence of the quantum yield from the photon energy, the determination of the mobility gap from photoconductivity data is probably ambiguous (Mott and Davis 1979). Defect levels located inside the gap that act as trapping or recombination centres can hinder the analysis of experimental results if several of those are present. It was suggested that information about defect states from photoconductivity measurements only is uncertain (Nagels 1979). Nevertheless, the experimental curves of the photocurrent vs. wavelength can provide useful working data with which specific glasses can be compared.

2.7.3 Infrared spectroscopy

Infrared absorption in both crystalline and non-crystalline semiconductors is determined by the interaction of light with vibrational modes via coupling with the oscillating dipole moment that accompanies the molecular vibration. Vibrational modes can be classified as acoustic,

due to bond-bending and due to bond-stretching and have increasing frequencies in this order.

However, and in contrast to the case for crystals where group theory imposes that only a few modes near the centre of the Brillouin zone can contribute to the infrared spectrum, in an amorphous material there is a disorder-induced breakdown of selection rules. As a consequence electromagnetic radiation coupling with vibrational modes that are not active in crystals is therefore possible and infrared spectra are expected to extend over the whole vibrational region. Broad bands are then generally anticipated in glasses with the I.R. spectrum resembling the phonon density of states although modulated by the matrix-element of the transition. So, in comparison with crystalline solids, spectra of their vitreous counterparts show no fine structure.

Interpretation of infrared data is generally made on the basis of one of the following approaches: by direct comparison between the spectra of the amorphous solid and the corresponding crystals with similar composition; by calculations considering small molecular entities which are either independent or effectively decoupled from the surrounding solid; by calculations considering clusters where terminator atoms with a different coordination number are present and give rise to "localized" modes, in terms of network dynamics if no independent molecular units can be identified and all the atoms present contribute to the vibrational modes; and by calculations based on a previous knowledge of the phonon density of states (obtained via other experimental sources).

Infrared spectroscopy can therefore provide direct structural information and, in particular, information about the short-range configuration of the glass.

2.7.4 Field effect

Departure from ohmic behaviour is quite a common effect in non-crystalline semiconductors. One or more of several physical reasons can be behind a non linear I-V characteristic.

In the first place problems can arise from contacts. When contacts form, the condition that the Fermi level should be the same in the metal electrode, the interface and the non-crystalline material has to be satisfied. This leads to a space charge region associated with a screening potential which depends on the density of states of the amorphous material. The smaller the density of localized states in the material the greater the width of the space charge region will be. Therefore the properties of thin films may be directly affected. In the case of semi-insulating or wide gap amorphous semiconductors such as Se, the problem is more acute since the density of the majority carriers is small and so it is difficult to establish electrical contact without perturbing that density. The space charge region is thus expected to be very large.

When an electric field is applied, the surface potential (and therefore the space charge adjacent to the surface) is changed. If one or both contacts provide a reservoir of carriers ready to participate in the conduction, departure from ohmic linearity will take place whenever the field strength is high enough to prevent, by dielectric relaxation, the charge balance. The deviation from ohmic regime is, in this case, said to be caused by "space charge limited currents" (S.C.L.C.).

The one carrier injection S.C.L.C. density J is, in a trap-free material, related to the applied voltage V and the sample thickness L by the quadratic law, (e.g. Fritzsche 1974)

$$J = \frac{9}{8} \mu\epsilon \frac{V^2}{L^3} \qquad (2.17)$$

where μ and ϵ stand for the mobility and the permittivity, respectively.

If localized states are present, a large number of the injected carriers will be trapped and so higher voltages are needed to originate S.C.L.C. At even higher voltages, whilst the trapping centres become filled, a higher voltage dependence of the current is observed before a new trap-free S.C.L.C. region is attained.

A typical I-V characteristic of an amorphous semiconductor where S.C.L.C. occur will therefore contain, in addition to an ohmic part, two square-law regions separated by a higher power regime (trap-filled limit). The specific form of the S.C.L.C. curve will obviously depend on the form of the localized state distribution and therefore the study of S.C.L.C. can be of importance in obtaining information on the defect structure of materials. Expressions for the special cases of exponential and uniform distribution of traps have been derived, amongst others, by Rose (1955) and Lampert and Mark (1970) respectively.

Other physical processes responsible for a non linear I-V curve include the Poole-Frenkel and Schottky effects. The former is due to the field assisted ionization of carriers from coulombic traps and yields a log I versus $V^{\frac{1}{2}}$ relationship. The Schottky mechanism is a similar one involving the emission of carriers from their image charge and is characterized also by an I-V curve of that form. Modifications of these models taking into account the probability of carriers escaping at all possible angles as well as models considering emission over other potential barriers and other emission processes (e.g. tunnelling through the barrier) have also been proposed.

S.C.L.C. due to double injection or to one carrier injection into a material for which the dielectric relaxation time is very large when compared to the carrier lifetime will account for I-V characteristics

which do not fit with the laws discussed above. In particular the latter mechanism leads seemingly to a sub linear ($I \propto V^{\frac{1}{2}}$) regime.

To be able to distinguish between non linearity arising from S.C.L.C. and that originating in other phenomena, the current dependence on the sample thickness should be investigated. According to the general relation for space charge currents in a homogeneous medium, of which eq. (2.17) is a special case, this means curves of J/L as a function of V/L^2 should superimpose (Roberts 1973).

CHAPTER III - EXPERIMENTAL METHOD

3.1 Glass preparation

3.1.1 Introduction

As already mentioned, it is now well established that some impurities, namely oxygen, have a very strong effect upon the electrical properties of selenium glass (Lacourse et al.1970; Twaddell et al. 1972; McMillan and Shutov 1977). At the same time the central aim of this work was to investigate the effect of other impurities. Therefore the main concern in choosing a method for the preparation of the samples was to ensure that, in general, and particularly with respect to oxygen, a very good degree of purity could be obtained. Since it was impossible to know what level of impurity contamination was present in each glass, the same procedure was followed for the preparation of all samples. Therefore it is reasonable to assume that all materials had a similar concentration of impurities.

Since vitreous selenium is quite fragile it was also desirable to choose a method where the necessity for post-preparation machining was reduced. Thus, as the intention was to work on bulk glasses, the method adopted consisted basically of forming a melt and quenching it at a sufficiently fast rate so that no crystallisation could occur. Such a rate is, for glassy selenium, established at $10\text{-}10^2$ $^oKs^{-1}$ (e.g. Zallen 1983).

3.1.2 The method

The actual method used comprised essentially the following:

The glasses were melted in silica ampoules for two hours at a

temperature of approximately 340°C, the only exception being the glasses of the Se-Te system for which a melting temperature of 500°C was used. The ampoule was frequently agitated to improve homogenization of the melt. After melting, the glass was rapidly quenched by pressing a drop of the molten material between two silicate plates attached to brass blocks.

The starting chemicals were obtained commercially from Aldrich Ltd., Koch Light Ltd. and Alfa Lab. and were claimed to be better than 99.99% pure, except for the case of selenium bromide and selenium tetrachloride claimed to be only better than 99.5% pure. In particular, the selenium used had a degree of purity of 6N. All the products were used directly in the form in which they were bought.

All the steps of the method, that is handling of the raw materials, melting and quenching, were carried out inside a glove-box filled with an oxygen-free nitrogen atmosphere. To provide further purification the nitrogen was passed through a desiccant and a tube containing hot copper pellets before entering the glove-box.

Prior to melting, the silica ampoule and plates were washed successively with a solution of hydrofluoric acid, methanol and distilled water. The ampoule and plates were then placed inside the glove-box, the ampoule heated up to 300°C and allowed to cool slowly. An indication of the dimensions of the ampoules and furnace is provided in fig. 3A.

3.1.3 Characteristics of the glasses

The glasses obtained were approximately disc-shaped with diameters that varied between 1 and 1.5cm and presented naturally mirror polished surfaces, being therefore ready for optical measurements. A typical glass sample is shown in fig. 3B.

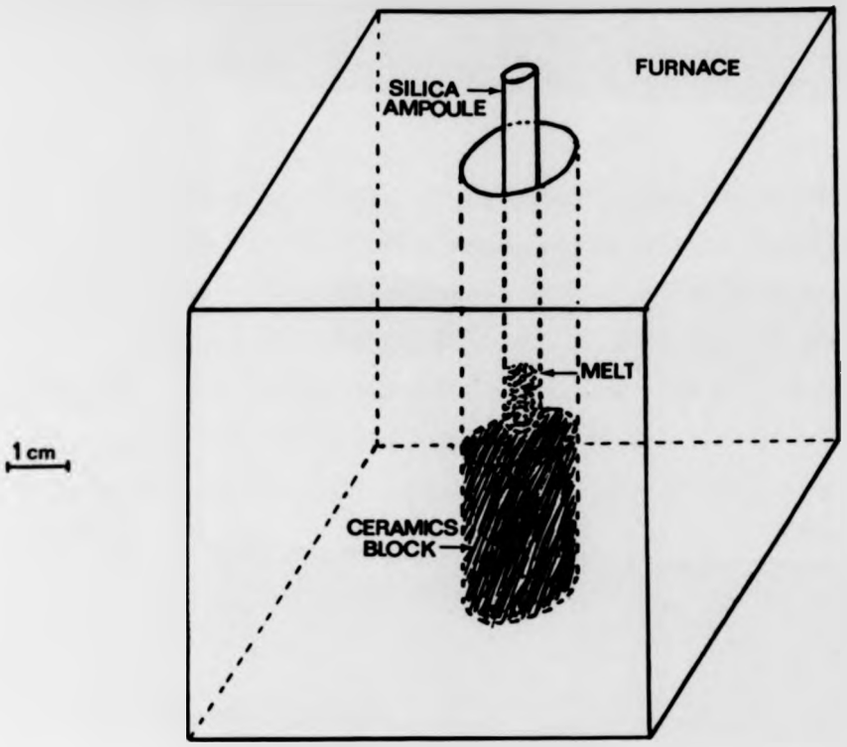

Fig. 3A - Melting furnace and silica ampoule.

Fig. 3B - Photograph of a Br-doped glassy selenium sample.

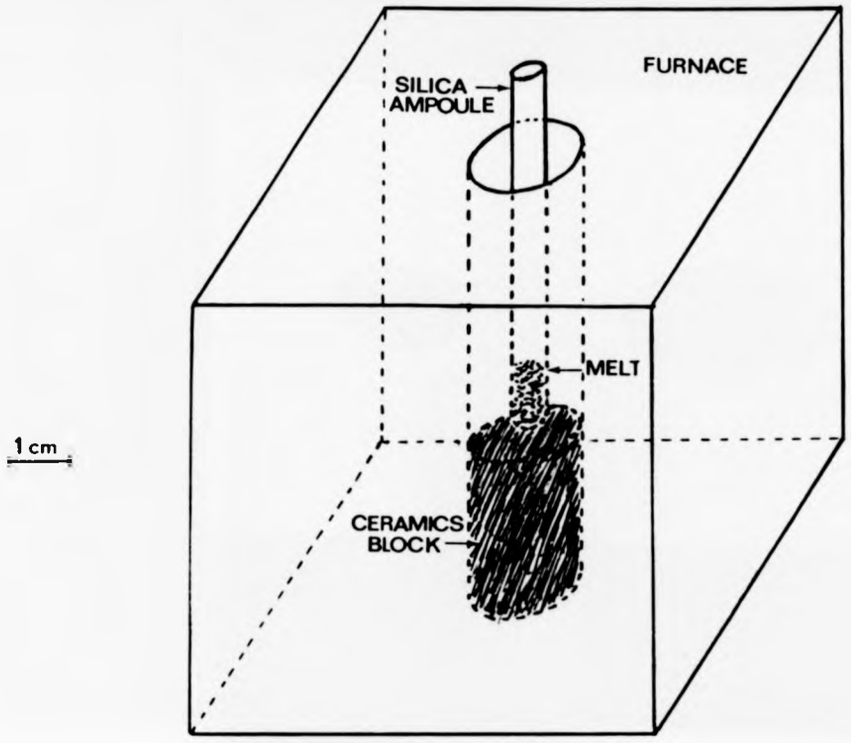

Fig. 3A - Melting furnace and silica ampoule.

Fig. 3B - Photograph of a Br-doped glassy selenium sample.

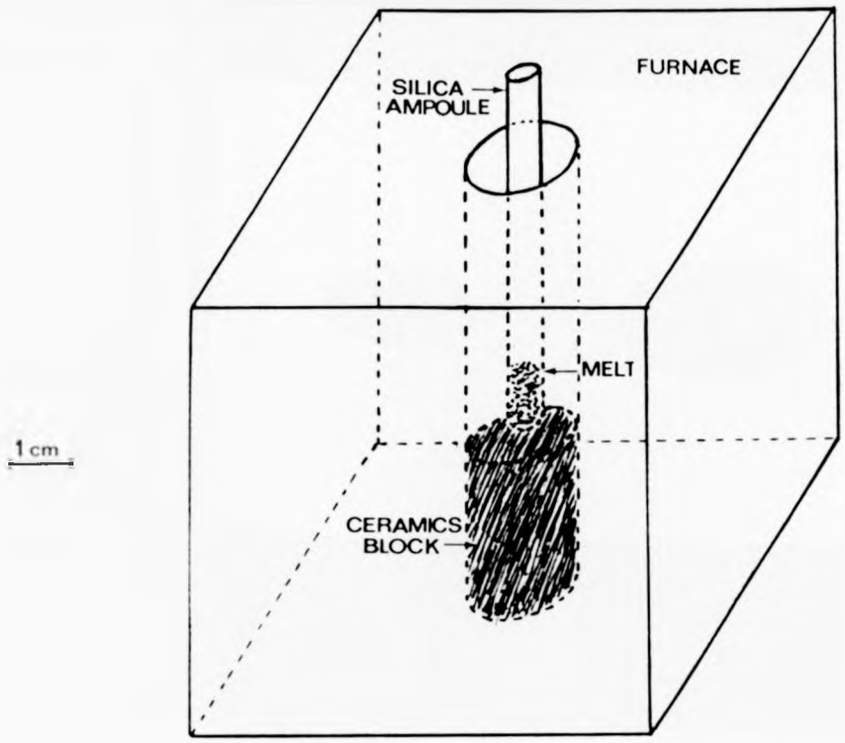

Fig. 3A - Melting furnace and silica ampoule.

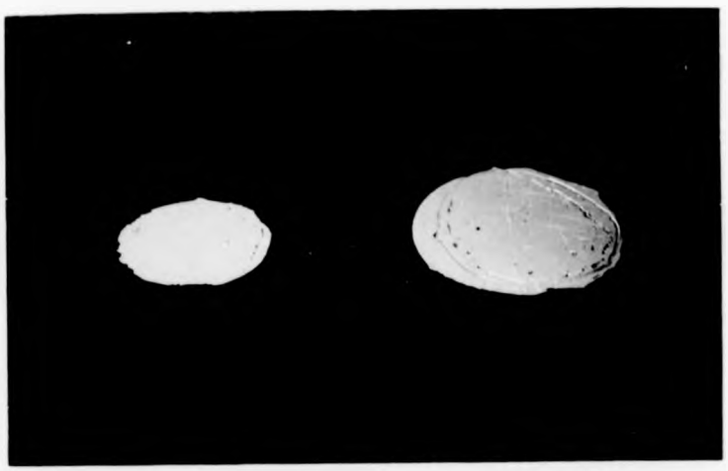

Fig. 3B - Photograph of a Br-doped glassy selenium sample.

The surfaces of fracture of all glasses showed the characteristic concoidal form, the surface being made up of round shaped convexities and concavities. Concoidal fracture, but for a few exceptions, is typical of the amorphous state (Bagley 1974) and so the above fact constitutes a first indication of the vitreous nature of the samples. Nevertheless fractography is a merely qualitative test and does not always allow a clear structural identification. The non-crystallinity of each material was therefore verified by X-Ray diffraction (X.R.D.). A typical X-Ray pattern for a pure selenium glass is shown in fig. 3C.

3.1.4 Sample purity control

The purity of the samples was estimated in two ways. In the first place no definite oxygen bands could be observed in the infrared spectra taken. According to Vasko et al. (1970) infrared spectra of a-Se are very sensitive to oxygen impurity and Twaddell et al.(1972) point even to the fact that amounts as small as two or three parts per million of oxygen can be detected by infrared spectroscopy. Hence the absence of oxygen bands indicates that should the impurity be present it will be at quite low levels. Moreover, there is some evidence that the melt purifies itself of oxygen. As a matter of fact it was necessary to add up to $\sim$ 4 at % of O in the form of selenium dioxide to actually obtain a modified Se infrared spectrum showing some oxygen bands. In fig. 4B the spectrum so obtained is compared with one of pure selenium. The self purification of Se in respect of oxygen has already been suggested by Vasko (1969).

The second way of estimating the oxygen content of vitreous selenium refers to its conductivity. A literature survey (Hulls 1970; Lacourse

The surfaces of fracture of all glasses showed the characteristic concoidal form, the surface being made up of round shaped convexities and concavities. Concoidal fracture, but for a few exceptions, is typical of the amorphous state (Bagley 1974) and so the above fact constitutes a first indication of the vitreous nature of the samples. Nevertheless fractography is a merely qualitative test and does not always allow a clear structural identification. The non-crystallinity of each material was therefore verified by X-Ray diffraction (X.R.D.). A typical X-Ray pattern for a pure selenium glass is shown in fig. 3C.

3.1.4 Sample purity control

The purity of the samples was estimated in two ways. In the first place no definite oxygen bands could be observed in the infrared spectra taken. According to Vasko et al. (1970) infrared spectra of a-Se are very sensitive to oxygen impurity and Twaddell et al.(1972) point even to the fact that amounts as small as two or three parts per million of oxygen can be detected by infrared spectroscopy. Hence the absence of oxygen bands indicates that should the impurity be present it will be at quite low levels. Moreover, there is some evidence that the melt purifies itself of oxygen. As a matter of fact it was necessary to add up to ~ 4 at % of O in the form of selenium dioxide to actually obtain a modified Se infrared spectrum showing some oxygen bands. In fig. 4B the spectrum so obtained is compared with one of pure selenium. The self purification of Se in respect of oxygen has already been suggested by Vasko (1969).

The second way of estimating the oxygen content of vitreous selenium refers to its conductivity. A literature survey (Hulls 1970; Lacourse

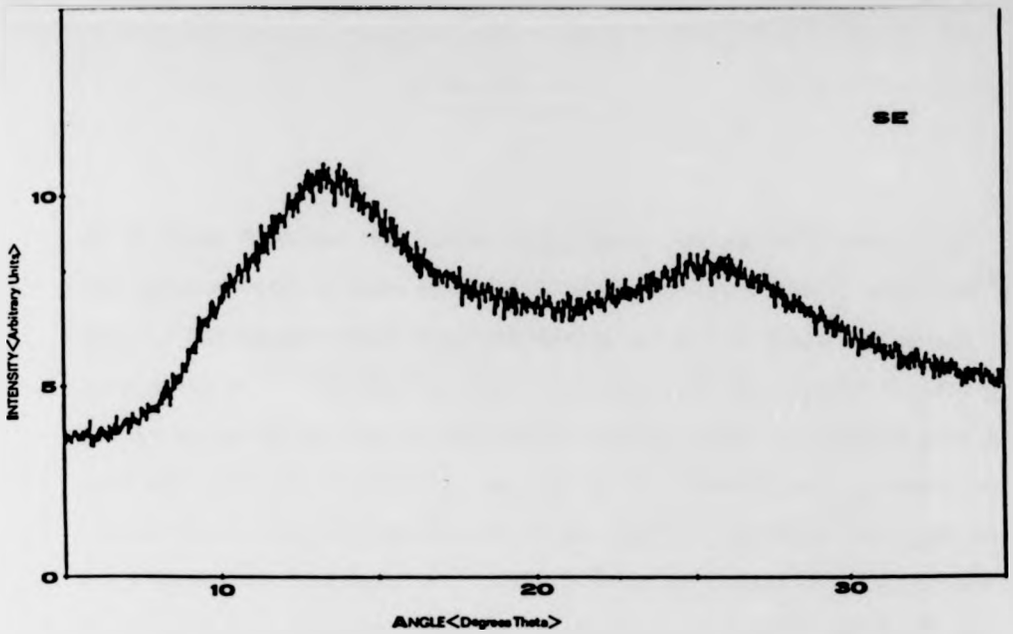

Fig. 3C - X-Ray diffractometer trace of a selenium glass at room temperature.

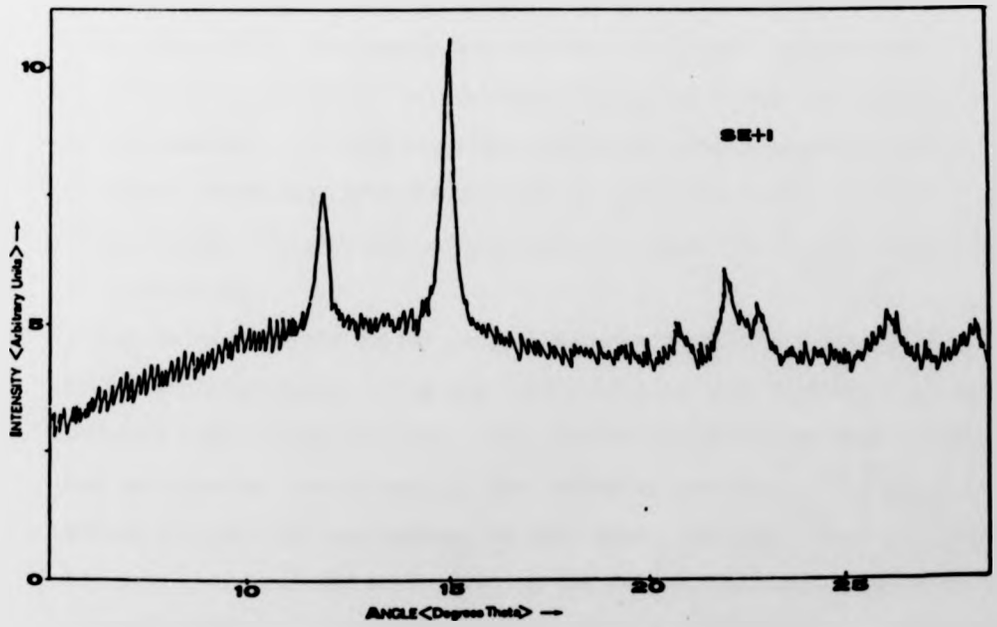

Fig. 3D - X-Ray diffractometer trace of a partially devitrified $Se_{97}I_3$ sample after staying 8 months at room temperature.

et al.1970; McMillan and Shutov 1977; Mehra et al. 1978) shows that the conductivity of pure Se glasses can be as low as 10^{-17} $ohm^{-1}.cm^{-1}$, whereas for oxygen doped Se glass the value of the conductivity can be as high as 10^{-11} $ohm^{-1}.cm^{-1}$. That is, oxygen can be responsible for a change up to six orders of magnitude compared with the conductivity of pure selenium and therefore a measure of the conductivity provides an indication of the oxygen content of glassy Se. The value obtained for a glass with 4 at % oxygen is close to that stated above as presented in chapter IV. For pure selenium a value of $\sigma = 3.10^{-15}$ $ohm^{-1}.cm^{-1}$ was obtained which would indicate that contamination by oxygen due to the method used is, at most, of a few p.p.m.

As also discussed in chapter IV, other factors can influence the conductivity of glassy Se and so some care should be taken in drawing conclusions about the oxygen content from electrical measurements only.

It was not possible to determine the actual oxygen concentration of the samples. A direct analysis could have been made at Harwell by a nuclear activation method but that was ruled out for economical reasons. Neither could the chemical analysis method suggested by Gobrecht (1969) be considered.

In as much as the purity problem is a very important one, a second method of glass preparation was tried, with the aim of comparing results before a choice could be made. The alternative method is quite a standard one and consists essentially of the following procedure: The glass is melted in a silica tube having, in this case, the shape shown in fig. 3E. The tube received the same cleaning and heating treatments, as previously described, before the raw materials in powder form were put in. The tube was then vacuum pumped and filled with argon prior to being sealed at

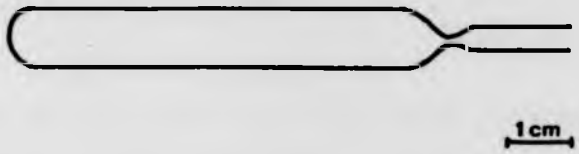

Fig. 3E - Shape of the silica ampoules used in the alternative method.

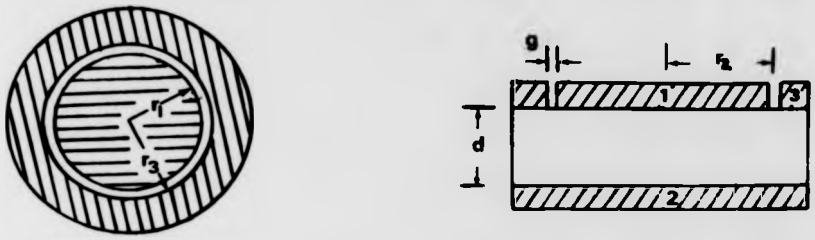

Fig. 3F - Electrode configuration of the three probe-method used.

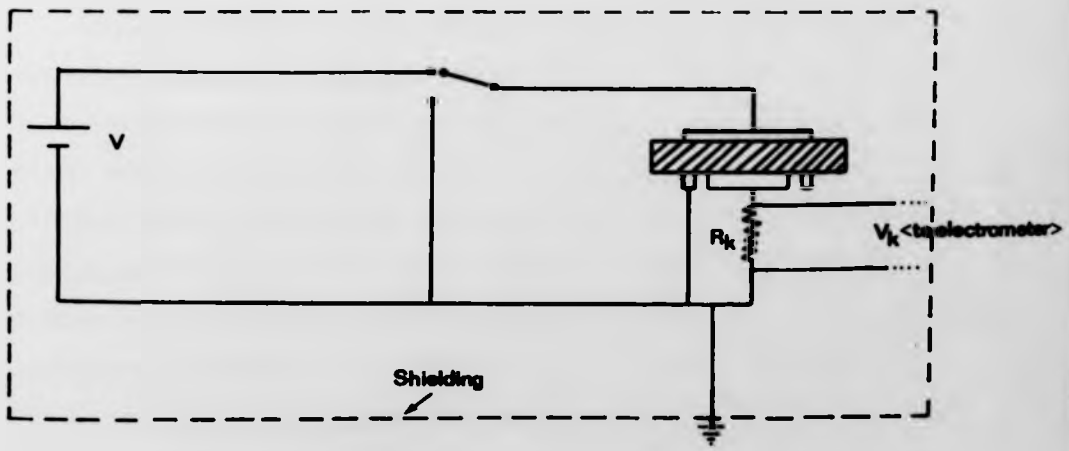

Fig. 3G - Experimental D.C. circuit. Shielding is schematically represented.

the narrow point and placed in a furnace with a rotating device. The silica ampoule was kept rotating about an axis, different from its natural ones, for two hours at $\sim 340^{\circ}C$. The glass was obtained afterwards by quenching the ampoule in cold water.

This alternative method, though ensuring a very good homogeneity, did not contribute to an increase of the resistivity of the glass; this was somehow expected (Hulls 1970; Mehra et al.1977, 1978). At the same time it had some practical disadvantages such as, for purity reasons, the need for powdering the raw materials and the fact that the samples had to be prepared from the bulk glass. The preparation of the samples implied the cutting of the glass as well as, for the case of optical specimens, its polishing which proved to be quite difficult due to the mechanical fragility of the glass and its low transition temperature. This method was therefore rejected.

3.1.5 Verification of the composition

Analysis of low levels of dopant in selenium is difficult as outlined earlier. Nuclear techniques (gamma photon, as employed by Savage (1982), or proton activation analysis) were not available. The alternative was to use energy dispersive analysis of X-rays (E.D.A.X.). This method, described in 3.6.2, is not quantitative for small amounts but can nevertheless provide some indications about the contents. The process followed was to measure separate glasses saturated with each dopant. Saturation occurred, in the case of halogens, for addition of about 3at% of the dopant and E.D.A.X. measurements indicated out that the final composition is similar to the initial one. So, it seems that compositions were not significantly altered during the melting process. In the case of additions of tellurium and sulphur the results are more reliable and also indicate an approximately constant composition throughout the melting.

The E.D.A.X. spectra are shown in chapter IV. The method could not be applied to two of the elements used as dopants, namely oxygen, due to its small atomic number and chlorine, because its K_α peak (main peak) occurs at the same energy as a selenium harmonic peak. The case of oxygen has already been discussed and chlorine was assumed to follow the trend shown by the other halogens: small or no alteration in composition during the melt.

3.1.6 Comments on the stability of the glasses

It was noticed that some of the preliminary halogen doped glasses, after being kept for some time at room temperature, underwent some structural transformations becoming partially crystallized. Fig. 3D shows evidence of crystallization that occurred in a selenium glass, doped with 2,8 at % of iodine after staying six months at room temperature. The peaks identify the crystallites as being of hexagonal selenium. No such effect has, so far, been observed in pure selenium glasses. Hence, it seems that the doping atoms might act as nucleating agents inducing Se to crystallize at a lower temperature.

To verify this some calorimetric measurements were undertaken and these will be discussed in chapter IV.

As the rate of crystallization is strongly temperature dependent all samples examined in this work were constantly kept in a refrigerator ($\sim 4^{o}C$) and this care proved to be sufficient to avoid crystallization over the timescale concerned.

3.2 D.C. conductivity measurements

3.2.1 The D.C. circuit

Since the resistivities to be measured could be as high as 10^{17} Ohm.cm the experimental apparatus had to be designed with high sensitivity.

The process adopted consisted in measuring the voltage across a known resistance placed in series with the specimen. As measuring device a vibrating reed electrometer - Electronic Instruments Ltd., model 62A - was used. Such an electrometer has an input impedance greater than 10^{16} Ohm.

One very important problem when dealing with very low conductivity materials is that one must ensure that the current is actually flowing through the bulk material and no short paths exist. "Easy" paths can exist either through the neighbouring atmosphere or across the specimen holder but, the most important source of shorting paths is, however, surface conduction. In order to avoid this source of error a three probe method was chosen (Blumenthal and Seitz 1974: Dunlop Jr. 1959). The basic electrode configuration for this method is shown in fig. 3F. The guard electrode was put at ground potential which was virtually the same as that of the central electrode (electrode 1), any surface conduction being therefore prevented. The conductivity of the sample was determined by means of the central and the top electrodes (electrodes 1 and 2) and since the reference resistor, R_K, was always at least two orders of magnitude smaller than the bulk resistance of the glass the value of the bulk conductivity, σ, could be simply calculated from the relationship

$$\sigma = \frac{d}{RA}$$

d being the thickness of the samples and $A = \pi[(r_1 + r_3)/2]^2$;

$R = \frac{R_k V}{V_k}$ represents the bulk resistance of the specimen, where V and V_k are respectively the D.C. applied voltage and the voltage measured across the known resistance (R_k). The D.C. voltage was applied using dry batteries of 25 Volt which provided good stable voltages. The circuit analogue of the experimental arrangement is represented in fig. 3G.

The switch S had the function of allowing any capacitance associated with the specimen to discharge between two readings.

3.2.2 The cryostat

A cryostat was designed and built in order to allow measurements for any glass to be taken in the largest range of temperatures possible, that is from the softening point of the glass down to the temperature where the resistance became impossible to measure. In practical terms this meant a range of temperatures between 150°K and 330°K, the latter temperature being above the softening point of all the materials investigated.

Careful consideration was given throughout the design of the cryostat and of the specimen holder to the need to overcome the usual problems connected with the measurement of very high impedances. These problems are identified with the so called noise voltages which are mainly thermoelectric voltages, electrostatic and inductive pick-up and transient signals and will be now briefly considered.

Thermoelectric voltages appear when there is a temperature gradient across the sample. To avoid such a gradient one needs a constant temperature surrounding the sample. This was made as good as possible by means of:

- Making the dimensions of the bath jacket quite large compared with the dimensions of the specimen holder.
- Allowing enough time between two measurements for the temperature to stabilize. The rate of temperature change of $0.3^{\circ}K\ min^{-1}$ was maintained for all samples.
- Providing an exchange gas (nitrogen) for better heat transport between the bath jacket and the specimen holder.

- Building the specimen holder mainly of metal.

The remaining error was minimized by taking the average between values obtained with the temperature increasing and decreasing. In practice this procedure proved to be unnecessary and was not continued.

Inductive pick-up from power sources around was shown to be a minor problem. The work was temporarily carried out in a specially shielded room but this turned out to be unnecessary. The very opposite happened with electrostatic pick-up. This problem became the most difficult to solve but was finally overcome through:

- The elimination of all moving parts of the measuring circuit. That was achieved by making the circuit of straight solid copper rods.
- Shielding of the whole circuit globally (and of each lead individually with brass), shorted to ground through a thick cable.

Noise was then lowered to about 5.10^{-16}Ampere which is of the order of magnitude of the input stray currents (detection limit) of the electrometer. In this way the maximum resistance that can possibly be measured with 25V is about 5.10^{15}Ohm when the signal in the electrometer is ten times greater than the noise. That represents, for the specimen configuration concerned, a lower limit for the conductivity of 5.10^{-17}Ohm^{-1}.cm^{-1}.

Transient signals were mainly introduced from the A.C. voltage via the thermocouples and were prevented by the use of a battery powered voltmeter for the thermocouple reading.

A diagram of the cryostat is presented in fig. 3H. Temperatures below room temperature were obtained by heat exchange with a jacket of either acetone or isopentane (2-Metylbutane). The liquid jacket was cooled by passing liquid nitrogen through a serpentine tube crossing the jacket. The liquid nitrogen was pumped from a rubber sealed dewar, the

- Building the specimen holder mainly of metal.

The remaining error was minimized by taking the average between values obtained with the temperature increasing and decreasing. In practice this procedure proved to be unnecessary and was not continued.

Inductive pick-up from power sources around was shown to be a minor problem. The work was temporarily carried out in a specially shielded room but this turned out to be unnecessary. The very opposite happened with electrostatic pick-up. This problem became the most difficult to solve but was finally overcome through:

- The elimination of all moving parts of the measuring circuit. That was achieved by making the circuit of straight solid copper rods.
- Shielding of the whole circuit globally (and of each lead individually with brass), shorted to ground through a thick cable.

Noise was then lowered to about 5.10^{-16} Ampere which is of the order of magnitude of the input stray currents (detection limit) of the electrometer. In this way the maximum resistance that can possibly be measured with 25V is about 5.10^{15} Ohm when the signal in the electrometer is ten times greater than the noise. That represents, for the specimen configuration concerned, a lower limit for the conductivity of $5.10^{-17} \text{Ohm}^{-1}.\text{cm}^{-1}$.

Transient signals were mainly introduced from the A.C. voltage via the thermocouples and were prevented by the use of a battery powered voltmeter for the thermocouple reading.

A diagram of the cryostat is presented in fig. 3H. Temperatures below room temperature were obtained by heat exchange with a jacket of either acetone or isopentane (2-Metylbutane). The liquid jacket was cooled by passing liquid nitrogen through a serpentine tube crossing the jacket. The liquid nitrogen was pumped from a rubber sealed dewar, the

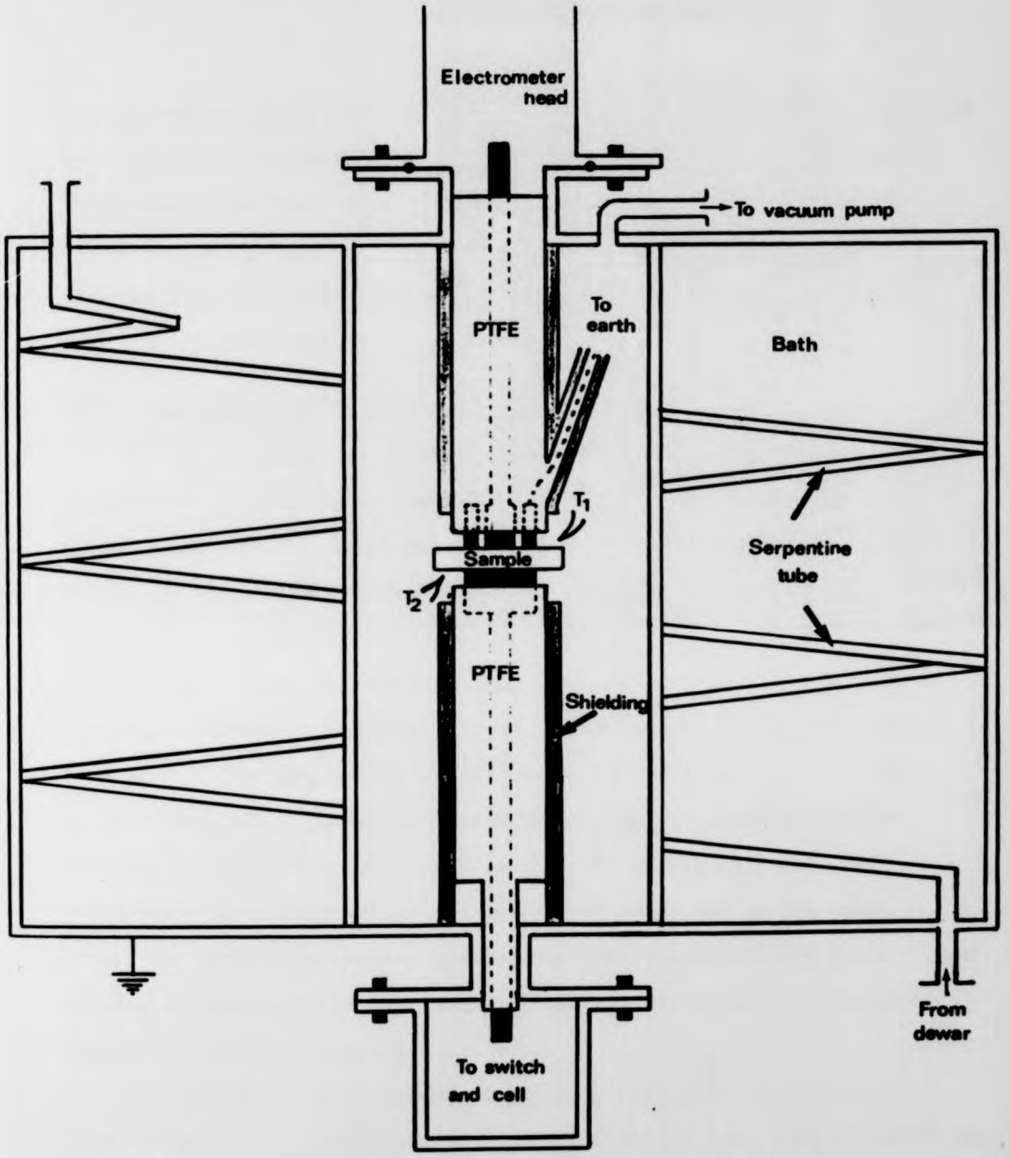

Fig. 3H - Schematic drawing of the cryostat and sample holder arrangements. The cryostat was made of steel. T_1 and T_2 represent thermocouples.

rate of pumping being determined by a Pye temperature controller connected to a powered resistance heater placed inside the dewar. Temperatures above room temperature were obtained using a similar system, with the difference being that the liquid pumped was hot water. The whole cryostat could be filled with a low condensation point gas to prevent shorting via condensation.

3.2.3 The sample holder and sample preparation

The sample holder is sketched as well in fig. 3H. The leads coming out from the electrodes to the cell and to the electrometer were solid straight copper wires which were insulated by passing through a hole drilled in P.T.F.E. 1cm thick rods. The electrodes were made from copper as well and were supported only by P.T.F.E. which formed a single block with the rod around the corresponding lead. The P.T.F.E. pieces were regularly cleaned with methanol to avoid the possibility of any surface conduction. The temperature of the sample was monitored by two nickel-chromium v.. nickel-aluminium thermocouples placed as near as possible to the sample (about 1mm away). One thermocouple was just above the surface of the sample and the other just below and at the opposite site. For both thermocouples a reference junction of melting ice was used being the temperature of the sample determined by taking the average of the two thermocouples voltages.

The specimens, as previously described, were discs of approximately 1 mm thickness and since they already had flat and polished surfaces, further preparation consisted only of the application of the electrodes. The choice of these was of some importance because one had to make sure that the high resistances measured were a characteristic of the glasses and not due to any effect at the metal-glass interface. On account of

that three different electrodes - sputtered gold, evaporated silver and "silver dag" were preliminarly tested on several samples and their performances compared: all of them gave similar values for the resistance of each specimen and exhibited ohmic behaviour in the region 1 to 50 volt.

Gold coating seemed the best choice for the reason that the gold is not easily eroded and the method makes it possible to apply a very precise shape. The method, however, presented in itself a problem since, due to the low transition temperature of the majority of the glasses, the temperature in the sputtering chamber was sufficient to soften the samples. Therefore, for practical reasons, one could only apply a very thin layer which, nevertheless, proved sufficient to make good contact. The resistance across the layer was checked for each sample and verified to be of the order of a few ohms.

The application of the electrodes was completed by painting "silver dag" (colloidal silver) onto the gold layer so that the sample could be fixed to the copper electrodes of the sample holder. No effect due to the possible migration of the silver ions into the surface of the glass was found.

3.2.4 The experiment

The experimental technique can be summarised as follows:
After the application of the gold electrodes the sample was glued with "silver dag" onto the copper electrodes of the sample holder, and next the cryostat was sealed and filled with nitrogen. Some preliminary measurements were then made starting with a low resistor ($R_k = 10^4$ Ohm) across the electrometer to establish the approximate value of the sample resistance and so to select the correct value of R_k. By doing so one prevented any possibility of damaging the very sensitive electrometer

by a wrong choice of R_k. The resistance of the specimen was measured afterwards as a function of temperature from a value close to Tg down to the temperature where the voltage reading was one order of magnitude higher than the noise. The readings were taken at intervals of 1.5 to 3 degrees Celsius and a cooling rate of 18 degrees per hour was maintained for all samples.

This experimental procedure was performed for each glass studied and the results concerning the conductivity σ, the activation energy E_σ and the pre-exponential factor C are presented in chapter IV. The values shown are always the average taken between the values for two or more samples of the same glass. The errors shown are the absolute errors regarding that average since in the case these were much larger than the uncertainties resulting from the readings of the voltage and from the measurements of the electrode radii and sample thickness.

To compare results and test the method used, and also to obtain further data, some D.C. measurements were performed in the cryostat of the Physics Laboratory of the University of Aveiro, Portugal. This cryostat works on a different basis having a permanent cold jacket (liquid nitrogen or helium), the temperature being changed by means of a power controlled resistance heater. The resistance of the samples was determined simply by measuring the current via a Keithley 610 C electrometer placed in series with the specimen. This method allows a much lower threshold of measurable resistances and obviously could not be used for all glasses. In the case of measurements being repeated the results obtained agreed fairly well with the ones previously established.

3.2.5 Field effect measurements

Complementary to the determination of the D.C. conductivity

variation with temperature the dependence of σ on the applied electric field was also investigated. The experiments were performed at a constant temperature of 25°C and took place in the D.C. apparatus already described.

With the purpose of studying the influence of the sample thickness, relevant in field effect experiments, samples 0.3 and 1mm thick were prepared. The application of electrodes was similar to that mentioned in 3.2.3.

The current intensity vs. applied field curves are presented and discussed in chapter IV.

3.3 Thermoelectric power measurements

3.3.1 Introduction

Three phenomena are commonly referred to as thermoelectric effects. They are the Thomson effect, the Peltier effect and the Seebeck effect. The objective was uniquely to measure the latter.

As is well known, the Seebeck effect appears when two different materials are joined together at both ends with the two junctions being kept at different temperatures. The effect consists of the setting up of a potential difference ΔV between the two junctions which is proportional to the temperature difference ΔT between the junctions. This potential difference is due to three contributions: a thermoelectrive force produced by the temperature gradients across the first material, i.e. across the contact wires; a thermoelectrive force produced by the temperature gradient across the second material, i.e. across the specimen; and a thermoelectrive force as a result of the difference in contact potentials at the two interfaces having different temperatures.

The potential difference per degree Kelvin is called the thermoelectric power or the Seebeck coefficient, S. It is defined as

$$S = \frac{\Delta V}{\Delta T}$$

when $T \rightarrow o$. S is customarily considered positive when the conventional current flows from the specimen to the contact wire at the colder junction (Frederikse et al. 1959; Wimmer and Bransky 1974).

In practice the thermoelectric power is obtained by using ΔT values as little as possible, generally of the order of magnitude of few percent of the temperature of the specimen. Therefore, the measurement of the Seebeck coefficient requires placing a sample between two electrodes and ensuring different temperatures at the two interfaces. The thermoelectric power of the sample is then referred to the substance of which the contact wires are made. These are usually metallic (copper or platinum). Absolute Seebeck coefficents can be determined by reducing the measured ones to the value with respect to lead which has, for $T > 20^{o}K$, a very small thermoelectric power.

Since S is dependent on temperature, the measurement of the thermoelectric power requires the determination of a potential drop, ΔV, and either two temperatures or a temperature and a temperature difference.

Although measuring the Seebeck coefficient seems, in principle, quite simple there are various experimental problems which can occur. These will be discussed in the next sections.

3.3.2 The measuring circuit

The main problem in choosing a technique to measure the thermoelectric power was, once more, the effect of the very high impedance of the materials involved (Keem 1975). This was, at room temperature, greater

than 10^7 Ohm for all samples. At this level the possibile occurrence of leakage paths had to be considered and therefore special care had to be taken to ensure that the ends of the sample were electrically isolated from each other at least two orders of magnitude better than the expected sample resistance.

The measuring circuit was originally suggested by Dr. Robert Petiffer and is based on the use of a commercially available operational amplifier, the 311 J, which is characterised by low drift, low noise and an input impedance greater than 10^{14} Ohm. The diagram of the circuit is shown in fig. 3I.

The arrangement of magnetic switches means that in position A (fig. 3J) it was possible to read simultaneously and independently the thermoelectric voltage and the temperature at one end of the specimen. The thermoelectric voltage and the thermocouple voltage were measured by means of, respectively, the 311 J amplifier (actual amplification = 315) and the LH 00 38 CD amplifier (actual amplification = 2.10^3). The thermocouple voltage was referred to a cold junction, placed in an ice-water bath. Switching to position B a reading of the temperature difference could be measured via the latter amplifier. Switching between A and B was achieved by sliding a magnetized material above the magnetic switches.

Copper wires were used to measure the thermoelectrical signals, whereas the temperature readings were made via a copper-constantan thermocouple. Therefore, the Seebeck coefficient was determined against copper. Both copper and constantan leads were very thin to make the thermal resistance very high and thus reduce errors resulting from thermal conduction.

Each magnetic switch was placed inside a glass sealed tube and the whole assembly was mounted on a teflon board. The P.T.F.E. and the glass

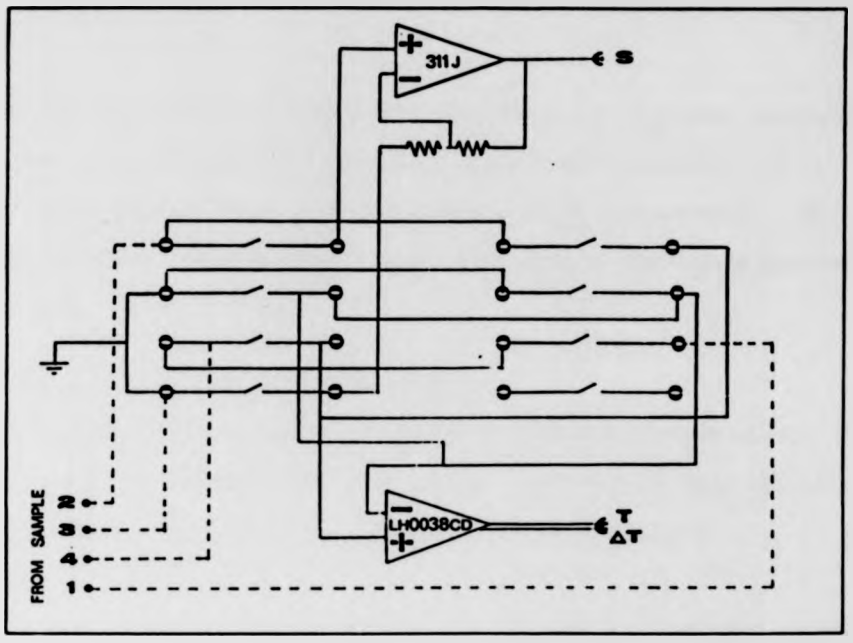

Fig. 3I - Diagram representative of the thermopower experimental circuitry.

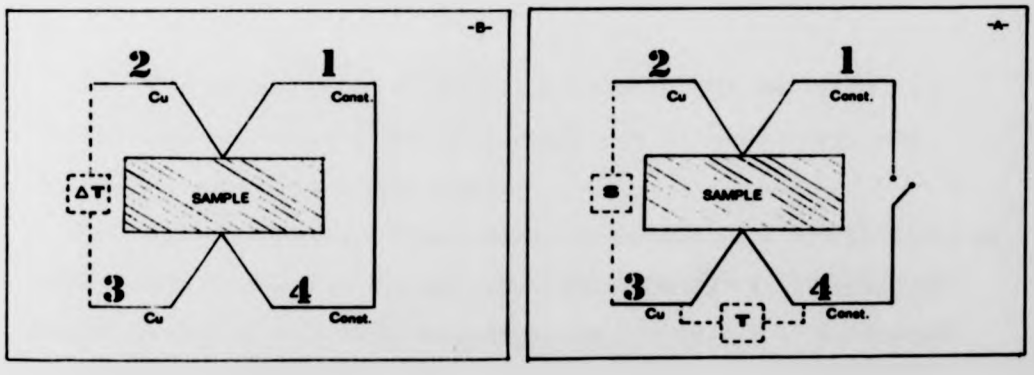

Fig. 3J - Schematic illustration of the two positions allowed by the magnetic switches ensemble: (A) The circuit is open so thermopower and temperature at one side of the sample can be measured simultaneously: (B) 1 and 4 are shorted permitting T to be measured.

surface were periodically cleaned and, therefore, a very good electrical insulation was maintained. For shielding reasons the circuitry was enclosed in a metallic box earthed through a thick copper cable. To diminish drifting the amplifiers were powered by a stabilized dry cells power supply (- 15, + 15V).

3.3.3 The cryostat and the sample holder

In designing the cryostat and sample holder the already stated need to avoid leakage paths and ensure proper shielding had to be kept in mind. The following additional precautions were made:

i) Good thermal contact between sample and wires at the interfaces, as well as between sample and heat sinks, is essential. Hence the sample was "glued" to lead - ends with "silver dag". At the same time the sample was placed between two copper discs which worked as heat sinks. The copper discs were electrically isolated from the wires, as shown in fig. 3K.

ii) The sample should be thermally isolated from the outside but for the inevitable leads. For that purpose teflon mounts were used to hold the sample and copper discs.

iii) Thermal radiation losses should be minimized so that temperature could remain constant inside the sample cell. Other than by external thermal shielding this could be achieved by evacuating the central part of the cryostat.

iv) The dimensions of the sample and the distance separating the two sample-leads interfaces should suit the characteristics of the material. Thus, in the case of doped silicon used as a test material, although electrical resistance constituted no problem, it was quite

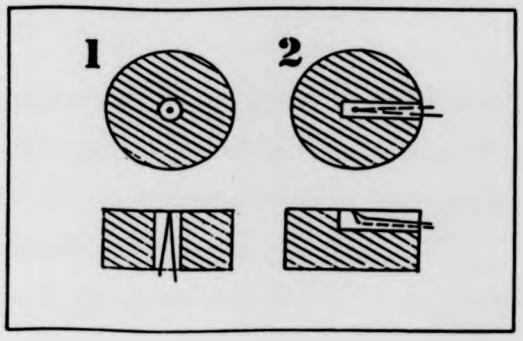

Fig. 3K – The way copper and constantan electrodes were installed in the copper blocks is shown in both top and cross-section views. White areas stand for the mounting glue (Araldite).

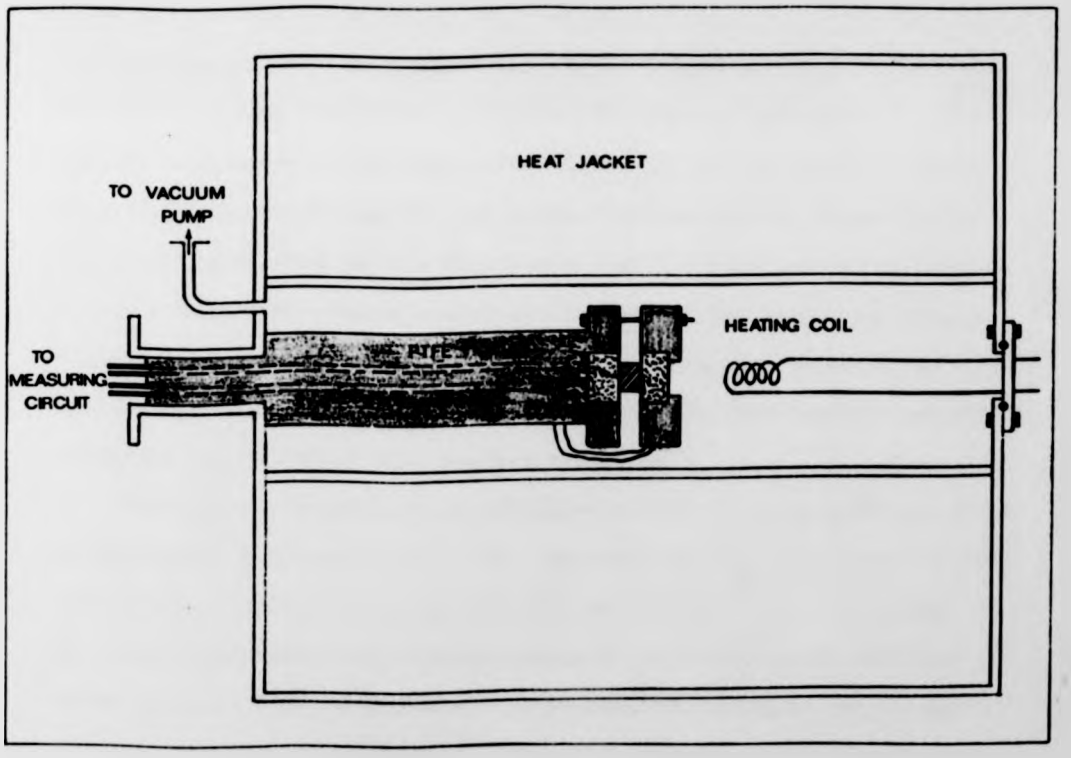

Fig. 3L – Representation of the cryostat and sample holder facilities for thermopower measurements. The two PTFE blocks were held together by three nylon screws.

difficult to establish a thermal gradient due to the high thermal conductivity of the samples. It was necessary to have a separation of $\sim$ 1cm between the two interfaces and a narrow sample cross-section to obtain a measurable temperature difference.

In the case of the glass materials, the very opposite happens. The materials showed quite a poor thermal conductivity and to create a thermal gradient was no problem. The need to reduce the electrical resistance then required the use of a thin specimen, but placed in a sandwich arrangement. The interface separation was approximately 1 mm.

The diagram of the cryostat and sample holder is shown in fig. 3L. The cryostat made from steel was thermally isolated externally by a foil of polystyrene. The temperature gradient was initially provided by a light source shining through a glass window on one of the copper discs. This allowed quite a fine control of the temperature difference. A simple resistance heater placed at one side of the sample was also installed as for one case a photovoltaic behaviour was observed and the light source had to be put aside. Other than that the results obtained using the two different heat sources agreed well.

The ambient temperature was obtained by heat exchange with a jacket placed around the sample cell. This proved to be the weak point of the apparatus. Temperatures going from the softening point of the glass to few degree centigrade were easily acquired by heat exchange with hot water or ice. This allowed both quite small fluctuations in average temperature and a small rate of temperature change and stable readings could be taken. For lower temperatures a jacket of dry-ice was used; however, the rate of temperature variation was too large as was the temperature instability in the sample surroundings. This fact,

together with the high impedances of the samples, made the measurements impossible in this region. The resolution of the problem or, at least, a great improvement could probably be achieved by introducing an arrangement similar to the one used for D.C. conductivity measurements.

3.3.4 The experiment

Prior to actual measurements on glass samples preliminary tests with known n-type and p-type doped silicon specimens were carried out. These were subjected to temperature gradients of both different amplitudes and opposite signals. The tests were then repeated for a glass sample. The objectives were in the first place to make sure that the actual thermopower was being measured and, second, to enable a decision about the most convenient temperature gradient to use. In that respect it was verified that the thermoelectric power response was linear with ΔT at least for $\Delta T < 2^{\circ}K$.

For each sample the following experimental procedure was then carried out. A sample was obtained by simply hand breaking a quenched disc. After the sample was glued in all the outputs were zeroed by use of the offset resistors. The jacket was then filled followed by the vacuum pumping of the cell. Some time was allowed for a temperature equilibrium between the sample and the bath to be attained. A set of values for each, ΔV, T and ΔT was then recorded.

The procedure was next repeated after putting on the resistance heater and allowing a new equilibrium at the same temperature to be established. To minimise the error, each value of the Seebeck coefficient, S, was calculated from the formula

$$S = \frac{\Delta V_{\text{resist. heater on}} - \Delta V_{\text{resist. heater off}}}{\Delta T_{\text{resist. heater on}} - \Delta T_{\text{resist. heater off}}}$$

with the denominator that is the differential temperature being in each case of, approximately, $0.7^{\circ}K$.

That same routine was then followed for various ambient temperatures so that the relation between S and T could be determined. For each sample two sets of readings were taken; one for increasing and the other for decreasing values of the temperature. The results seemed to agree within experimental error.

The curves of S versus $1/T$ are presented in chapter IV. Each point on the graph has an error determined by $\sqrt{\frac{\Sigma (S_i-\bar{S})^2}{n(n-1)}}$ since the number, n, of readings was large. The values for the activation energy (E_S) and the ordinate at the origin (γ) were taken applying the linear regression method for each run. When two different runs were made for the same glass the results presented correspond to the average values and the errorsare absolute errors. Otherwise the errors ΔE_S and $\Delta\gamma$ were determined by the expressions (Topping 1962),

$$\frac{\Delta\gamma^2}{\Sigma S_i^2} = \frac{\Delta E_S^2}{n} = \frac{\Sigma d_i^2}{n-2\ \left[n\Sigma S_i^2 - (\Sigma S_i)^2\right]}$$

where $d_i = E_S \frac{1}{T_i} + \gamma - S_i$

3.4 Photoconductivity measurements

For the purpose of measuring the photoconductivity as a function of the incident photon energy the experimental arrangement shown in fig. 3M was set up. A tungsten lamp was used as the light source. The monochromator consisted of a silica prism and was calibrated against several monochromatic lamps (Hg, Cd-Zn, Na, He, K and Rb) and the He-Ne laser. A calibration curve in the range 300 to 1100 nm could thus be obtained and

with the denominator that is the differential temperature being in each case of, approximately, $0.7^{o}K$.

That same routine was then followed for various ambient temperatures so that the relation between S and T could be determined. For each sample two sets of readings were taken; one for increasing and the other for decreasing values of the temperature. The results seemed to agree within experimental error.

The curves of S versus $1/T$ are presented in chapter IV. Each point on the graph has an error determined by $\sqrt{\frac{\Sigma (S_i-\bar{S})^2}{n(n-1)}}$ since the number, n, of readings was large. The values for the activation energy (E_S) and the ordinate at the origin (γ) were taken applying the linear regression method for each run. When two different runs were made for the same glass the results presented correspond to the average values and the errorsare absolute errors. Otherwise the errors ΔE_S and $\Delta\gamma$ were determined by the expressions (Topping 1962),

$$\frac{\Delta\gamma^2}{\Sigma S_i^2} = \frac{\Delta E_S^2}{n} = \frac{\Sigma d_i^2}{n-2\ \left[n\Sigma S_i^2 - (\Sigma S_i)^2\right]}$$

where $d_i = E_S \frac{1}{T_i} + \gamma - S_i$

3.4 Photoconductivity measurements

For the purpose of measuring the photoconductivity as a function of the incident photon energy the experimental arrangement shown in fig. 3M was set up. A tungsten lamp was used as the light source. The monochromator consisted of a silica prism and was calibrated against several monochromatic lamps (Hg, Cd-Zn, Na, He, K and Rb) and the He-Ne laser. A calibration curve in the range 300 to 1100 nm could thus be obtained and

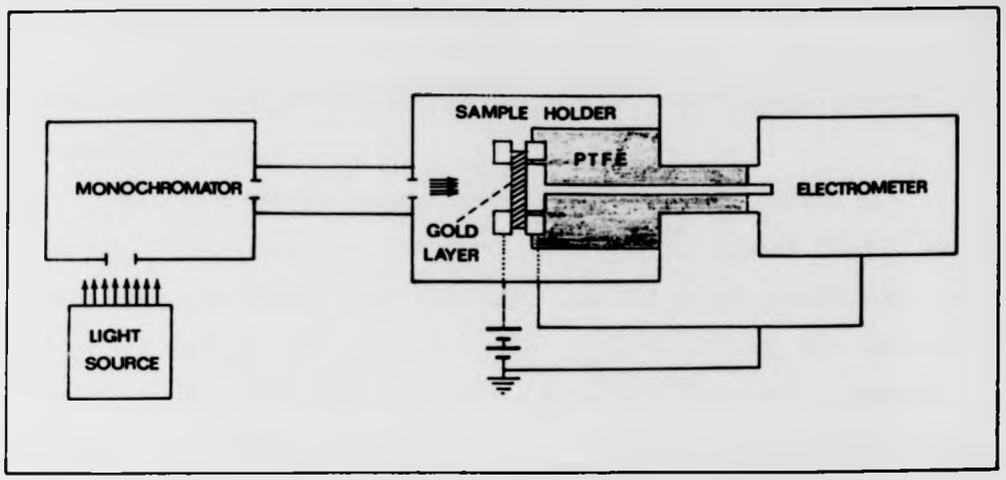

Fig. 3M - Block diagram of the experimental apparatus for photoconductivity measurements.

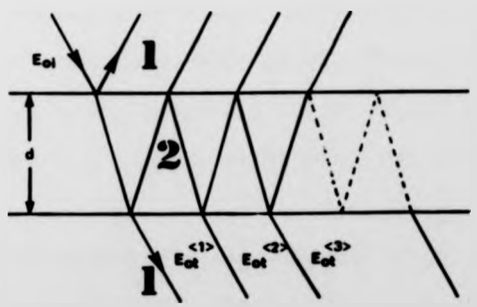

Fig. 3N - Transmitted electric fields E_{ot} corresponding to an incident E_{oi} after crossing a parallel faced sample of thickness d.

was checked using the BPX 25 phototransistor whose typical spectral response is known.

For the electrical part a three electrode configuration as in fig. 3F was chosen in connection with the D.C. circuit of fig. 3G. Once more a straight, thick and very short copper rod provided the lead from the central top electrode to the electrometer head, the electrometer being the one referred to in 3.2.1. The bottom electrode consisted of a copper ring. Good contact with the sample was ensured by positioning of the ring on the outer part of a gold layer sputtered onto the corresponding side of the sample. A gold layer having a longitudinal resistance of $\sim$ 100KΩ proved:-

- To provide a good semi-transparency (the reduction of intensity was less that 10%),
- To allow the setting of a nearly uniform electric field, and
- To form an ohmic contact.

This last point was of particular importance since photoconductivity may depend on the possibility of charge carriers being freed to the sample from the contact electrodes (e.g. Bube 1959). The constancy of the thin gold film transparency in the range 0.6 - 1.1 μm was verified by comparing the transmission spectra of a glass slide with and without a sputtered gold coating.

Photoconductivity curves were taken in the range 1.2 to 3.2 eV. The photoconductivity intensities were firstly corrected for the spectral distribution of black body radiation being normalized to the wavelength $\lambda^* = 850$nm. This resulted in a correction factor (c.f.) given by

$$\text{c.f.} = \frac{H(\lambda^*, T)}{H(\lambda, T)}$$

where T and H(λ,T) are respectively the absolute temperature and the radiant emittance of a black body. Assuming the Wien approximation ($\lambda T < 0.21$ cm. degree) the factor can be written as (Rutgers 1958)

$$c.f. = \frac{\exp(-c_2 / \lambda^* T)}{\exp(-c_2 / \lambda T)} \left(\frac{\lambda}{\lambda^*}\right)^5$$

c_2 being a constant with the value 1.438 cm.degree. Because the actual radiant intensity, $I(\lambda, T)$ emitted by a non-black body thermal radiator differs from $H(\lambda,T)$ by a factor $\alpha(\lambda,T)$, called the emissivity, that is,

$$I(\lambda,T) = \alpha(\lambda,T) \cdot H(\lambda,T) ,$$

the correction factor was modified accordingly (De Vos 1954, Larabee 1959).

Finally, to present the photoconductivity response in the form of normalized intensity per photon incident, a further correction was added. As the number of photons that reach the sample per second is $N = \frac{\Delta p}{hc}\lambda$ where Δp is the incident power, the correction factor was finally determined as

$$c.f. = \exp\left[-\frac{c_2}{T} \cdot \left(\frac{1}{\lambda} - \frac{1}{\lambda^*}\right)\right] \left(\frac{\lambda}{\lambda^*}\right)^4 \cdot \frac{\alpha(\lambda^*,T)}{\alpha(\lambda,T)}$$

Using the I_{CE} vs. V_{CE} characteristic curve of the BPX 25 phototransistor it was possible to make an estimation of the incident illumination and so of Δp. This allowed calculation of absolute values of the photocurrent intensity per incident photon times electron charge, $\frac{I_{ph}(\lambda)}{eN}$. Nevertheless due to the difficulty involved in this estimation, absolute values should be critically regarded.

The results, in the form of $\frac{I_{ph}(\lambda)}{eN}$ vs. photon energy curves, are presented in chapter IV. The curves correspond to an average of values obtained with increasing and decreasing wavelengths.

3.5 Optical absorption experiments

3.5.1 General features

Optical absorption measurements were carried out with two aims. In the first place infrared transmission curves were taken in the wavelength range of 2 to 55.5 μm (wave number range of 5000 to 180 cm^{-1}). These curves, as stated before, can provide useful structural information about the glasses. A Perkin Elmer Spectrometer (PE 983) was the instrument employed to measure the specimens which consisted of slabs, 1mm thick, with parallel mirror polished surfaces, formed directly from the quenching process.

A second set of optical experiments was performed to obtain transmission spectra in the visible and near infrared regions (wavelength range of 0.5 to 2 μm). These measurements allowed the determination of the absorption coefficient vs.photon energy curves at the optical absorption edge. From such curves an estimation of the optical gap (and therefore of the mobility gap) is possible.

The instrument employed to obtain the transmission data was, in this second case, a Grubb Parsons Spectromaster Spectrophotometer. Once more samples with parallel mirror polished surfaces were used. The discs measured had thickness of 0.3 and 1.0 mm, allowing the determination of the optical absorption coefficients up to only 10^2 cm^{-1}. For higher values of the absorption coefficient, thinner samples were required and a significant improvement would have meant, at least, an order of magnitude thinner. However, due to the mechanical weakness of the glasses, no mechanical thinning accompanied by a good polishing finish was possible to that extent and the experiment could not be improved.

3.5 Optical absorption experiments

3.5.1 General features

Optical absorption measurements were carried out with two aims. In the first place infrared transmission curves were taken in the wavelength range of 2 to 55.5 μm (wave number range of 5000 to 180 cm^{-1}). These curves, as stated before, can provide useful structural information about the glasses. A Perkin Elmer Spectrometer (RE 983) was the instrument employed to measure the specimens which consisted of slabs, 1mm thick, with parallel mirror polished surfaces, formed directly from the quenching process.

A second set of optical experiments was performed to obtain transmission spectra in the visible and near infrared regions (wavelength range of 0.5 to 2 μm). These measurements allowed the determination of the absorption coefficient vs.photon energy curves at the optical absorption edge. From such curves an estimation of the optical gap (and therefore of the mobility gap) is possible.

The instrument employed to obtain the transmission data was, in this second case, a Grubb Parsons Spectromaster Spectrophotometer. Once more samples with parallel mirror polished surfaces were used. The discs measured had thickness of 0.3 and 1.0 mm, allowing the determination of the optical absorption coefficients up to only 10^2 cm^{-1}. For higher values of the absorption coefficient, thinner samples were required and a significant improvement would have meant, at least, an order of magnitude thinner. However, due to the mechanical weakness of the glasses, no mechanical thinning accompanied by a good polishing finish was possible to that extent and the experiment could not be improved.

3.5.2 Method for the computation of the absorption coefficients

According to Maxwell's curl equations, a linearly polarized wave travelling in the x direction is, in a conducting medium, governed by the following wave equation:

$$\frac{\partial^2 \mathbf{A}}{\partial x^2} - \mu\varepsilon \cdot \frac{\partial^2 \mathbf{A}}{\partial t^2} - \sigma\mu \cdot \frac{\partial \mathbf{A}}{\partial t} = 0 \qquad (3.1)$$

A represents either the electric or the magnetic field vector of a plane electromagnetic wave; μ, ε and σ are, respectively, the permeability, the permitivity and the conductivity of the medium considered.

Equation (3.4.1) yields solutions of the type

$$\mathbf{A} = \mathbf{A}_0 \cdot e^{i\left[\omega\left(t - \frac{n^* x}{c}\right) + \delta\right]} \qquad (3.2)$$

where ω is the angular frequency, c the velocity of light in vacuum, δ is a phase factor and n^* is the complex refractive index. If n^* is written in the form

$$n^* = n - im \qquad (3.3)$$

equations (3.1) and (3.2) give

$$n^2 - m^2 = \frac{\mu\varepsilon}{\varepsilon_0\mu_0}, \quad 2nm = \frac{\sigma\mu}{\omega\varepsilon_0\mu_0}$$

that is

$$n^2 = \frac{1}{2}\left[\sqrt{\frac{\varepsilon^2\mu^2}{\varepsilon_0^2\mu_0^2} + \frac{\sigma^2\mu^2}{\omega^2\varepsilon_0^2\mu_0^2}} + \frac{\mu\varepsilon}{\mu_0\varepsilon_0}\right] \quad m^2 = \frac{1}{2}\left[\sqrt{\frac{\mu^2\varepsilon^2}{\varepsilon_0^2\mu_0^2} + \frac{\sigma^2\mu^2}{\mu_0^2\omega^2\varepsilon_0^2}} - \frac{\mu\varepsilon}{\mu_0\varepsilon_0}\right]$$

(3.4)

ε_0 being the vacuum permitivity.

If (3.3) is introduced in (3.2) it is clear that the wave is attenuated by the factor $\exp(-m\frac{\omega x}{c})$. At the same time the energy flow

is determined by the Poynting vector of average scalar magnitude,

$$S_{av} = \frac{1}{2} E_o H_o \cos \Delta$$

where Δ is the phase difference between the electric and magnetic fields. The average power per unit area is then proportional to both, the electric, E_o, and magnetic, H_o, field amplitudes which means that the attenuation in intensity is determined by the term $\exp(-2m \frac{mx}{c})$.

Defining the absorption coefficient, α, by the condition that the intensity falls off by $\frac{1}{e}$ after the wave travels the distance of $\frac{1}{\alpha}$ cm, then,

$$\alpha = \frac{2m\omega}{c} \qquad (3.5)$$

The absorption coefficient may be related to the accessible experimental data, that is, the transmitted and reflected fractions. This can be done by considering fig. 3N where transmission across a slab of a material (medium 2) placed in air (medium 1) is represented, by the multiple reflection contribution. Assuming that the various transmitted fields do not have phase coherence, the total transmitted intensity, I_t, is given by the sum of the intensities of the individual components. As medium 1 is air, the average power per unit of area is therefore $\propto \frac{E_o^2}{2}$ and for normal incidence it is possible to write,

$$I_t = \frac{(E_{oi})^2}{2} (t_{12}t_{21})^2 e^{-\alpha d} [1 + (r_{12}r_{21})^2 e^{-2\alpha d} + \ldots + (r_{12}r_{21})^{2n} e^{-(2n)\alpha d} + \ldots]$$

where the coefficients t_{12}, t_{21}, and r_{12}, r_{21} are the ratios respectively between transmitted and incident, and between reflected and incident, amplitudes of the electric field at the corresponding interface. Since σ is small the dielectric approximation is suitable and gives, for the case of normal incidence,

$$t_{12} = \frac{2}{n+1} \quad , \quad t_{21} = \frac{2n}{n+1} \quad , \quad r_{12} = -r_{21}$$

The fraction of transmitted intensity is then,

$$\frac{I_t}{I_i} = \left[\frac{4n}{(n+1)^2}\right]^2 e^{-\alpha d} \Big/ \left[1 - (r_{21})^4 e^{-2\alpha d}\right] \qquad (3.6)$$

The transmission, T, and reflection, R, coefficients for intensity at the interface between the material and the atmosphere are

$$T = \frac{1}{n} t_{21}^2 = \frac{4n}{n+1} \qquad R = r_{21}^2 = \frac{n-1}{n+1}^2$$

since the medium is non-magnetic. This allows equation(3.6) to be rewritten in the form

$$\frac{I_t}{I_i} = \frac{T^2 e^{\alpha d}}{e^{2\alpha d} - R^2} = \frac{(1-R)^2 e^{\alpha d}}{e^{2\alpha d} - R^2} \qquad (3.7)$$

For values of α small enough to make the sample actually transparent, eq. (3.7) reduces to

$$\frac{I_t}{I_i} = \frac{1-R}{1+R} \qquad \text{and so}$$

$$\frac{I_r}{I_i} = \frac{2R}{1+R} \qquad (3.8)$$

Equation (3.7) provides an implicit relationship between the absorption coefficient and the transmitted data allowing, as long as R is determined, the calculation of the α values.

The determination of R, however, was a problem since it was not possible to measure the sample reflectivity at normal incidence and so to obtain this coefficient directly. Hence it was necessary to estimate R from the transmission output as well. This was done along the following

lines: In a wavelength region where the absorption is negligible, that is where $\alpha < 1$, the losses are practically only a consequence of reflection. This region is situated below the absorption edge and extended for most of the glasses up to 5 μ m. The transmission traces of two specimens with different thicknesses (1 and 0.3mm) in that range were effectively very similar and constant throughout the whole range (2 to 5μm) as shown in fig. 30. This proved the constancy of the coefficient R in the long wavelength part of the spectra and made it possible to compute its value there. An average value of R = 0.215 was found corresponding to an average transmittance of 64.5%, values that are close to others reported elsewhere (Hagen and Derks 1984; Vasko 1969).

It was then assumed that the R value encountered remained constant also in the absorption edge range. To justify the validity of this assumption an independent estimation of the scalar magnitude of the absorption coefficients was made. The transmittances of two specimens with different thicknesses d_1, d_2 was measured and using the formula

$$\text{Relative transmittance} = \frac{e^{-\alpha d_1}}{e^{-\alpha d_2}}$$

α was determined. This expression does not take into account the multiple reflections, and so it is only a reasonable approximation if the values of α are high, but gives nevertheless an idea of the order of magnitude of α. The values obtained were less than 100cm^{-1} and similar to the ones expected (Hartke and Regensburger 1965). The error in not considering the value of m in the correct expression for R (as for a medium with $\sigma \neq 0$) is then negligible. In fact, considering the general expression for R (Born and Wolf 1959)

$$R = \frac{(n-1)^2 + m^2}{(n+1)^2 + m^2}$$

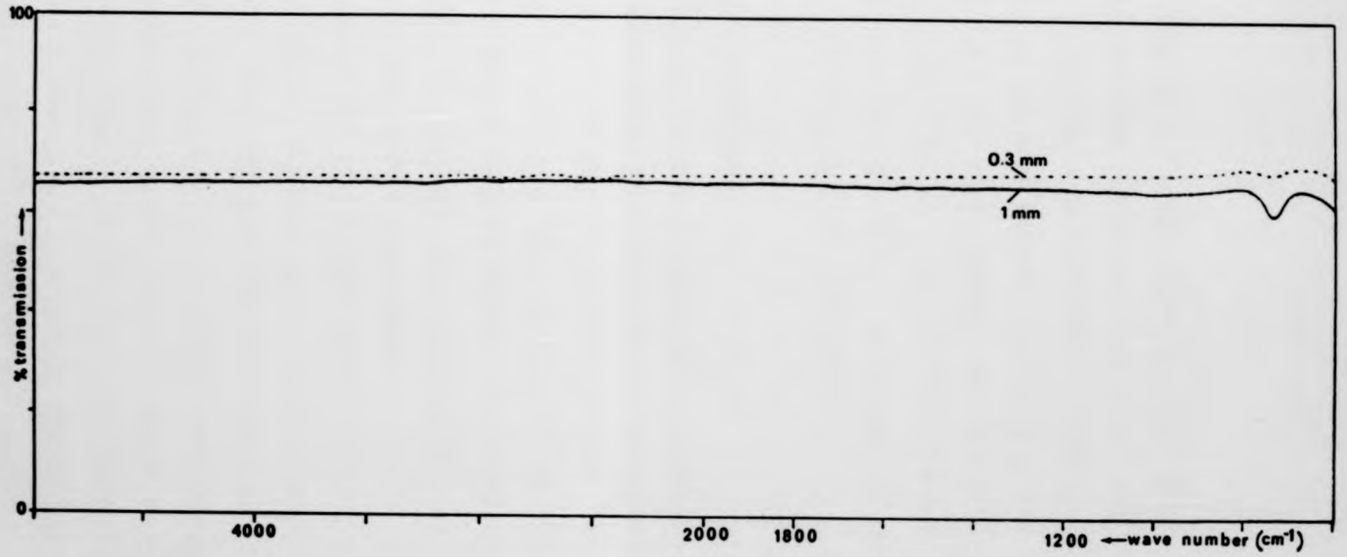

Fig. 3 0 - IR traces of samples with different thicknesses proving the constancy of R over the range 2-5 μm.

where the value of n is taken from the long wavelength region ($n_{average}$ $\sim$ 2,7) and comparing with (3.4) and (3.5) it is easily seen that the error in omitting m is very small (< 1%) up to values of $\alpha \sim 10^4 cm^{-1}$.

In the experimental procedure and to minimize errors a value of R was computed for each glass system. Once the value of R was calculated, α values in the range 0.7 to 1.5 μm were determined employing numerical tables constructed from (3.7). The results are presented in chapter IV in the form of log α vs. photon energy curves.

3.6 Other experiments

3.6.1 Differential Scanning Calorimetry (D.S.C.)

Differential Scanning Calorimetry is a comparative technique in which the rate of heat absorbed by a sample relative to a standard is measured directly as a function of either temperature or time. D.S.C. is thus, like Differential Thermal Analysis (D.T.A.) a structure-sensitive technique but has advantages in precision and reproducibility as a consequence of a more accurate temperature measurement.

D.S.C. experiments were carried out as a function of temperature allowing information about glass transition, crystallization and melting properties of the glass, to be obtained. The D.S.C. curves were taken over the temperature range 285°K-480°K using a SETARAM Calorimeter.

The samples studied were solid ($\sim$ 100 mg in weight) being measured against a similar amount of alumina powder employed as the standard. Both materials were placed in identical platinum crucibles and a constant scanning rate of $90°h^{-1}$ was used for all samples.

The upper temperature limit was set as a protection for the experimental apparatus due to the great volability of the specimens. This limited the investigations on the melting properties.

3.6.2 Scanning Electron Microscopy and Energy Dispersive Analysis of X-Rays (E.D.A.X.)

Scanning Electron Microscopy (S.E.M) in the back scattered mode was performed over a number of glasses to determine the eventual existence of inhomogeneities. The microscope resolution in the working conditions was estimated as being between 500 and 1000Å.

As referred to in paragraph 3.1.5 Energy Dispersive Analysis of X-Rays was carried out as a way of checking the presence of the added impurities in the glasses. The method is based upon the idea that a thin section of a sample containing two elements, A and B, with concentrations N_A and N_B should show X-Ray intensities I_A and I_B whose ratio is given by

$$\frac{I_A}{I_B} = \frac{1}{K_{AB}} \frac{N_A}{N_B}$$

where K_{AB} is a correction factor related to fluorescence emission, detector efficiency and ionization cross-section. K_{AB} is then dependent on the atomic numbers Z_A and Z_B of the elements present. Full E.D.A.X. of bulk samples requires as well a correction for absorption (A) and secondary fluorescence (F).

The analysis were performed using an E.D.A.X. detector coupled with a S.E.M. An accelerating voltage of 20 KeV was used as a higher voltage would damage the samples. Comparison of K line intensities was made except for the elements I and Te in which case, for obvious reasons, L lines had to be considered. An interfaced microcomputer permitted the visualization and complete (ZAF) correction of the spectra so that the relative elemental percentages could be directly computed.

Each sample was analysed in several different areas and an average value was taken. With the accelerating voltage referred and the take-off

angle of 39° chosen an relative accuracy of ± 5% is expected.

In both, S.EM. and E.D.A.X. experiments, the samples had flat and polished surfaces. Carbon coating was provided to present surface charging.

3.6.3 X-Ray diffractometry (X.R.D.)

X-Ray diffractometry is a well established experimental method and will therefore not be discussed in detail. It was used mainly as a test to verify the amorphous nature of the samples. X-Ray diffraction in a crystal exhibits maxima at scattering angles 2Θ, for which the Bragg condition,

$$n\lambda = 2d \sin\Theta$$

where λ is the wavelength of the incoming X-Rays, d is the spacing of crystal planes and n is an integer, is obeyed. In amorphous materials the Bragg condition is obviously not fulfilled and no sharp peaks occur. Instead characteristic broad maxima are observed.

It is possible (Klug and Alexander 1974) to establish a relationship which gives an estimate of the size of the crystals present. The crystallite size, D, equation may be written in terms of the full angular diffraction line width at half maximum intensities, $\beta_{1/2}$, as

$$D = \frac{0.89\lambda}{\beta_{1/2}\cos\Theta}$$

This equation sets a theoretical limit for the resolution of fine crystallites.

The experiments took place in a standard Philips diffractometer using Cu K_α radiation. The X-Ray generator operated at 40kV and 30mA. In order to achieve the best resolution possible the slowest scanning speed available (1/8° 2Θ/min) was employed. The samples in form of discs were mounted in aluminium holders and made level with them. X-Ray diffraction

traces could be obtained directly in an interfaced PET computer. The Debye-Scherrer method using finely powdered samples was initially and occasionally used as well. Samples partially devitrified were identified by the Hanawalt method.

3.6.4 Electron spin resonance (E.S.R.)

E.S.R. also known as electron paramagnetic resonance (E.P.R) is a dynamical magnetic phenomenon associated with the total angular momentum of electrons. When a magnetic field is applied on a paramagnetic centre there is a splitting of its magnetic ground state. The transitions between the resulting states occur in an energy range such that resonant absorption can be obtained by coupling to microwave electromagnetic radiation.

The energy, E, of a magnetic dipole moment, M, in the presence of a magnetic field, H, is in classical terms given by

$$E = -\vec{M}.\ \vec{H}$$

In quantum mechanics M can be written in terms of the operator representing the total angular moment, J, that is

$$M = - g\ J\beta$$

where g is the Landé factor with a value for pure spin states (zero orbital contribution) of approximately 2 ($g = 2.0023$) and β is the Bohr magneton ($\beta = \frac{e\hbar}{2m}$). The energy of the interaction between the field and the magnetic dipole moment, assuming no interaction with surrounding dipoles, is then determined by the hamiltonean

$$\mathcal{H} = -g\ \beta H J_Z,$$

H and J_Z being the operators representing respectively the magnetic field and the J component along the field axis. The eigen-values of the

energy are given by the expression

$$E = g \beta H m$$

and m is the magnetic quantum number (m = -J, -J+1, ... J+1, J). Resonance absorption takes place when Δ m = 1, that is for frequencies

$$\upsilon = \frac{g \beta H}{h}$$

In more general terms absorption depends, not only on the ground state, but also on the paramagnetic centre environment.

E.S.R. experiments can be of considerable value in chalcogenide glasses which are materials free of paramagnetic ions and where the contribution from conduction electrons to E.S.R. is very small. The observation of E.S.R. signals in those materials is therefore dependent on the presence of coordination defects of a paramagnetic nature. In the scope of this thesis the main aim of the ESR. experiments performed was simply to establish the presence of unimpaired spins in the glasses due to impurity induced defects.

The experiments were carried out in the E-109 Varian Spectrometer at Oporto, Portugal. A fixed frequency of 8.895 GHz was used and the spectra were produced by variation of the magnetic field. In these conditions, if a value of g=2 is assumed, absorption should take place at $3.18\ 10^3$ Gauss. The results are shown in chapter IV. Unfortunately, no absolute values for the number of spins present could be determined.

CHAPTER IV - EXPERIMENTAL RESULTS

4.1 Pure and oxygen doped selenium glasses

4.1.1 D.C. conductivity experiments

A large number of pure selenium samples were measured in total, since each time a new additive was introduced it was necessary to check the melting conditions in the globe-box. Some variation in the value of conductivity was obtained. As a result an average value of $\sigma_{RT} = 3.4\ 10^{-15}$ $ohm^{-1}.cm^{-1}$ was determined but, although most of the samples presented conductivities below 10^{-15} $ohm^{-1}.cm^{-1}$, some values as high as $\sim 10^{-14}$ $ohm^{-1}.cm^{-1}$ were also measured.

The average value is comparable to others reported elsewhere (Hulls 1970; McMillan and Shutov 1977; Mehra et al. 1977, 1978) and is higher than those obtained (Lacourse et al. 1970) on samples prepared by a special deoxygenation method (Kosyrev 1959). The variation of conductivity could be due to some impurity dust existing inside the glove-box, as a consequence of previous melts, or to residual oxygen being trapped during the pressing process. Some of the variation in σ may instead be attributed to variations in the pouring process resulting in different cooling times and quenching temperatures from sample to sample. This difference in fictive temperatures between samples can result in varying proportions of chains and rings and so lead to different values of the conductivity. There is, in fact, evidence of the importance of the preparation conditions (Grochowski and Brenner 1971) which seems corroborated by the D.S.C. thermograms obtained (see fig. 4F). At the same time the former authors found values more than one order of magnitude apart, despite using the same method (pre-evacuated silica ampoule) and selenium of similar quality, and so having, apparently, the same purity

conditions. Thus, even though there is a well established relationship between the oxygen content and the conductivity (Lacourse et al.1970), and the oxygen factor is in itself sufficient to explain all the differences observed, it may not be the only variable involved. A clarification of the problem will indeed need a precise determination of the oxygen contamination.

The plots of log σ versus $1/T$, as far as the small temperature range allows, show a linear fit for all samples indicating either a single activation energy, E_σ or a constant dependence of the activation energy on temperature. The values obtained for E_σ and for the pre-exponential factor C were respectively $E_\sigma = (0,88 \pm 0,06)$eV and C = 12 $ohm^{-1}.cm^{-1}$ with C values spreading over two orders of magnitude. This large error is attributed mostly to the very narrow range of temperatures over which the curves were obtained.

The value for the activation energy is similar to others quoted in the literature for bulk vitreous selenium (Lakatos and Abkowitz 1971; Mehra et al. 1977, 1978; McMillan and Shutov 1977). Juska et al.(1969) however observed a higher value (1.1 eV). The value of E_σ is also close to the difference $E_F - E_V = \frac{1}{2} E_g - \epsilon$ where E_g is the optical gap as determined from optical absorption data (see 4.1.2) and ϵ is the shift of the Fermi level towards the valence band as a result of the defect states. At the same time most of the values of C obtained fell somewhere between what one would expect for transport occurring just below the mobility edge, E_V, due to carriers excited into the extended states ($> 100 \Omega^{-1}.cm^{-1}$) and the values anticipated assuming that conduction takes place via thermally activated hopping in the localized states ($< 10 \Omega^{-1}.cm^{-1}$). Both facts taken together (it is supposed that glassy Se has p-type behaviour as liquid Se) suggest that electrical transport probably occurs via extended

states with the carriers being trapped and released during transit by localized states above E_V, their mobility being therefore reduced.

In fact, supposing that conduction occurs by hopping the activation energy for conductivity should be compatible with the relation

$$E_\sigma = \tfrac{1}{2} B - \varepsilon - \text{Width of the localized states} + W \quad (4.1)$$

Assuming that W, the activation energy for hopping, is of the order of kT (~ 0.025 eV) a value for the width of the localized band of 0.03 eV is obtained. Such a value is too small a value for the width of the localized states which would be expected to fall between ~ 0.15 eV (width of the disorder induced tail) and 0.28 eV, the measured activation energy for hole drift mobility- Marshall and Owen 1972-(which may represent a band of localized gap states at that energy above the valence mobility edge). Nevertheless, given the uncertainties affecting the parameters involved in the above calculation the possibility of hopping conduction cannot be excluded.

The D.C. conductivity of samples of oxygen doped selenium were also measured. As stated in chapter III this had the main aim of testing the experimental set-up since, as already mentioned, the effect of oxygen has been quantitatively determined. The samples were made by adding selenium dioxide to selenium pellets in order to form the alloy $Se_{96}O_4$ but as also discussed in chapter III there were indications that the actual impurity content was much smaller.

The room temperature conductivity measured was $\sigma_{RT} = 2.6.10^{-11}$ $ohm^{-1}.cm^{-1}$ which agrees very well with the "saturation" value determined by Lacourse et al. but is much higher than that indicated by McMillan and Shutov. The actual oxygen concentration in the latter sample might however be very small as no definite IR oxygen bands were observed. The pre-exponential coefficient was determined as $C = 6.5$ $ohm^{-1}.cm^{-1}$ which is

close to the value observed in pure selenium suggesting that the mechanism of conduction is the same. The increase in conductivity can be explained by the verified decrease in activation energy from 0.38 eV to 0.66 eV. This value is in agreement, within experimental error, with the value determined by Twaddell et al. and is slightly higher than the value predicted according to Mott (1976). Mott and in addition Popov (1978), supposed that the oxygen atoms will form O^- centres by adsorption at D^- chain ends with a high probability and discusses the activation energy change in terms of both the principle of "detailed balancing" and Boltzmann statistics. Since selenium is supposedly p-type and oxygen doped Se was also determined as showing p-type thermopower signal (see 4.1.3) the expected activation energy according to Mott's calculation would then be,

$$E_\sigma = \frac{2}{3}\left(\frac{1}{2} E_g - \epsilon\right) = 0.59 \text{ eV}$$

which is in reasonable agreement with the experimental value.

The D.C. conductivity results for pure and oxygen containing selenium are summarised in table A and illustrated in fig. 4A.

4.1.2 Infrared data

Infrared measurements were taken in the range of 20.000 to 180cm^{-1}. The transmission curves of all pure selenium samples show a flat part of, on average, 65% from 5000 cm^{-1} to 600 cm^{-1}. Bands appear at 740, 488 and 248 cm^{-1}, the latter being most probably a double band at 255 and 233 cm^{-1} as better shown by the I.R. spectrum of a 0.3mm thick sample (fig. 4B). A shoulder is present at $\sim$360cm^{-1}. The results are similar to those described elsewhere (see for example Vasko 1969). According to Lucovsky et al. (1967), who compared the glassy response with the spectra of the crystalline forms of trigonal (Se long chains) and α - monoclinic

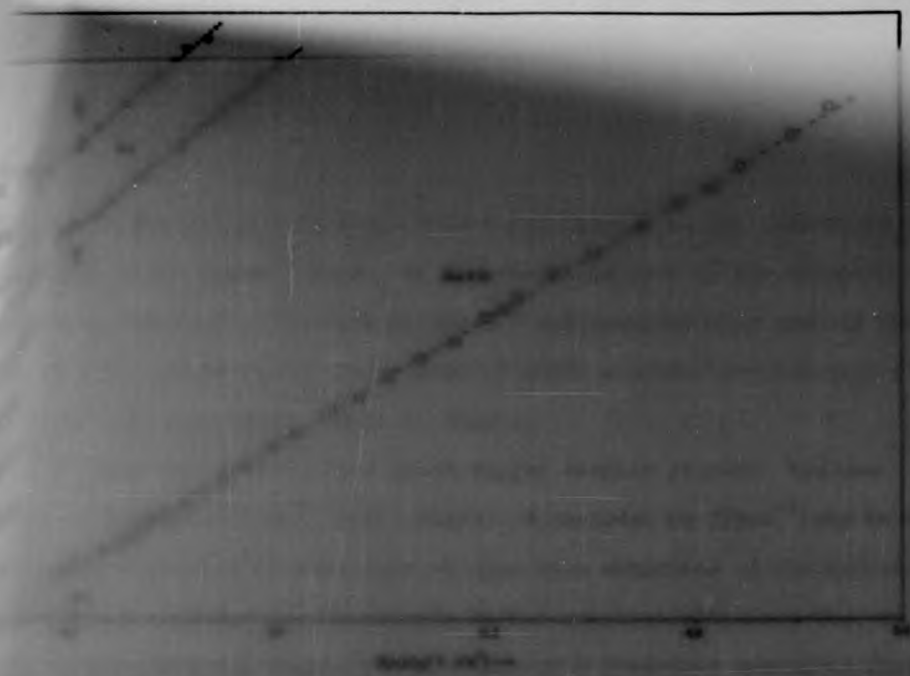

Fig. 14 - Temperature dependence of the resistivity, ρ, of Se and copper containing Se glasses. Lower Se sample shows average slope while upper curve represents the highest resistivity glass for which activation energy was determined. The arrows illustrate the range of resistivities observed for "pure" vitreous Se.

close to the value observed in pure selenium suggesting that the mechanism of conduction is the same. The increase in conductivity can be explained by the verified decrease in activation energy from 0.88 eV to 0.66 eV. This value is in agreement, within experimental error, with the value determined by Twaddell et al. and is slightly higher than the value predicted according to Mott (1976). Mott and in addition Popov (1978), supposed that the oxygen atoms will form O^- centres by adsorption at D^- chain ends with a high probability and discusses the activation energy change in terms of both the principle of "detailed balancing" and Boltzmann statistics. Since selenium is supposedly p-type and oxygen doped Se was also determined as showing p-type thermopower signal (see 4.1.3) the expected activation energy according to Mott's calculation would then be,

$$E_\sigma = \frac{2}{3}\left(\frac{1}{2} E_g - \epsilon\right) = 0.59 \text{ eV}$$

which is in reasonable agreement with the experimental value.

The D.C. conductivity results for pure and oxygen containing selenium are summarised in table A and illustrated in fig. 4A.

4.1.2 Infrared data

Infrared measurements were taken in the range of 20.000 to 180cm^{-1}. The transmission curves of all pure selenium samples show a flat part of, on average, 65% from 5000 cm^{-1} to 600 cm^{-1}. Bands appear at 740, 488 and 248 cm^{-1}, the latter being most probably a double band at 255 and 233 cm^{-1} as better shown by the I.R. spectrum of a 0.3mm thick sample (fig. 4B). A shoulder is present at $\sim$ 360cm^{-1}. The results are similar to those described elsewhere (see for example Vasko 1969). According to Lucovsky et al. (1967), who compared the glassy response with the spectra of the crystalline forms of trigonal (Se long chains) and α - monoclinic

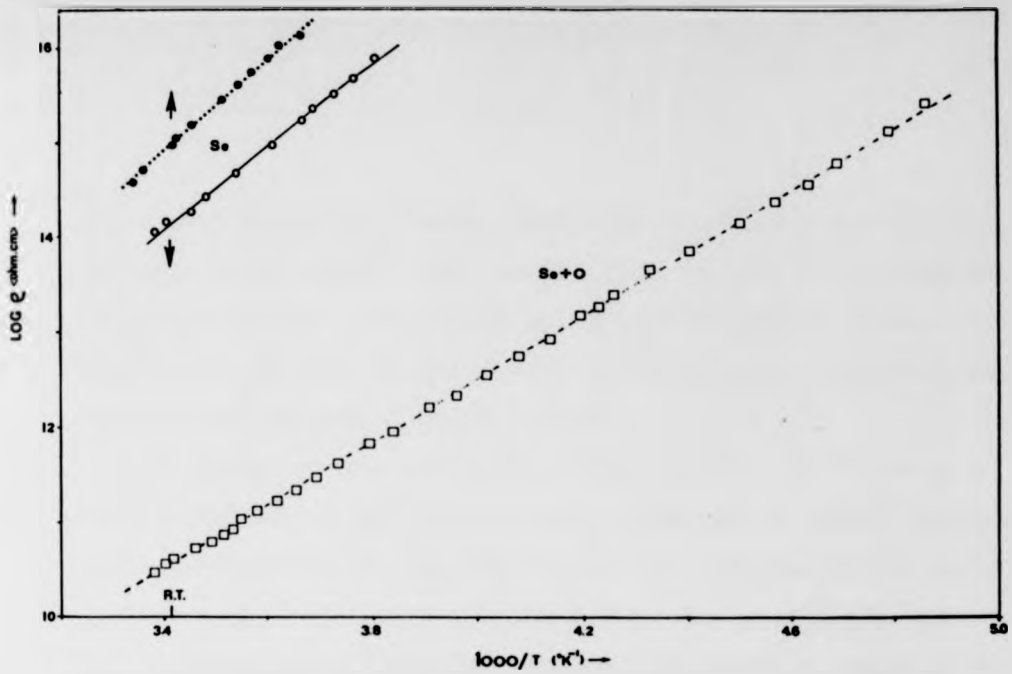

Fig. 4A - Temperature dependance of the resistivity, ρ, of Se and oxygen containing Se glasses. Lower Se sample shows average slope while upper curve represents the highest resistivity glass for which activation energy was determined. The arrows illustrate the range of resistivities observed for "pure" vitreous Se.

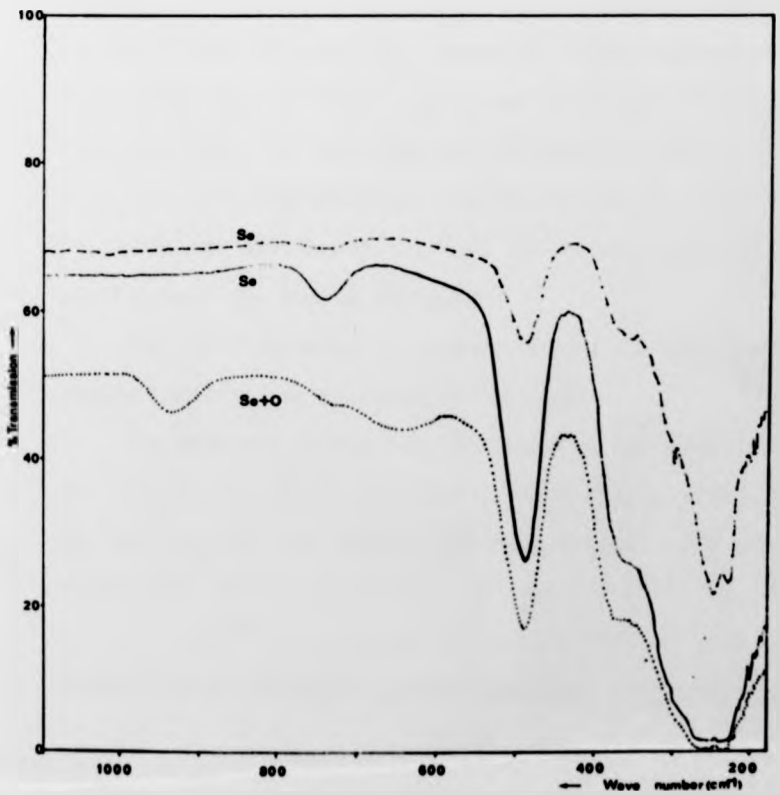

Fig. 4B - Infrared spectra of "pure" and oxygen doped vitreous selenium. The upper curve was obtained with a 0.3mm thick sample while the others refer to thicknesses of 1mm.

(Se eight-fold rings) selenium, these bands may all be due - with the exception of the 233cm^{-1} band - to the ring like part of the selenium amorphous structure. The band at 233cm^{-1} was assigned to a mode of the long chains. However, in the context of later studies (see Lucovsky 1979) definite band assignment cannot be made .

The spectra of the 4 at % added oxygen samples present two new bands at 935 and 648 cm^{-1} (very broad). A shoulder at 735cm^{-1} may be due to the corresponding Se band only or also to a vibration of the O-Se-O unit (Tausend 1969). As the spectra differ substantially from that of SeO_2 in bulk they may denote the presence of a dissolved monomeric form of SeO_2 as suggested by Burley (1968). However, the bands observed by this author were slightly shifted towards lower frequencies. A similar spectrum has been interpreted by MacKenzie (1970) as due to a SeO_2 terminated selenium chain and on this he based an explanation of the increase in electrical conductivity. However, since vibrations of both, Se-O and Se=O groups are reported to be near 11 microns (Tausend 1969) the absorption at 935cm^{-1} may also be related to an oxygen terminated chain, as considered in 4.1.1. The difference in frequencies is probably a result of the different structural coupling of the oxygen-selenium entity in crystalline SeO_2 and in the glass.

The I.R. transmission curves of pure selenium and selenium containing oxygen impurity are compared in fig. 4B.

The analysis of the I.R. response in the region 0.5 to 2 μm allowed the computation of the absorption coefficient, α, as a function of the photon energy at the optical absorption edge. The curves all showed exponential behaviour (Urbach edge type) for E > 1.4 eV presenting a tail of $\alpha < 1.5\text{cm}^{-1}$ for energies below that value. This is similar to the general shape exhibited by most amorphous semiconductors.

The value of E_t, the slope of the exponential absorption region (see eq. 2.17) was determined as being $(10.6 \pm 2.3)eV^{-1}$. This is at the low end of the range of values observed in semiconducting glasses (Connell 1979) and smaller than that indicated by other authors (Vasko 1969, Hartke and Regensburger 1965). According to Vasko (1969) defects may be responsible for the observed discrepancy.

To obtain the optical gap from optical absorption data Stuke suggested the intercept at $\alpha = 10^4 cm^{-1}$ which Owen and Robertson (1970) arguably consider a good criterion. Since, in the curves obtained, the slopes were comparatively low and the highest α values measured $\sim 50cm^{-1}$ it was considered preferable to extrapolate the optical gap as the energy for which α was $10^3 cm^{-1}$. Thus the value determined was $E_g = (2.03 \pm 0.08)eV$. This estimation is similar to the energy value at 10^4 cm^{-1} as reported by other authors (e.g. Hartke and Regensburger 1965).

A plot of the absorption coefficient as a function of the photon energy is presented in fig. 4C. The LR data referred to above are contained in table A.

4.1.3 Photoconductivity measurements

The room temperature D.C. photoconduction response of glassy selenium is shown in fig. 4D. The photo response per absorbed photon shows a peak at an energy of $E_{Ph} = (1.65 \pm 0.03)eV$. That is smaller than the expected for inter-band transition corresponding to the optical gap and is comparable to the value determined by McMillan and Shutov (1977).

It is generally believed that the D^- centres act as traps for the holes produced by light absorption. The D^+ centres will constitute traps for the electrons. The trapped carriers are afterwards released thermally to the respective band, thus giving rise to photoconductivity. At the same time photoconduction due to direct optical excitation from those

The value of E_t, the slope of the exponential absorption region (see eq. 2.17) was determined as being $(10.6 \pm 2.3)eV^{-1}$. This is at the low end of the range of values observed in semiconducting glasses (Connell 1979) and smaller than that indicated by other authors (Vasko 1969, Hartke and Regensburger 1965). According to Vasko (1969) defects may be responsible for the observed discrepancy.

To obtain the optical gap from optical absorption data Stuke suggested the intercept at $\alpha = 10^4 cm^{-1}$ which Owen and Robertson (1970) arguably consider a good criterion. Since, in the curves obtained, the slopes were comparatively low and the highest α values measured $\sim 50cm^{-1}$ it was considered preferable to extrapolate the optical gap as the energy for which α was $10^3 cm^{-1}$. Thus the value determined was $E_g = (2.03 \pm 0.08)eV$. This estimation is similar to the energy value at 10^4 cm^{-1} as reported by other authors (e.g. Hartke and Regensburger 1965).

A plot of the absorption coefficient as a function of the photon energy is presented in fig. 4C. The LH data referred to above are contained in table A.

4.1.3 Photoconductivity measurements

The room temperature D.C. photoconduction response of glassy selenium is shown in fig. 4D. The photo response per absorbed photon shows a peak at an energy of $E_{Ph} = (1.65 \pm 0.03)eV$. That is smaller than the expected for inter-band transition corresponding to the optical gap and is comparable to the value determined by McMillan and Shutov (1977).

It is generally believed that the D^- centres act as traps for the holes produced by light absorption. The D^+ centres will constitute traps for the electrons. The trapped carriers are afterwards released thermally to the respective band, thus giving rise to photoconductivity. At the same time photoconduction due to direct optical excitation from those

TABLE A

	Se	Se + O
σ_{RT} ($Ohm^{-1}.cm^{-1}$)	$3.4\ 10^{-15}$	$(2.6 \pm 0.8)\ 10^{-11}$
E_σ (eV)	0.88 ± 0.06	0.66 ± 0.03
C ($Ohm^{-1}.cm^{-1}$)	12	6.5
E_t (eV^{-1})	10.6 ± 2.3	
E_g (eV)	2.03 ± 0.08	
E_{Ph} (eV)	1.65 ± 0.03	~ 1.70
S_{RT} (mV/degree)		1
I.R. bands (cm^{-1})	233; 255; ~360; 488; 740	648; 935
D.S.C. peaks (°K)		
- endothermic	318 ± 2	
- exothermic	375 ± 5; (398 ± 4)	
E.S.R.	broad signal at $g \sim 2.3$	

Summary of results for pure and O containing Se glasses: I.R. bands listed for the latter are additional bands only.

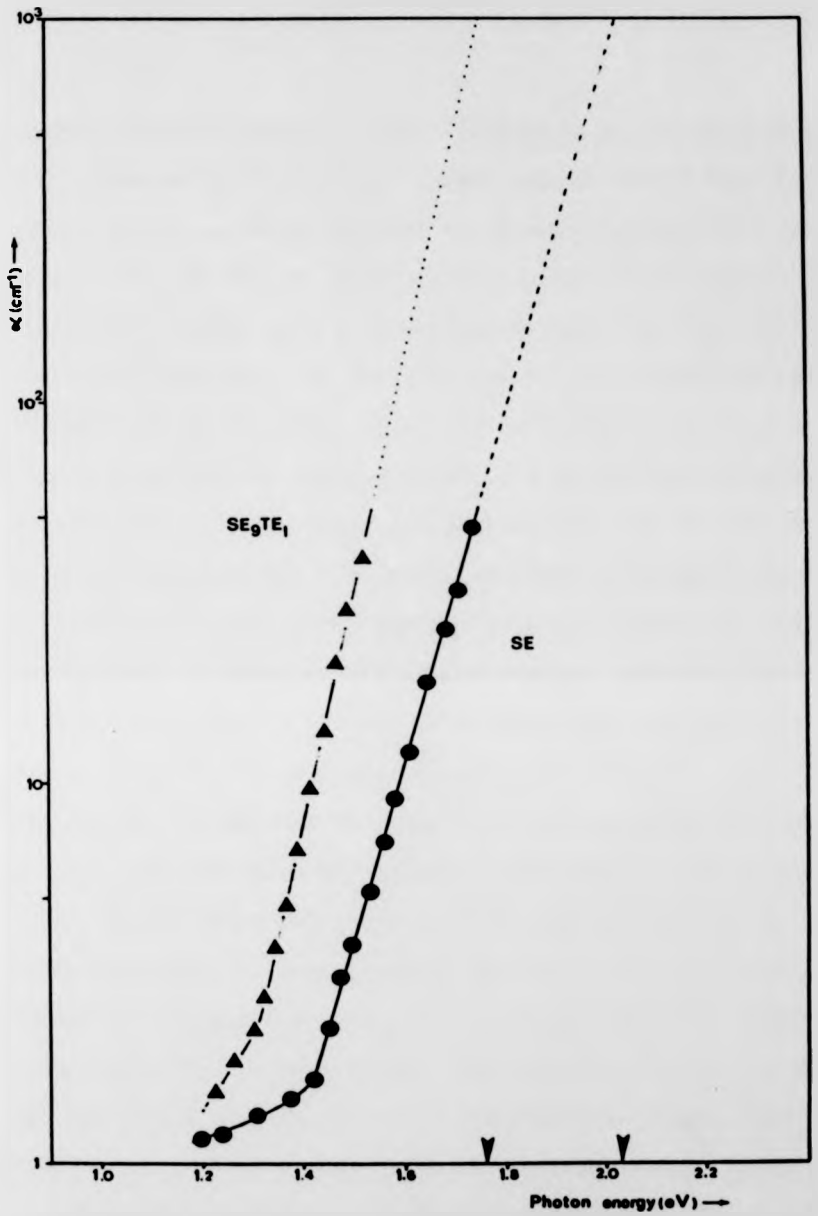

Fig. 4C - Logarithmic plot of the absorption coefficient α versus the photon energy at the optical absorption edge for bulk amorphous selenium (●) and $Se_{90}Te_{10}$ (▲) glasses. The straight part of the curves follow the equations $\alpha = 4.2\ 10^{-7} \exp\frac{h}{0.094}$ and $\alpha = 6.5\ 10^{-9} \exp\frac{h}{0.067}$, respectively. The arrows indicate estimations of the optical gap.

centres is also envisaged. Both mechanisms can account for a low value of E_{Ph} when compared with the optical gap, the difference $E_g - E_{Ph}$ being related to the energies required to thermally excite the respective carrier from the defect centre to the valence or conduction band. These quantities assessed as the activation energies for hole and electron drift mobilities have been determined as being 0.28 eV and 0.33 eV respectively (Marshall and Owen 1972), and according to the energy scheme of fig. 2N, where trap levels are denoted by D^o, the possibility of optical transitions is described by levels above and below these. As the smallest direct energy gap is expected to be much less than the observed peak energy it is therefore suggested that the photocurrent maximum is related to excitations of holes (electrons) from the conduction (valence) band to $D^-(D^+)$ centres. According to the considerations above and even if the excess energy necessary for photogeneration is not known, the peak may be expected to occur at an energy higher than Eg- ($\sim$0.30) $\simeq$1.73 eV and not below as observed. The possible energy dependence of either the recombination process or the mobility may be responsible for thediscrepancy. The experimental results also deviate generally from the data on quantum efficiency due to Knight and Davis (1974) although their work refers to a-Se films. The increase in photoconduction in the high energy part is, however, qualitatively in accordance with the verified exponential energy dependence of the quantum efficiency.

It is interesting to compare the observed spectral distribution of photoconductivity (before being normalized to photoresponse per absorbed photon) with that reported by Abdullayev et al.(1969a) corresponding to polycrystalline Se containing both monoclinic and hexagonal forms (see fig. 4E). The agreement is good which seems to give evidence for the presence in vitreous selenium, simultaneously, of

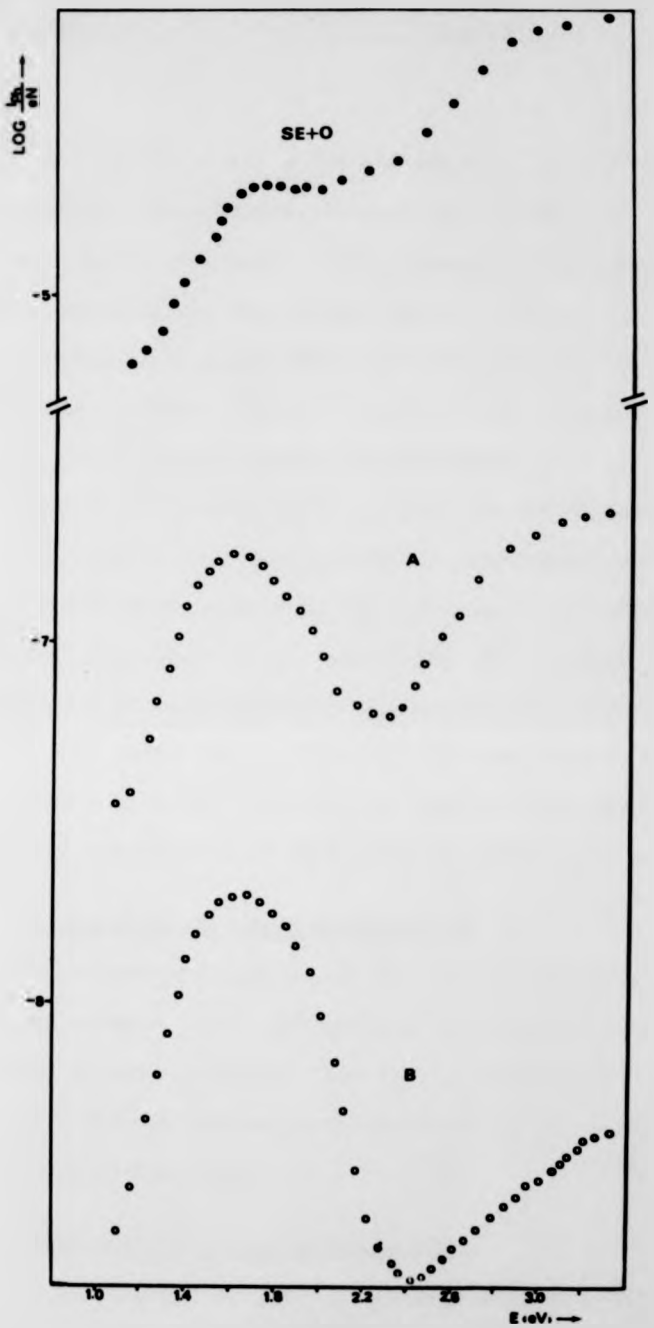

Fig. 4D - Photoresponse curves normalized per absorbed photon (○ ref refer to pure selenium glass with A and B as extreme cases; ● correspond to oxygen doped samples). I_{Ph} represents the photocurrent intensity and N the estimated number of photons incident onto the sample surface.

eight ring molecules and polymeric chains. It was not possible, however, to establish a relationship between the measured electrical conductivity and the relative intensity ratio between the two observed photoconductivity peaks. Nevertheless the interpretation is dubious as a second peak, at a photon energy much larger than the mobility gap, has been reported in chalcogenide glasses (Tohge et al.1983) and explained as being probably produced at the sample-electrode interface.

Addition of oxygen causes an increase in the photocurrent by two to three orders of magnitude which is comparable with previous observations (McMillan and Shutov 1977), although these recorded a smaller increase. The shape of the curve (fig. 4D) follows, in this case, more closely, even if only qualitatively, the quantum efficiency data already referred (Knight and Davis 1974). Although the peak is not very well defined its position does not seem to have suffered any appreciable shift (non normalized response peaks at 715 nm against the 755 nm observed in pure Se).

4.1.4 Thermoelectric power measurements

The Seebeck coefficient of the sample containing oxygen was ascertained as being $\sim$ 1000 μV/degree at room temperature. The measurements indicated p-type behaviour. Due to the experimental limitations discussed in chapter III the temperature dependence of the thermoelectric power could not be determined.

4.1.5 Differential Scanning Calorimetry

DSC thermograms of pure selenium glasses are depicted in fig. 4F. They are of two kinds. Both kinds are characterized by a single endothermic peak at 318 $\pm$ 2 ^{o}K which can be assigned to the glass transition phenomenon, but differ with regard to exothermic behaviour.

Most of the glasses showed a single exothermic peak at 375 $\pm$ 5 ^{o}K

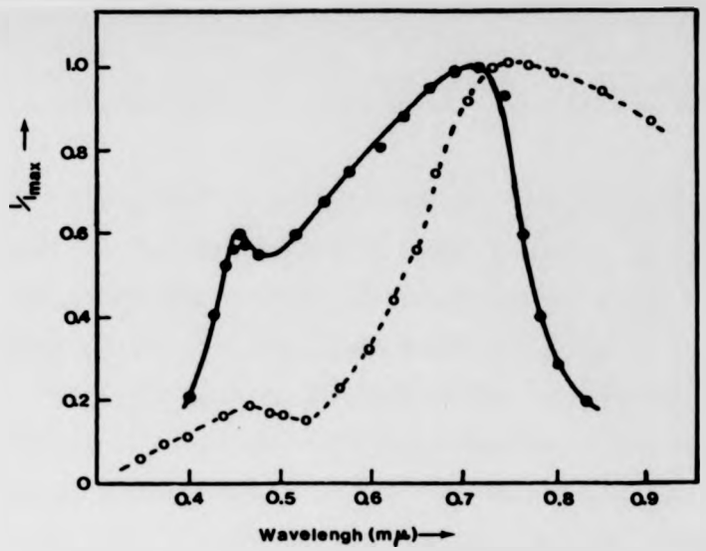

Fig. 4E - The spectral distribution of photoconductivity of glassy selenium (o) is compared with the results reported by Adbullaev et al.(1969a) and referring to a sample of monoclinic selenium partially converted to the hexagonal form (●).

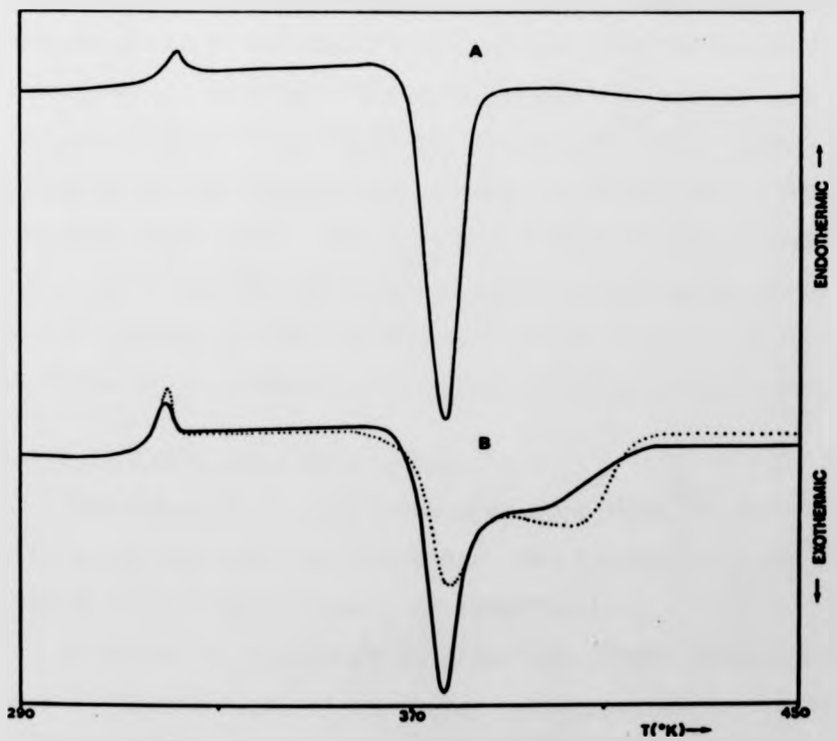

Fig. 4F - D.S.C. thermograms for pure vitreous selenium
A - Typical response; B - The two samples showing a shoulder are represented.

identified with the crystallization process. These types of curve are similar to the ones obtained by Gobrecht (1969). However, contrary to this author's observation it was found that even freshly prepared samples presented a small glass transition peak.

Two of the samples exhibited a different shape with regard to the exothermic region, with a shoulder appearing at the high temperature side, in the region 395 - 402°K. The reason for such a behaviour can be attributed, in accordance with work performed by Nagels et al.(1983), to the existence of different quenching temperatures. According to those authors, the shoulder occurs for the samples quenched at the lowest temperatures.

In fact the equilibrium concentrations of eight fold Se rings and long Se chains in the liquid state has been reported as strongly temperature dependent with the ring concentration decreasing as temperature increases (Keezer 1969; Grochowski and Brenner 1971). Therefore, different ratios of the two species might be expected in the glass, depending on the quenching temperature. The existence of rings in non-crystalline selenium has nevertheless been considered controversial (Lucovsky 1979). In this respect the DSC thermograms observed could be taken as an indication of the Se rings presence in the vitreous state, giving rise to the shoulders.

4.1.6 Electron spin resonance data

The ESR signal of glassy selenium was studied, at room temperature, within a g value range of 0.8 to 6.3. The standard used was DPPH and samples were powdered prior to measurements.

According to the charged dangling bond models, already discussed, no ESR absorption would be expected since all the defect centres are doubly occupied. Published results seem to confirm the electron pairing

at the Se chain ends as no signal compatible with the eventual existence of $\sim 3.6\ 10^{17}$ paramagnetic centres /cm^3 - assuming 10^5 atoms per chain (Eisenberg and Tobolsky 1960)-was found (Abkowitz 1967). In terms of the Mott model a paramagnetic signal having its origin in the states near the Fermi level should nevertheless occur but it is predicted to be small (Agarwal 1973).

The results obtained showed, however, a very broad (> 0.5 kGauss) signal at $g \sim 2.3$ (see fig. 40). ESR signals in selenium have been reported by Abdullaev et al.(1969b) who interpreted the results in terms of a charge-transfer complex model. However, these results refer to a sharp absorption and were obtained only after heat treatment of the amorphous powder. A broad signal has been reported in the literature (Sampath 1966) and interpreted as due to hydrocarbon impurities (Abkowitz 1967). This could also be the case of these samples since they had been stored inadvertently in plastic boxes. The non-reproducibility of signals, discussed in paragraph 4.2.6, also seems to support this hypothesis.

4.2 The Se-Br and Se-Cl systems

4.2.1 Introduction

Two series of samples were made by adding selenium bromide (Se_2Br_2) or selenium tetrachloride ($Se\ Cl_4$) to selenium pellets. The range of added proportions varied from 4 at % to 50 p.p.m. in the case of bromine, and from 4 at % to 10 p.p.m. in the case of chlorine.

As discussed in chapter III an indication of the actual composition of bromine doped glasses was obtained using energy dispersive analysis of X-Rays. For samples of a glass in which 3.2 at % of bromine had been added in, EDAX measurements gave 2.6 at % which indicates that the actual composition is, at least, of the same order of magnitude as that intended.

The EDAX spectrum of that glass is shown in fig. 4G. For the reasons already mentioned no EDAX results could be obtained for the Se-Cl system.

During the preparation of the glasses of both systems it was observed that, for compositions around 3.5-4 at %, an adsorbed layer was apparent on the surface of the glass after quenching. It therefore appears that the saturation level has been reached for atoms of Br or Cl in selenium. It was not possible then to prepare samples with greater content of bromine or chlorine than 4 at %.

The experimental results whose description follows are summarized in table B.

4.2.2 D.C. conductivity experiments

For each glass prepared, the room temperature D.C. conductivity was determined by measuring at least two distinct samples. A plot of the D.C. resistivity at 20°C versus the composition of the glass for the Se-Br system is shown in fig. 4H. Each error bar represents the absolute error. The main features are, in first place, the strong dependence of the resistivity upon the composition, for bromine contents smaller than ~0.3 at %, whereas for impurity concentrations greater than that, the resistivity seems to become constant. For the "flat" part of the curve an average value for the conductivity of $\sigma_{RT} = (2.7 \pm 0.6)\ 10^{-9}\ ohm^{-1}.cm^{-1}$ was obtained. The second main feature is that, compared with the value of the conductivity of non-doped selenium glasses, a dramatic change of six to seven orders of magnitude was observed.

The results concerning the chlorine doped glasses are very similar to those obtained for the Se-Br system. Once more for impurity contents greater than a value around 0.5 at % a region of constant resistivity is attained. This corresponds to a conductivity maximum of, on average, $(2.8 \pm 0.9)10^{-9} ohm^{-1}.cm^{-1}$ which is in excellent agreement with the value

TABLE B

	Se + Br	Se + Cl	Se + I
σ_{RT} ($Ohm^{-1}.cm^{-1}$)	$(2.7 \pm 0.6)10^{-9}$	$(2.8 \pm 0.9)10^{-9}$	$(4.5 \pm 0.8)10^{-11}$
E_σ (eV)	0.60 ± 0.02	0.61 ± 0.01	0.75 ± 0.05
C ($Ohm^{-1}.cm^{-1}$)	68	87	180
E_t (eV^{-1})	9.8 ± 2.0	10.1 ± 1.8	10.0 ± 1.4
E_g (eV)	2.04 ± 0.04	2.06 ± 0.03	2.01 ± 0.05
E_{Ph} (eV)	1.69 ± 0.05	1.66 ± 0.04	1.60 ± 0.05
S_{RT} (mV/degree)	1.57 ± 0.12	~ 0.8	0.96 ± 0.08
E_S (eV)	1.02 ± 0.11		1.18 ± 0.08
γ (eV/degree)	$(1.84 \pm 0.21)10^{-3}$		$(2.98 \pm 0.23)10^{-3}$
I.R. bands (cm^{-1})	none	335; 960	none
D.S.C. peaks (°K) - endothermic - exothermic			 313 ± 2 379 ± 3
E.S.R.	no extra signal	no extra signal	no extra signal

Summary of results for vitreous Se doped with halogens.
(Results refer to saturated glasses - see text).
I.R. bands listed are additional bands only.

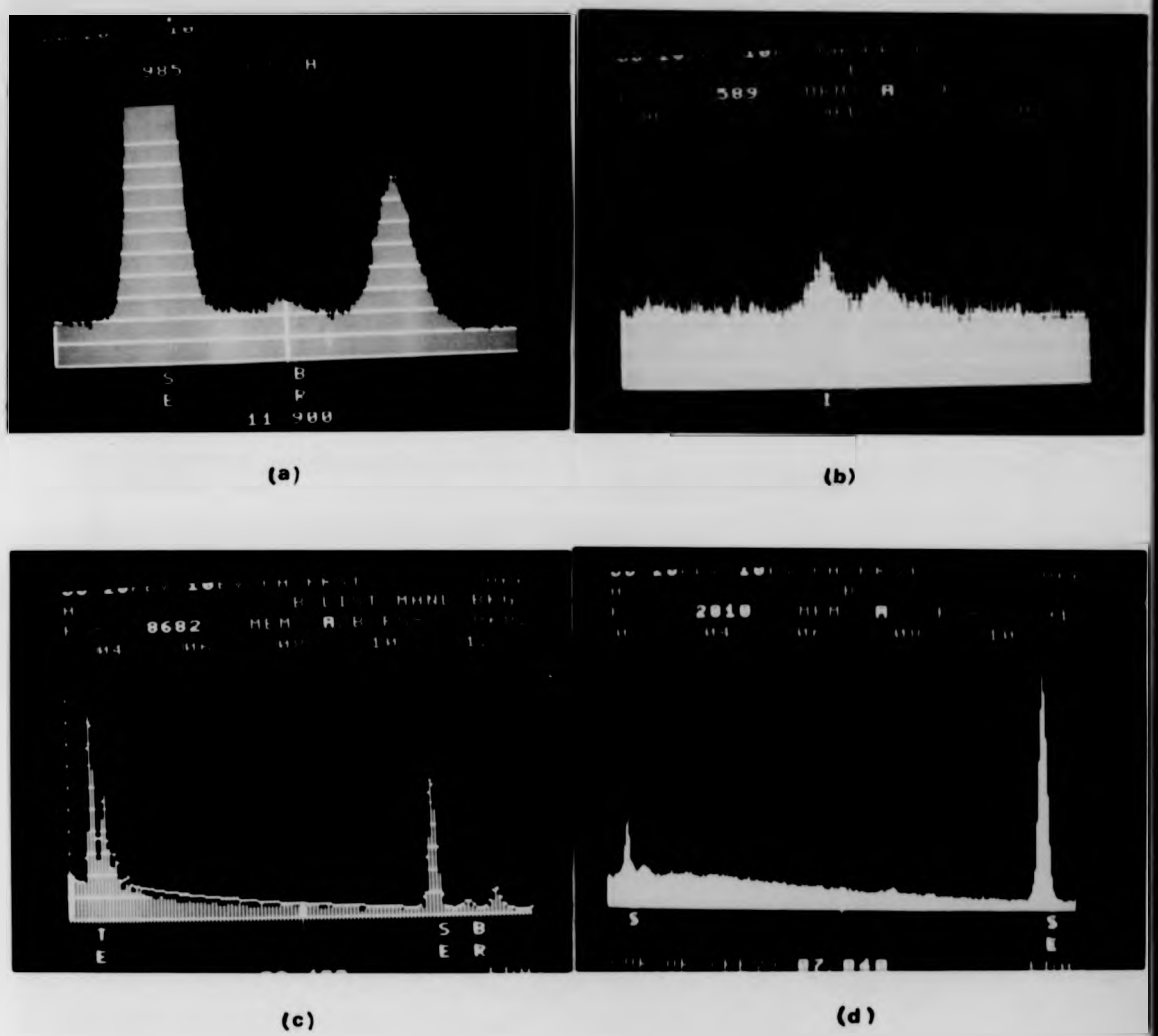

Fig. 4C - The spectra resulting from EDAX analysis of various samples are shown: (a) $Se_{9.68}Br_{3.2}$ glass. K_α line of Br is compared with K_β line of Se (on the right). On the left appears part of the K_α selenium line.
(b) $Se_{97.3}I_{2.7}$ glass being evident the L_α and L_{β_1} lines of iodine.
(c) $Se_{80}T_{18}Br_2$ glass (Tellurium L lines).
(d) $Se_{90}S_8Br_2$ glass (Sulphur K line).

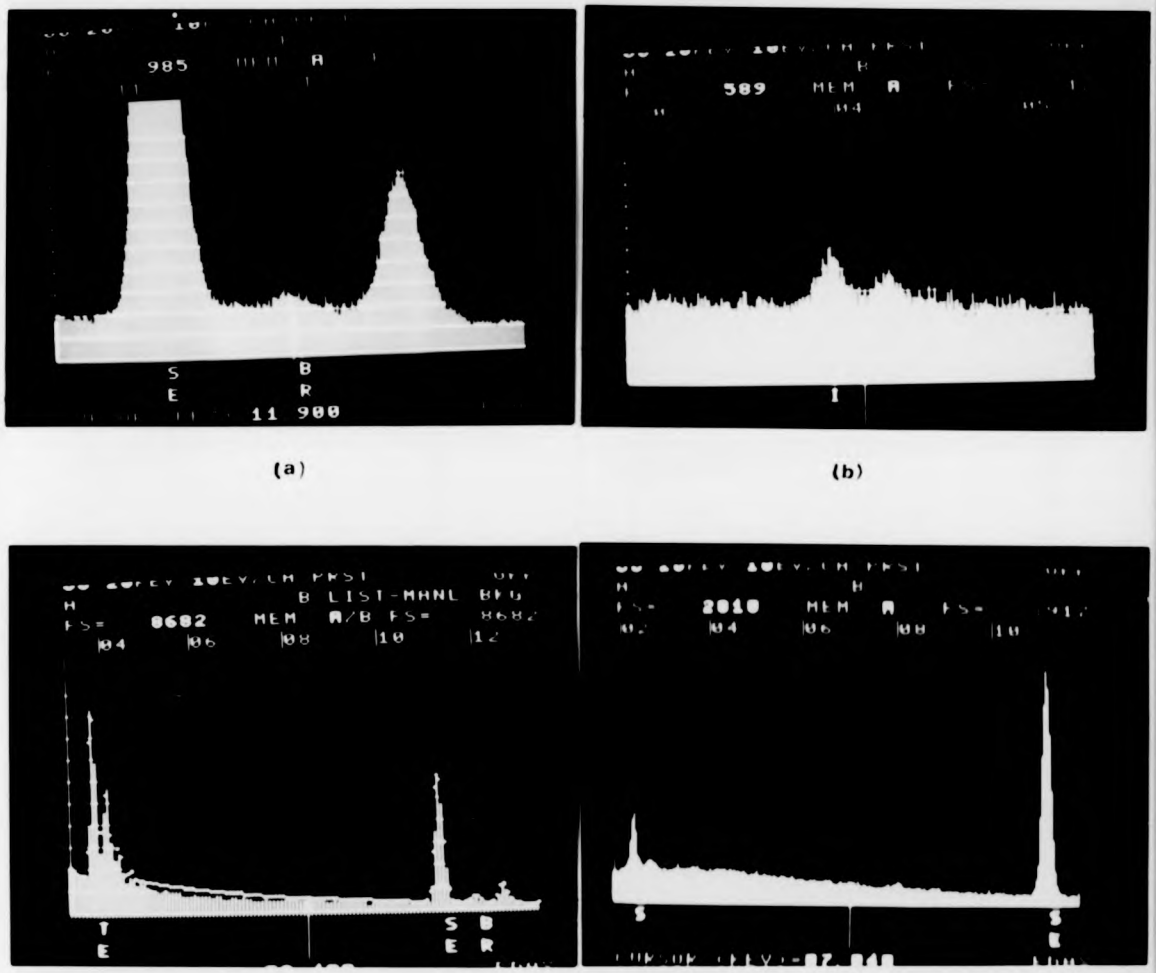

(a) (b)

(c) (d)

Fig. 4G - The spectra resulting from EDAX analysis of various samples are shown: (a) $Se_{96.8}Br_{3.2}$ glass. K_α line of Br is compared with K_β line of Se (on the right). On the left appears part of the K_α selenium line.
(b) $Se_{97.3}I_{2.7}$ glass being evident the L_α and L_{β_1} lines of iodine.
(c) $Se_{80}T_{18}Br_2$ glass (Tellurium L lines).
(d) $Se_{90}S_8Br_2$ glass (Sulphur K line).

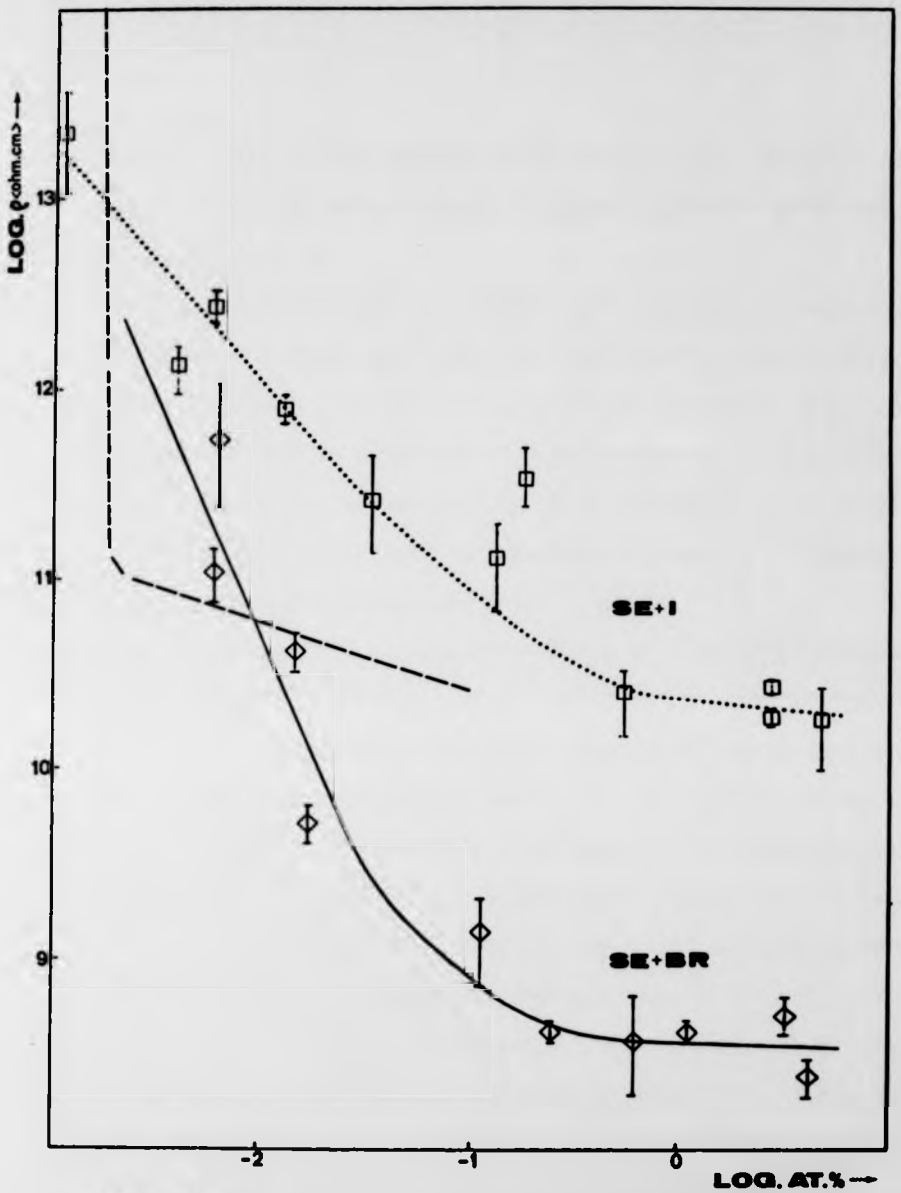

Fig. 4H - Room temperature D.C. resistivity of Br and I doped selenium glasses is represented as a function of the additive concentration. The broken line is the theoretical interpretation by Popov (1978) of oxygen doped selenium data of Lacourse et al. (1970).

characteristic of the bromine containing glasses. The room temperature D.C. conductivity versus composition curve for the Se-Cl system appears in fig. 4I.

For a certain number of samples of both glass systems an analysis of resistivity dependence upon the temperature was also made. All samples showed a well defined exponential behaviour, Arrhenius type, with respect to the inverse of the temperature. So a single activation energy seems to be characteristic of all glasses. In fig. 4J are plotted Arrhenius curves of bromine doped glasses. Chlorine containing glasses showed identical behaviour.

The values of the activation energy E_σ are represented in terms of the composition in fig. 4K(a). It should be noticed that due to experimental limitations different temperature ranges were used. The curve shows also a quasi-flat part which corresponds to the same region of compositions ($\gtrsim$ 0.5 at %) as observed in the resistivity plots, as expected. (The shape of the activation energy vs. composition curve will be rediscussed later). For the compositions corresponding to the approximately constant part, an average value of $E_\sigma = (0.60 \pm 0.02)$eV was found for the bromine containing glasses, whereas the glasses of the Se-Cl system showed the very similar value of $E_\sigma = (0.61 \pm 0.01)$ eV. These are substantially smaller than the value obtained for the activation energy of pure vitreous Se (0,88 eV) as illustrated in fig. 4J.

In the case of the values of the pre-exponential factor C it seems that the introduction of the additive (Br or Cl) has a small effect. The average values of C obtained for the more heavily doped glasses were 68 $ohm^{-1}.cm^{-1}$ for Br and 87 $ohm^{-1}.cm^{-1}$ for Cl, that is less than one order of magnitude greater than the value observed for non-doped Se. As an increase could not be consistently observed when the impurity concentration

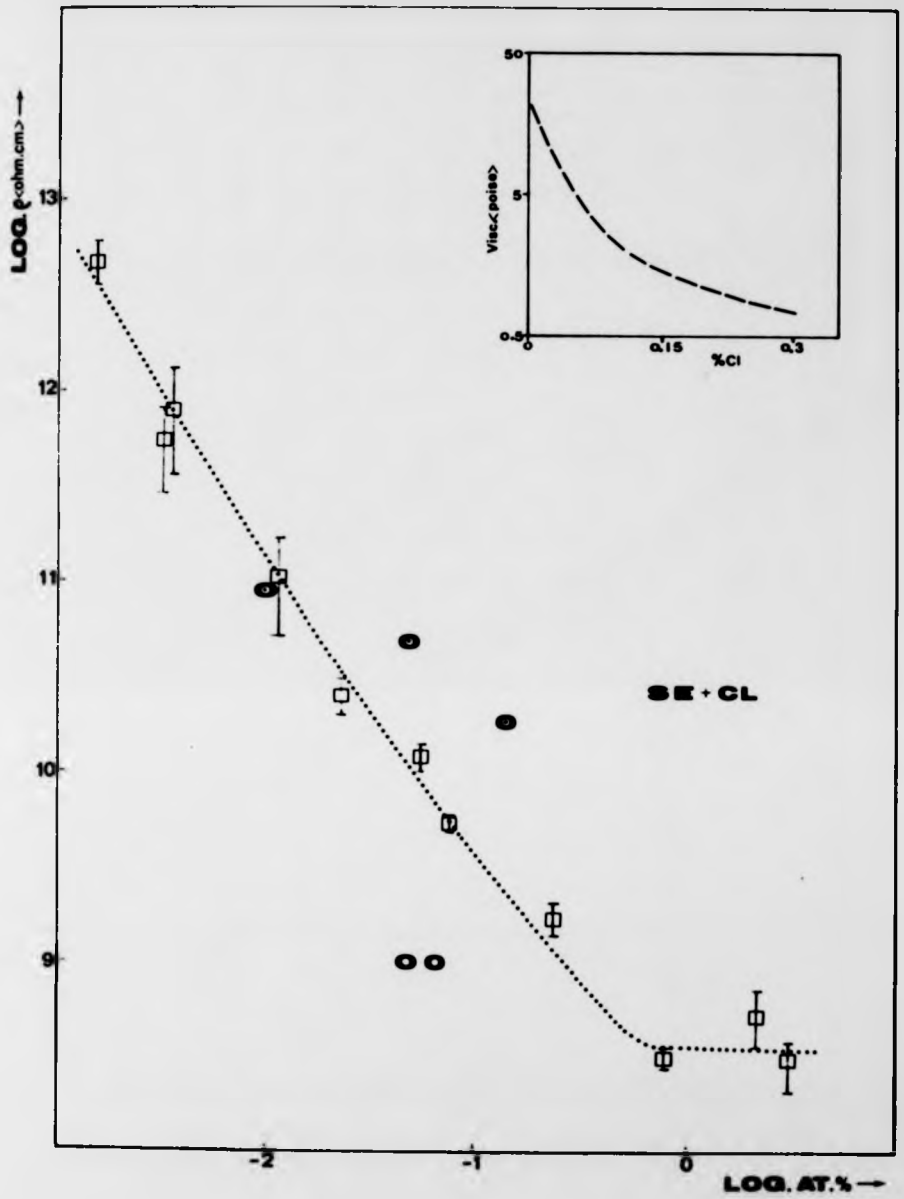

Fig. 41 - Room temperature D.C. resistivity versus impurity concentration for vitreous Se containing Cl is shown. Other points are the published results (Twaddell et al. 1972). In the upper right hand corner the influence of Cl upon the viscosity of liquid selenium (Shirai et al. 1963) is presented.

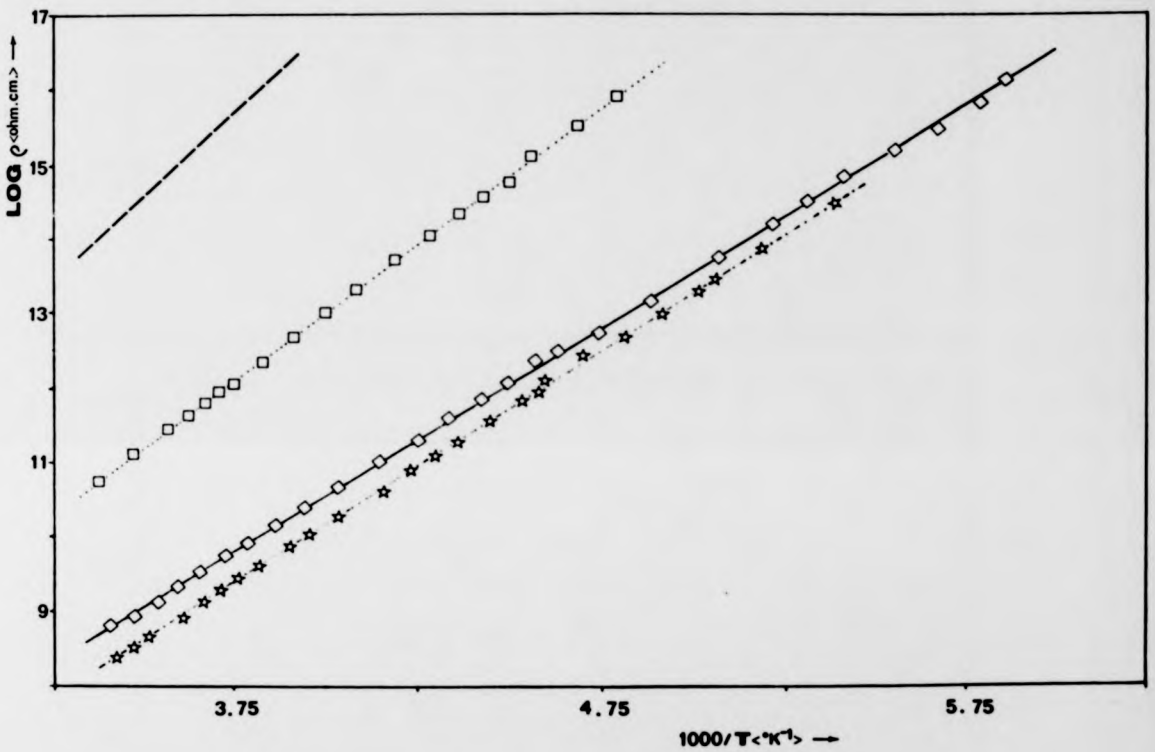

Fig. 4J - The Arrhenuis curves for $Se_{97}Br_3$ (✡), $Se_{99}Br_1$ (◇) and $Se_{99.98}Br_{0.02}$ (□) are compared with the average curve for "pure" selenium glass (broken line).

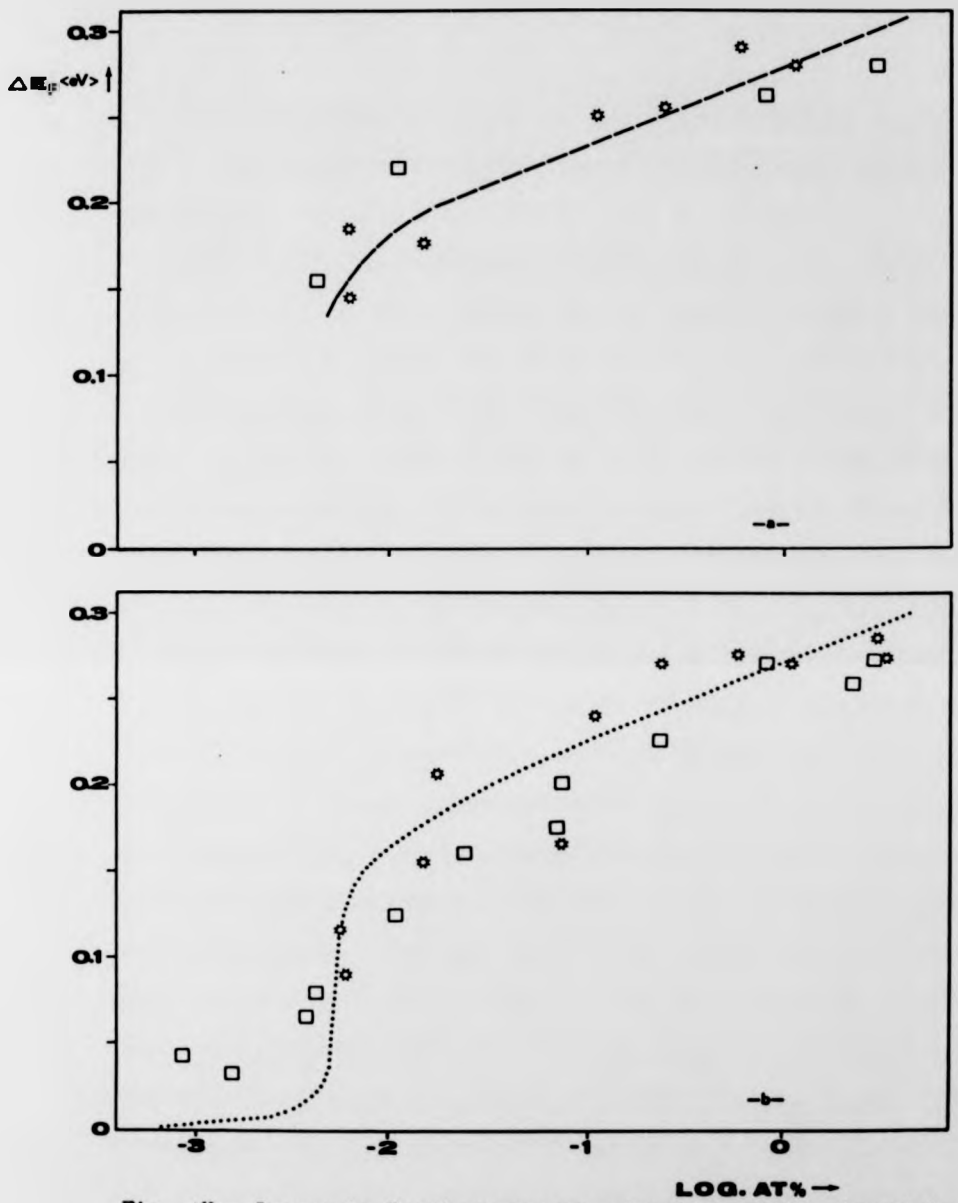

Fig. 4K - Change in Fermi energy as a function of the dopant level. Experimental points refer to bromine (✲) and chlorine (□) and were obtained from activation energy curves (a) or determined from resistivity results (b). Curves refer to theoretical estimations (see section 4.2.2).

was raised from zero to its higher value it is difficult to draw a definite conclusion as also the temperature ranges used differed a great deal.

Since bromine and chlorine containing glasses have proved to be p-type (see 4.2.4), the effect of the Cl upon the transport properties of selenium, expected from the published data, was effectively small. In fact, Takasaki et al.(1983) determined that although the effect of adding Cl upon the electron range is great, the hole range stays practically unchanged. Other results on drift mobility measurements (Schotmiller et al.1970) indicate a similar behaviour. The values of C, in any case, are both smaller than 100 and so seem to point out a conduction mechanism similar to that observed in non-doped selenium, i.e. band conduction limited by carrier trapping at localized sites.

The increase in conductivity is 10^5 greater than the apparent change of C; it appears therefore to be, if not solely, at least principally related with the decrease in the activation energy. The observed change in conductivity is close to that previously reported on Cl doped glasses (Twaddell et al.1972) although the activation energies found are vastly different. Such an increase in conduction was interpreted by Mott (1976) (on the supposition that the doped materials were n-type) as due to absorption of Cl atoms at the D^- ends. This will be accompanied by the liberation of electrons to interstitial Cl atoms with the resulting Cl^- ions having a role of donors. However, as stated, thermopower measurements, which have been asserted as a reliable indication of the type of conduction (Mott and Davis 1979), indicate conduction by holes and so it is necessary to look for an alternative interpretation.

It is noticeable that the "saturation" value of the activation energy is very approximately $\frac{1}{3}$ less than the value observed for pure selenium, i.e. $\frac{2}{3}$ ($E_g - \epsilon$). This suggests a similar process to that observed in oxygen doped glasses, that is the halogen atoms go to the D^- centres so forming halogen terminated chains. Since the extra electron is expected to be weakly bound, it will probably be captured by interstitial halogen atoms. The D^- centres are destroyed and since the electron affinity of halogens is very high it is believed that no electrons can be generated. That leaves the D^+ centres which, assuming that they have remained intact, will originate holes with the fall of the activation energy. Those interstitial atoms are eventually responsible for the observed cessation of electron drift mobility. However, with the disappearance of the D^- centres, a rise in the hole mobility might be expected since such defects are generally considered as hole traps. That, as discussed, could not be established.

On the other hand it is suggested by viscosity measurements (see fig. 41) that halogens break the selenium chains. In chemical terms the attack of the Se-Se bond is justifiable by the electronegativity difference between selenium and chlorine (0.6 eV) and selenium and bromine (0.5 ev). In addition infrared spectra (see 4.2.3) seem to corroborate that halogens are chain terminators. It is interesting to compare the shape of the σ versus composition curve with that of the corresponding viscosity data. Viscosity becomes approximately constant for concentrations >0.3 at % which is a value close to the beginning of the "flat" part of the σ (and also E_σ) curves. This value may indicate the incapability of further incorporation of halogen atoms in a chain situation and so the similarity of behaviour may be taken as an indication that the conduction process is somehow associated with chain breaking. Since

one would anticipate the saturation conductivity to be attained, as it happens in oxygen (see fig. 4H), when the number of impurities becomes of the same order that the number of topological defects (Popov 1978) -which occur in a concentration estimated in 10-100 atoms per million, (Eisenberg and Tobolsky 1960; Keezer and Bailey 1967)-the observed value of $\sim$ 0.5 at % might mean that halogen atoms "prefer" to break chains prior to being adsorbed at D^- ends. Infrared data shown in 4.2.3 indicates that some competition with interstitial selenium-halogen molecules also takes place.

On that basis an alternative hypothesis may also be envisaged considering that, on addition of either Br or Cl to selenium, the balance between the charged dangling centres, D^- and D^+, remains unchanged throughout the process, with the halogen atoms being bound only at the neutral ends formed after chain breaking. If the equality $n(D^+) = n(D^-)$ is maintained the unpinning of the Fermi energy will be achieved uniquely by the introduction of electronically active impurities (with creation of a new energy level) in higher concentration than those numbers. Since the neutral Br and Cl ends are presumably not electronically active it is suggested, based on the high electron affinity of these elements, that halogen atoms, staying interstitially, constitute acceptor states causing a shift of the Fermi energy towards the mobility edge of the valence band. As the D^- centres (hole traps) are assumed to remain unchanged this hypothesis would account for the invariant hole mobility value.

An estimation of the expected shape of the E_F variation in terms of statistical mechanics is now undertaken. This follows the calculations by Adler and Ioffa (1976) for a semiconductor containing defects which are characterized by a negative correlation energy. That is believed to

be the case of selenium. As discussed in chapter II, in glassy Se the topological defects (dangling bonds) can have zero, (D^-), one (D^o) or two holes (D^+). If the energy to extract a first electron from a D^- centre (which will become D^o) is $E + |U|$, the energy to extract the second (transforming the centre into D^+) is only E due to the negative correlation energy U that describes the electron pairing (Anderson 1975). That is equivalent to say that a donor level lies at E whereas an acceptor level lies at $E - |U|$ (see fig. 2N) and consequently the Fermi level is fixed midway at $E - |\frac{U}{2}|$. If an extra defect level is introduced at an energy W, there will be a significant alteration of the E_F position only when the concentration of additive exceeds the (D^+,D^-) concentration as will be shown.

For the case where W is a single particle level, as it was assumed, an implicit expression for E_F is given by Khan and Adler (1984) in the form,

$$N \cdot \frac{\exp(+2\beta\Delta E_F) - 1}{1 + 2\left[\exp\beta\left(\Delta E_F - |\frac{U}{2}|\right)\right] + \exp(2\beta\Delta E_F)} = M \cdot \frac{1}{\exp\beta\left(\Delta E_F - W + E - |\frac{U}{2}|\right) + 1} \qquad (4.2)$$

where ΔE_F is defined by

$$E_F = E - |\frac{U}{2}| + \Delta E_F \qquad (4.3)$$

N represents the concentration of dangling bonds of selenium, which as stated, is supposed to be independent of the halogen concentration and M is the concentration of the halogen impurities electronically active. The concentration of holes in the valence band was neglected. The variation of the Fermi level, ΔE_F, since the problem concerns hole conduction, must be interpreted as the "increase" of E_F towards the valence band.

According to the drift mobility data (Marshall and Owen 1972) and considerations of paragraph 2.6, $|\frac{U}{2}|$ is expected to be of the order of $\sim$ 0,7 eV for selenium. The middle term in the denominator of the first part of equation (4.2) is therefore negligible. So equation becomes successively

$$N \cdot \frac{\exp(\beta\Delta E_F)[\exp(\beta\Delta E_F)-\exp(-\beta\Delta E_F)]}{\exp(\beta\Delta E_F)[\exp(\beta\Delta E_F)+\exp(-\beta\Delta E_F)]} = \frac{M}{1+\exp\beta(\Delta E_F+E-|\frac{U}{2}|-W)}$$

and

$$N \tanh(\beta\Delta E_F) = M\,[1+\exp\beta(\Delta E_F + E - |\tfrac{U}{2}| - W)]^{-1} \qquad (4.4)$$

For all measured activation energies $\beta\Delta E_F$ is great enough to make $\tanh(\beta\Delta E_F)$ effectively equal to unity. It is therefore possible to write (4.4) in the form

$$\Delta E_F = W - E + |\tfrac{U}{2}| + kT \ln(\tfrac{M-N}{N}) \qquad (4.5)$$

For values of M large when compared with N, eq. (4.5) yields a small dependence of W on the N value. It is possible, accordingly, to estimate the impurity energy level from the activation energies for the larger impurity concentrations. That gives $W-(E-|\frac{U}{2}|) = (0.175 \pm 0.04)$ eV, i.e. W is located $\sim$0.70 eV above the valence band. The error includes the uncertainty of considering the range of possible N values extending from 3.10^{17} cm^{-3} to 10^{19} cm^{-3} which is based on the estimation of the selenium chain length.

The best fitting of the activation energy data for that value of W is shown in fig. 4K(a). It yields an apparent value for N of $\sim 1.5\ 10^{18} cm^{-3}$ This seems reasonable according to the values quoted above. However, the resistivity vs. composition data suggests that the effective M could be rather smaller than the impurity concentration, therefore implying an apparent value of N greater than that observed.

The experimental points in fig. 4K(a) are insufficient to arrive at an unambiguous conclusion. So, with the purpose of clarifying the problem and since the pre-exponential factor C was observed to undergo little change, a new plot of ΔE_F as a function of the amount of additive present was made. This was derived using activation energies calculated directly from the room temperature resistivities and assuming that C was invariant. This should be a more reasonable approach as the error resulting from the use of different temperature ranges (some of which were particularly narrow) is avoided. The new curve of ΔE_F is represented in fig. 4 K(b).

At small values of ΔE_F where eq.(4.4) reduces to

$$N(\mathrm{Tanh}\ \frac{\Delta E_F}{kT}) = M,$$

it was possible to determine a value for N of $\sim (1.8 \pm 1.0)10^{18} cm^{-3}$. From the larger concentrations eq. (4.4) yields $W - E_F = |\frac{U}{2}| = (0.16 \pm 0.02)$ eV. These values are very close to the ones obtained previously. Thus it looks like the effectiveness of the impurity in changing the activation energy is high for concentrations similar to that of the defects; i.e. whatever chemical process is taking place, new electronically active centres are created in significant percentage from the beginning of the addition process.

At the same time, adding halogen atoms apparently leads to the formation of a new energy state at ~ 0.17 eV below the Fermi level for pure selenium. As the values of electron affinities are 3.53 eV for Br and 3.75 eV for Cl (Moeller 1961), that means the mobility edge at the valence band being located ~ 4.4 eV below vacuum, a high value when compared with that obtained from photoemission experiments (5.7 eV) (Mort 1973). The difference in electron affinities might suggest that

contrary to experimental observation, Cl doping and Br doping should lead to distinct results.

Those considerations might favour the idea of halogens being adsorbed at D^- centres. In this case, however, one would anticipate results similar to those observed in the oxygen doped selenium glasses. The difference seems too large to be justified by experimental error.

A third alternative explanation may also be considered since there are reasons to believe that in liquid state a selenium chain breaks after deformation is caused by halogens at a regular selenium site - C_2^o state in the notation of Kastner et al. - (Yao et al. 1983). Due to the electronegativity difference a Br (or Cl) atom will attract one electron from the lone pair of the Se atom leading to hole formation (aC_2^+ centre, probably). When the glass is formed some of these centres will be quenched in. The C_2^+ centres will act as acceptors and could constitute the states at $\sim$ 0.70 eV. As the centres are certainly very dependent on the temperature, the number of them in the glass will depend on the quenching conditions, which will eventually account for some of the error observed. This interpretation seems consistent with the experimental evidence that results concerning Br and Cl are similar.

4.2.3 Infrared data

Once again infrared spectroscopy comprised in the first place the transmission response in the range between the optical absorption edge and 180 cm^{-1}. A considerable expectation was attached to those measurements since some useful information concerning the structural modification due to the introduction of the Br and Cl atoms could be obtained. The results were unfortunately not very rewarding especially those for bromine.

As in the case of pure selenium, the infrared spectra showed for both Br and Cl doped glasses, a constant transmission from 5000 cm^{-1} to $\sim$ 1000 cm^{-1} of, on average, 66% indicating good homogeneity of the glasses.

In the region 1000 cm^{-1} - 180 cm^{-1} some Cl containing glasses show two new bands at 960 and 335 cm^{-1}. This behaviour occurred in all glasses with Cl content larger than $\sim$ 700 p.p.m. Contrary to observations by Lucovsky (1969) no sample showed only one of those bands. Concentrations smaller than 700 p.p.m. contained no new bands. The band at 960 cm^{-1} was interpreted by Tausend (1969) as a combination of some of the six fundamental vibrations of the Se_2Cl_2 molecule (Stammreich and Forneris 1956). However, combination of some of the Raman frequencies of the $SeCl_4$ molecule as determined by Gerding and Houtgraaf (1959) also lead to a similar result. Since there is an excess of selenium it is considered more likely that the band derives from monochloride rather than tetrachloride. According to a similar reasoning and based on the Raman spectra of selenium monobromide given by Stammreich and Forneris a band should appear, in the Br doped glasses, at $\sim$ 670 cm^{-1}. Such a band could not be observed in any sample. The interpretation above may indicate that some chlorine is not incorporated in the glass structure but remains interstitially in a molecular form.

Lucovsky (1969) suggested that the band at 335 cm^{-1} can be attributed to a vibrational mode of a chlorine capped chain. That is compatible with viscosity data and also with the observation that the additive causes no change in the intensity of Se bands which would be expected if halogen atoms preferentially broke the Se_8 rings. The reason for the non-appearance of a corresponding band in the bromine case, although the above considerations are equally applicable, is most likely a result

of the similarity between Se and Br masses. Therefore localized Se-Br vibrations are not distinguishable from Se-Se vibrations. In bromine doped glasses it was not thus possible to observe any new band.

The optical gap was also determined from the absorption coefficient vs. energy data at the optical absorption edge. This was carried out for the $Se_{99}Br_1$ and $Se_{97}Cl_3$ glasses and yielded the values for Eg of 2.04 eV and 2.06 eV respectively, which are very similar to the value for pure selenium glasses. The slopes of the exponential absorption region and the general shape of the curves were also very close to those observed in pure selenium. The data shows therefore no significant alteration in the mobility edge as expected.

The I.R. transmission curves of selenium glass containing Br or Cl are shown in fig. 4L.

4.2.4 Thermopower measurements

The determination of the thermopower, S, was a key experiment since there was the possibility that halogen addition might change the conduction from p-type, as for vitreous selenium, to n-type behaviour as early experiments (Twaddell et al 1972) seemed to indicate in Cl doped selenium. However it was not possible to confirm this result. Both Cl doped and Br doped glasses showed positive thermopower sign, and so, if S is taken as a guide, these glasses are p-type.

In the case of bromine doped selenium two glasses containing 0.6 at % and 1 at % of the impurity were analysed. Both showed similar results. For the $Se_{99}Br_1$ glass, from which two different samples were measured, a value of + 1.57 $mV.^{o}k^{-1}$ was found for the Seebeck coefficient at the temperature of 23°C. The absolute error obtained was 0.12 $mV.^{o}K^{-1}$. The dependence of S as a function of the inverse of the temperature for those

samples is plotted in fig. 4M. The linear regression method determined on average activation energy for the process of E_S =(1.02 $\pm$ 0.11) eV and a value for γ of 1.84 10^{-3} $eV.^oK^{-1}$.

This value for the activation energy is much higher than the value for the activation energy characteristic of the conductivity curve, E_σ whereas, if conduction is via extending states, those values should agree with each other. If hopping is involved, the discrepancy would be worse. No proper interpretation can be given to the discrepancy. However attention should be drawn once more to the narrow temperature ranges over which data was obtained. It should also be noticed that values obtained in liquid chalcogenides (see Mott and Davis 1979) also show a discrepancy of the same signal although not as large. The existence of mixed conduction mechanisms has been suggested as a possibility of explaining the difference between the two activation energies.

The value of γ , the temperature coefficient of the difference E_F-E_V, is of the same order of magnitude as values obtained in various liquid chalcogenides (Mott and Davis 1979) and is not too different from typical values for the temperature coefficient of the optical gap (10^{-4} - 10^{-3} eV/degree) (Donald and McMillan 1978; Mott and Davis 1979).

In the case of Cl doped glasses a sample containing 0.8 at % of the impurity was analysed. The sign of S was, as stated, also positive. S presented a value at room temperature of 0.8 mV K^{-1} which is smaller than that observed for Br. This numerical result however needs confirmation. The result also indicated that the activation energy, E_s, and γ values are close to those of the $Se_{99}Br_1$ glass. The results can be compared with data published on chlorine doped liquid selenium (Yao et al.1983) that also shows positive thermopower and a value for S of a similar order of magnitude.

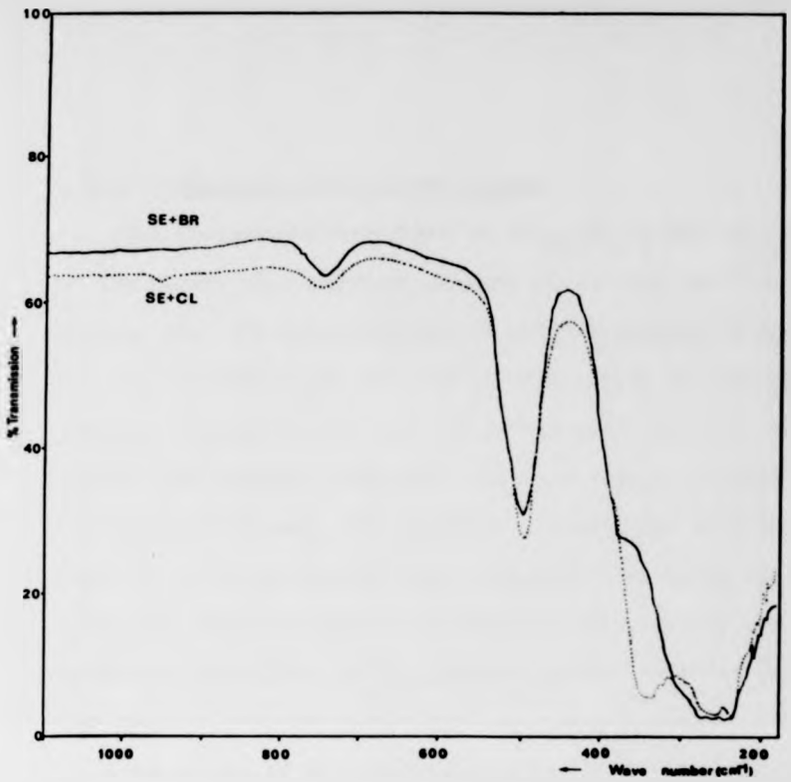

Fig. 4L - Infrared transmission spectra for $Se_{99}Br_1$ and $Se_{99.2}Cl_{0.8}$ are compared. The former is identical to the pure selenium curve.

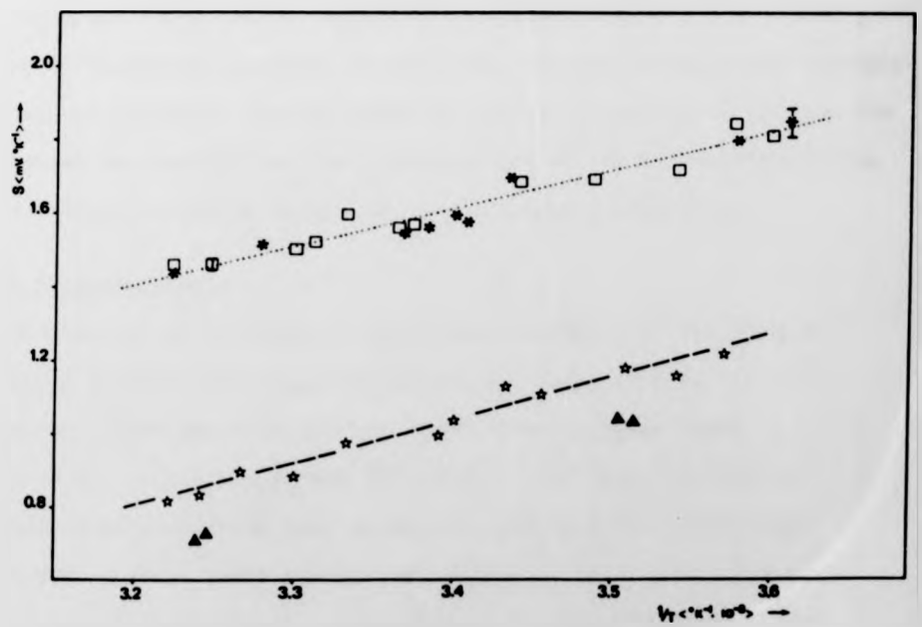

Fig. 4M - Thermopower for selenium glasses containing 1 at % of Br (upper curve referring to two different samples) and 2.7 at % of I (lower curve) as a function of the reciprocal absolute temperature are depicted. Results concerning the $Se_{99.2}Cl_{0.8}$ glass are also shown (▲).

4.2.5 Photoconductivity measurements

The photoresponse spectra of $Se_{99.4}Br_{0.6}$ and $Se_{99.2}Cl_{0.8}$, typical of the higher concentration glasses of the two systems, are displayed in fig. 4N. The photoresponse of both is similar presenting peaks at $\sim$ 1,69 eV and $\sim$1,66 eV respectively, which are close to the one verified for pure selenium. This supports the previous finding that the optical gap remains unchanged. No information on impurity centres could thereby be obtained. The spectral distribution of photoconductivity prior to being normalized also resembles that found in glassy selenium (fig. 4E) with maxima at $\sim$450 nm and $\sim$760 nm. It was not possible to detect any affect of the impurity on the relative intensity of the two peaks.

The values of the photocurrent per incident photon are much larger than those in non doped (four to five orders of magnitude) and oxygen containing (two orders of magnitude) glasses, showing that the photoresponse is strongly dependent on the impurity. As photoconductivity is a product of the quantum yield, lifetime and mobility of the photocarriers it is obvious that Cl and Br cause a common, increment in one or more of these parameters.

4.2.6 E.S.R. measurements

The ESR spectra of vitreous Se containing respectively 0.8 at % of chlorine and a similar percentage of bromine are shown in fig. 4O. It is obvious, by comparison with the non-doped Se curve, that those impurities do not contribute to any ESR signal. The broad absorption was not consistently observed (for example it appeared in a preliminar experiment with another Se-Br sample) and has to be attributed to some cause not inherent to the glasses themselves. It is therefore believed that those doped glasses, like pure Se and most chalcogenide glasses, are diamagnetic.

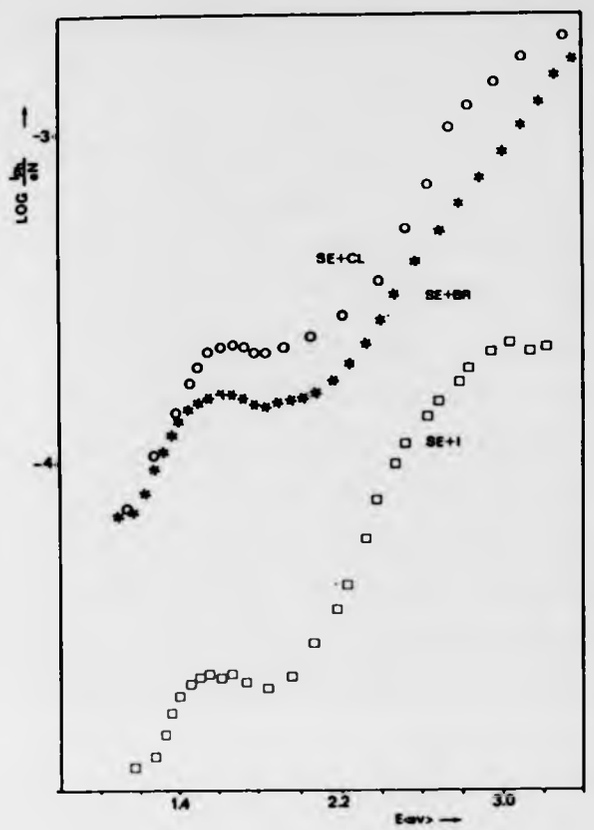

Fig. 4N - Spectral photoconductivity response per absorbed photon for $Se_{99}Br_1$ (•), $Se_{99.2}Cl_{0.8}$ (o) and $Se_{99.4}I_{0.6}$ (□) glasses.

Fig. 4O - E.P.R. spectra for selenium glasses containing 0.8 atoms of Cl and 0.6 at % of Br are displayed. The result for non doped selenium is also shown.

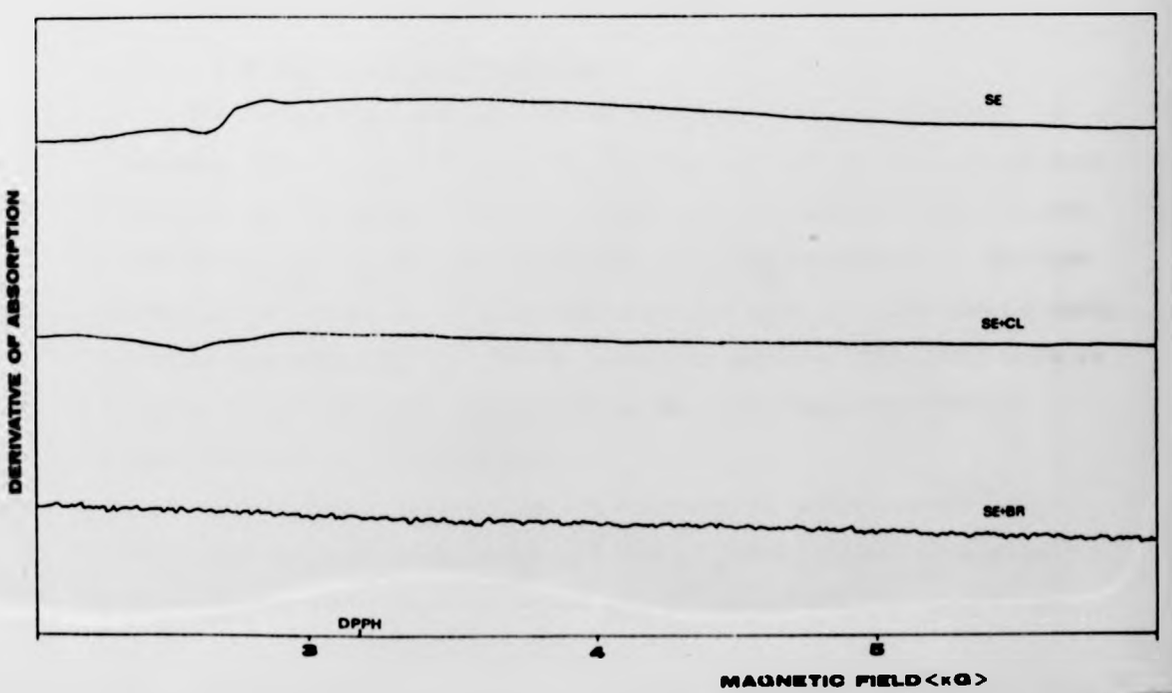

4.3 The Se-I system

4.3.1 Introduction

A set of glasses was produced in the compositional region of 10 p.p.m. to 3 at % by addition of elemental iodine to selenium pellets. The iodine used was claimed to be better than 4N pure.

Energy dispersive analysis of X-Rays was taken on some of the higher concentrations samples. For glasses prepared by addition of 4 and 2.3 at % of I, EDAX data indicated (3.2 ± 0.5) and (2.2 ± 0.6) atomic percent respectively (fig. 4.G). Actual iodine contents in the glasses are not therefore expected to differ substantially from nominal ones.

All samples were checked by XRD and showed no long-range order. For the reason mentioned in 4.2.1 it was not possible to prepare glasses with iodine concentration greater than approximately 4 at %.

The experimental results concerning this set of glasses are summarized in table B where they can be compared with the data obtained for the glasses doped with the other halogens.

4.3.2 D.C. conductivity experiments

The D.C. conductivity was determined, for all glasses prepared, by measuring two or more different specimens of the same nominal composition. The graph of the resistivity as a function of the additive atomic concentration is shown in fig. 4H, where each error bar represents the absolute error value. As it can be seen from there the curve presents qualitatively a close resemblance to that for Br containing glasses. Once more there is limited incorporation of the halogen in the glass which restrict the possible reduction in resistivity.

Quantitatively, however, Br and I effects do differ a great deal. The higher concentrations iodine containing glasses present an average value for the resistivity of $(2.2 \pm 0.4)10^{10}$ ohm.cm which is almost two

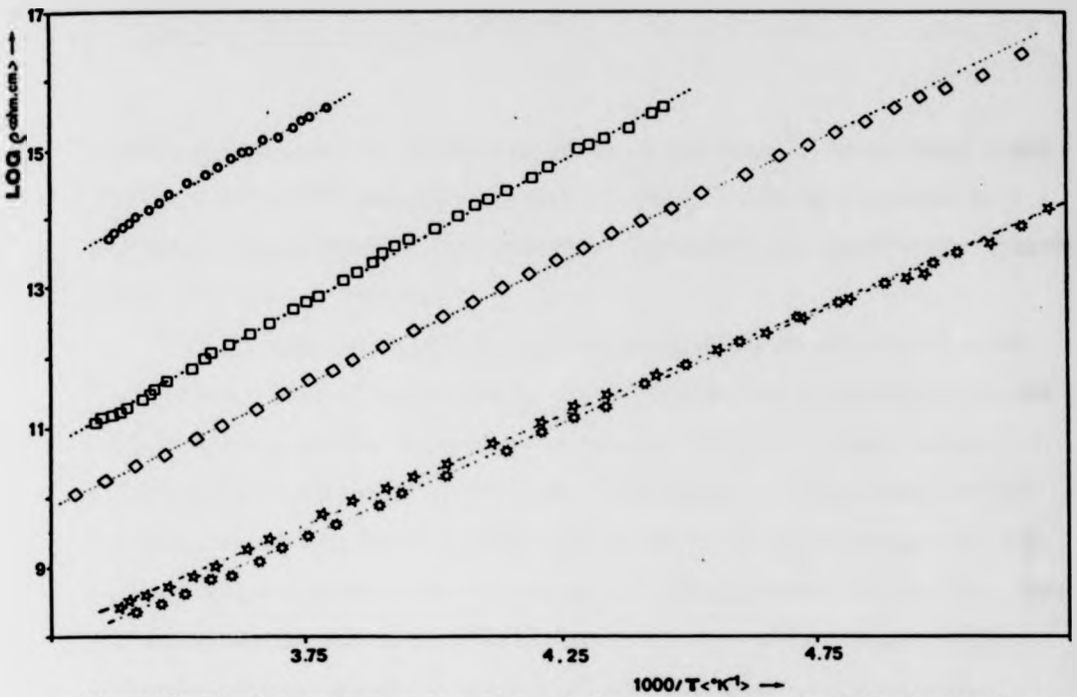

Fig. 4P -The log of ρ as a function of the reciprocal absolute temperature curve for the $Se_{97.3}I_{2.7}$ glass (◇) is compared to analogue curves for Se glasses, doped with similar amounts of Br (✡) and Cl (☆). The Arrehenius curves for glasses containing 0.1 at % of I (□) and 10 ppm of the same element (O) are also shown.

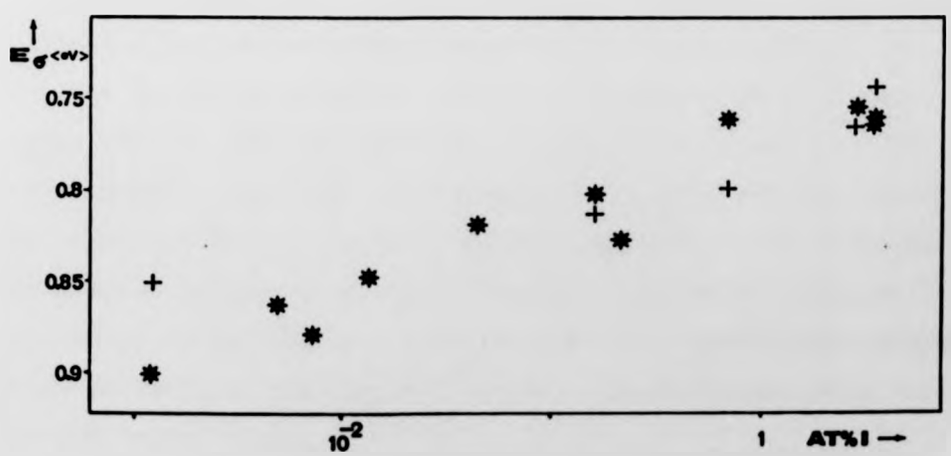

Fig. 4Q - The activation energy for iodine doped glasses is plotted against composition. (+) represent values as directly measured from activation curves; (✱) refer to values obtained from room temperature resistivities.

decades larger than the corresponding value for bromine or chlorine doped glasses. In comparison with the resistivity of vitreous Se itself a decrease of approximately five orders of magnitude was nevertheless achieved by the addition of iodine.

The D.C. electrical resistivity was also measured as a function of temperature. Some of the curves of log ρ versus the reciprocal absolute temperature are plotted in fig. 4P. From the slopes of those curves, values for the activation energy were determined. Although the overall effect is relatively small a reduction in the activation energy with the increase of iodine was observed and is graphically shown in fig. 4Q. For the higher iodine concentrations (> 0.5 at %) an average value for the activation energy of (0.75 ± 0.05) eV was found. That is indeed much higher than the values determined in the case of the other halogens as it is put in evidence in fig. 4P.

From the log ρ versus the reciprocal absolute temperature curves the pre-exponential factor C was also determined for each case. For the higher iodine levels an average value of $180 ohm^{-1}.cm^{-1}$ was obtained, which is of the same order of magnitude as the values observed in the chlorine and bromine containing glasses and therefore just one decade higher than the value for "pure" Se. As iodine glasses also manifest hole conduction (see 4.3.3) the above fact is in correspondence with the verified small sensitivity of the hole range towards iodine doping as occurs in the case of Cl doping (Takasaki et al. 1983). Thus, the increase in conductivity as a consequence of iodine incorporation appears to be due mainly to the observed decrease in the activation energy for the D.C. conductivity.

From fig. 4P it can be seen that the highest I content curve does not show a perfectly exponential behaviour with a departure from the

straight line taking place at $\sim -65^{\circ}C$. Due to the non-continuous nature of the change it cannot be explained by any eventual non linear temperature dependence of the mobility gap. It might therefore be a consequence of an increased role of hopping transport. However, as some glasses of the same system do not show the same behaviour and the region where the effect occurs is small and located at very high resistivity values, it is not possible to come to a definite conclusion about the process involved. The effect may be due simply to experimental error.

Iodine has less effect on resistivity than comparable doping level of the other two halogens (v.s.). This was somewhat expected in so far as the electronegativity difference between selenium and iodine is almost nought (0.1eV) in marked dissimilarity to the selenium-chlorine (0.6) and selenium-bromine (0.5) differences. The effectiveness of the selenium-selenium bond attack by iodine should therefore be rather small as the non-existence of selenium iodides in crystalline form seems to corroborate. Data on crystal growth from halogen doped Se melts also shows clear differences between iodine and bromine or chlorine doping (Keezer 1969). In addition, iodine has some tendency to form short chains by itself (e.g. Moeller 1961) which might introduce a competitive process and contribute as well to the limited incorporation of I in the glass structure.

At the same time it is also reasonable to assume that the reactivity of iodine with the terminal D^- centres will be of lesser importance. In either case, whether the activation energy is reduced by creation of C_2^+ centres or by destruction of negatively charged dangling bonds, the decrease of resistivity with the addition of iodine will be expected to differ quantitatively, as it does, with the observed in the Br-Se and Cl-Se systems.

Due to the relatively small change in activation energy, the experimental errors involved and the lack of further information about the iodine role in selenium, a detailed quantitative discussion is rather difficult. In particular, the application of equation (4.4) is not unambiguous, although fig. 4Q shows reasonable qualitative agreement, in the higher concentration part, with fig. 4K. However a clear jump in the Fermi level is not observed and so an estimation of the intrinsic defect states concentration N is not possible. Of course N can be assumed as equal to the value deduced from fig. 4K(b) and consequently, from the larger iodine additions, it is concluded that an impurity energy level is introduced at 0.04 eV below the Fermi level instead of the 0.18 eV found for the Cl and Br doped glasses. Nevertheless a question concerning the number M (effective concentration of impurity defects) should be raised since that number, as argued before, might be much smaller than the iodine concentration introduced. If this is so, then the above energy calculation is meaningless.

4.3.3 Thermoelectric power measurements

The determination of the Seebeck coefficient at room temperature was carried out for the glasses containing 2.7 at % and 0.6 at % of iodine. Both showed, as the other halogens doped glasses did, a positive S indicating p-type behaviour. The thermoelectric power values obtained were also of a similar order of magnitude.

For the first of the glasses the S dependence of the temperature was analysed (fig. 4M). From the slope of the Seebeck coefficient plotted as a function of the reciprocal absolute temperature an activation energy for thermoelectric power of (1.18 ± 0.08) eV was established. The ordinate intercept at the origin gave a temperature coefficient γ value

of 2.98 10^{-3} eV/degree. This activation value is higher than that obtained for the $Se_{99}Br_1$ glass and is of course much larger than the activation energy for conductivity. This result, although not understood, is in accordance with the earlier measurement (bromine doped glass). The value of γ is also close to the one measured for the $Se_{99}Br_1$ glass.

The 0.6 at % of iodine glass showed a higher value for S, suggesting that this might decrease with increasing dopant level. Recently other authors (Nagels et al.1983) reported the same effect in an iodine doped Se-Te glassy alloy. They also found p-type behaviour and values for the Seebeck coefficient of the same magnitude as those reported here.

4.3.4 Other experimental data

Other measurements included: IR spectroscopy, photoconductivity, D.S.C and E.S.R.

Absorption data at the optical edge for the $Se_{99.3}I_{2.7}$ glass indicated values for the optical gap, E_g, of 2.01 eV and for the slope of the exponential region, E_t, of 10 eV^{-1}. These resemble the values already described for the other glasses and so no significant alteration to the behaviour represented in fig. 4C (pure Se) was observed.

Infrared transmission curves show no special feature with the Se bands being preserved and no new band being found. That does not necessarily rule out the possibility of iodine atoms capping the Se chain. If a localized mode due to that grouping is possible, then relative to the position of the corresponding band in the Se+Cl glasses (29.8 μm), a shift towards higher wavelengths will be expected according to equation:

$$\upsilon = \frac{(c_{11}\, a)^{1/2}}{2\pi} \sqrt{\frac{1}{M_{Halogen}} + \frac{1}{nM_{Se}}}$$

In fact the $\sqrt{\frac{M_I}{M_{Cl}}}$ ratio largely dominates the bond lengths ratio $\frac{a_{Cl}}{a_I}$ and the elastic modulus c_{11} is larger for the smaller halogen. So the frequency ν shift creates overlap with the large selenium band at $\sim 40\,\mu m$.

The average IR. transmission was $\sim 64\%$ at the lower wavelengths. No dependence of the band intensity on iodine content was observed.

Photoconductivity results were obtained for the glasses containing 2.7 and 0.6 at % of iodine. The curve from the latter is shown in fig. 4N. From the figure it can be seen that the photoresponse resembles the ones obtained for Cl and Br doped glasses although a reduction in photocurrent by a factor of ~ 10 is observed.

DSC. experiments were carried out for the $Se_{97.3}I_{2.7}$ and $Se_{98}I_2$ glasses. The thermograms show an endothermic and an exothermic peak placed respectively at 313°K and 379°K. This indicates a small shift of the softening point of the glass towards lower temperatures which might be due solely to experimental error. The crystallization peak appears at a similar position and shows a shape like that for pure selenium (form A of figure 4F) and contrary to other reports (Nagels et al. 1983) the peak shows no assymetry. According to the discussion of 4.1.5, and since iodine will not act as a ring former this behaviour is expected.

EPR. experiments were performed for the $Se_{99.4}I_{0.6}$ glass. No new feature was observed further confirming that halogen impurities do not contribute to any magnetic absorption signal. Namely the sharp line at g = 2.0035 reported in literature (Abdullaev et al.1969b) could not be detected. As that line, obtained for heat treated materials, was interpreted as being due to a charge-transfer complex, built of an iodine molecule absorbed at a chain end, it is presumed that such a situation does not apply to iodine doped vitreous selenium.

4.4 Bromine doped Se-Te and Se-S glasses.

4.4.1 Introduction

Glasses with the following compositions $Se_{90}Te_{10}$, $S_{80}Te_{20}$, $Se_{90}S_{10}$ and $Se_{50}S_{50}$ were prepared by mixing Te or S power with selenium pellets. Glasses with similar concentrations (excepting the latter) but containing approximately 2 at % of bromine impurity were also prepared by adding the required amount of selenium bromide.

EDAX analysis of the samples showed good agreement with the compositions stated above. The EDAX spectra of some of those samples are shown in fig. 4G.

X-Ray diffractometer traces of all samples were also taken showing total absence of sharp peaks. The first broad peak occurs at a similar angle ($\theta = 13.7^{o}$) to that in the pure Se case and so there seems to be no significant modification in the average atomic distance inside the glass. However, the addition of tellurium contributes to a relative lowering of the second peak intensity which may be related to an increase in disorder.

4.4.2 DC conductivity measurements

The temperature dependence of the conductivity was measured for each one of the compositions with the exception of the $Se_{50}S_{50}$ glass. As discussed in 4.4.5 addition of sulphur diminishes Tg which makes the glass with that composition "unstable" (rubbery consistency) at room temperature and so impossible to measure with the experimental conditions available. It is in fact well known (Rawson 1967) that pure sulphur, if quenched to room temperature, is amorphous (plastic sulphur) but rapidly crystallizes.

The plots of the resistivity as a function of the reciprocal absolute temperature are shown in fig. 4R. As a first important feature

4.4 Bromine doped Se-Te and Se-S glasses.

4.4.1 Introduction

Glasses with the following compositions $Se_{90}Te_{10}$, $S_{80}Te_{20}$, $Se_{90}S_{10}$ and $Se_{50}S_{50}$ were prepared by mixing Te or S power with selenium pellets. Glasses with similar concentrations (excepting the latter) but containing approximately 2 at % of bromine impurity were also prepared by adding the required amount of selenium bromide.

EDAX analysis of the samples showed good agreement with the compositions stated above. The EDAX spectra of some of those samples are shown in fig. 4G.

X-Ray diffractometer traces of all samples were also taken showing total absence of sharp peaks. The first broad peak occurs at a similar angle ($\theta = 13.7^{o}$) to that in the pure Se case and so there seems to be no significant modification in the average atomic distance inside the glass. However, the addition of tellurium contributes to a relative lowering of the second peak intensity which may be related to an increase in disorder.

4.4.2 DC conductivity measurements

The temperature dependence of the conductivity was measured for each one of the compositions with the exception of the $Se_{50}S_{50}$ glass. As discussed in 4.4.5 addition of sulphur diminishes Tg which makes the glass with that composition "unstable" (rubbery consistency) at room temperature and so impossible to measure with the experimental conditions available. It is in fact well known (Rawson 1967) that pure sulphur, if quenched to room temperature, is amorphous (plastic sulphur) but rapidly crystallizes.

The plots of the resistivity as a function of the reciprocal absolute temperature are shown in fig. 4R. As a first important feature

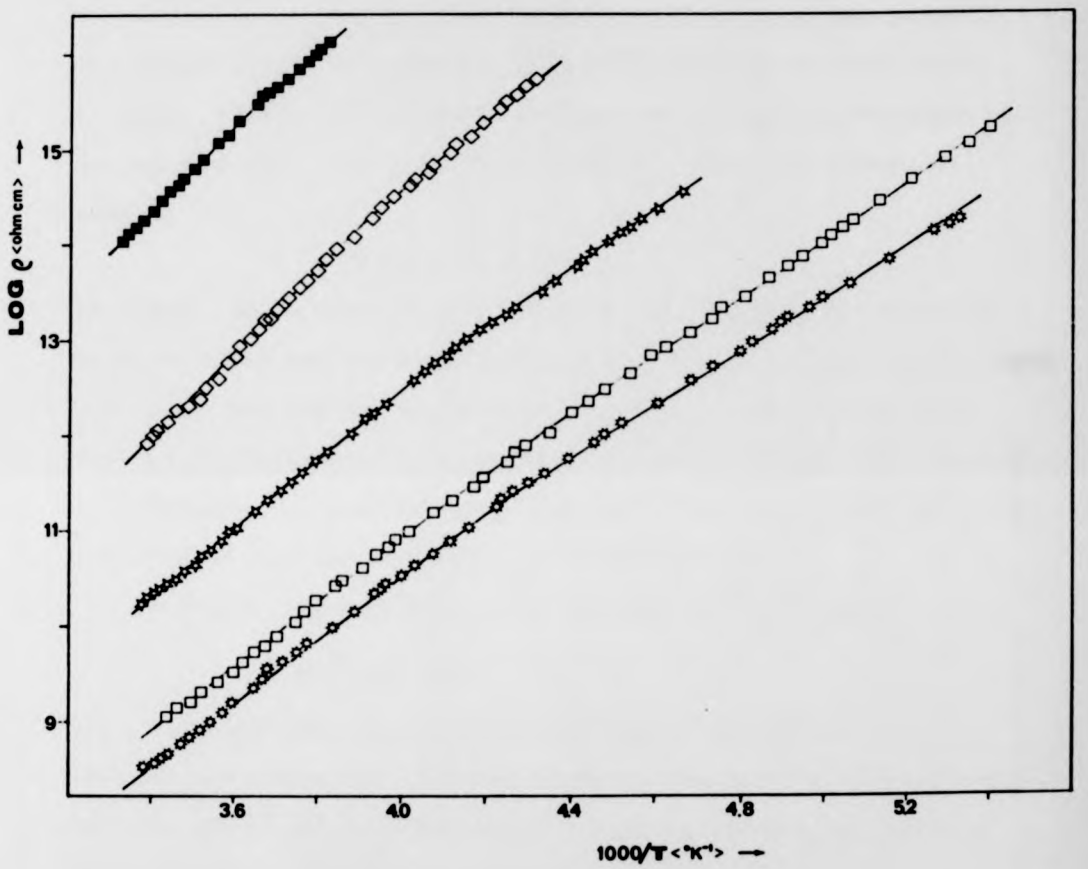

Fig. 4R - Log ρ vs. $^{1}/_{T}$ curves for several selenium containing glasses: (■) $Se_{90}S_{10}$; (◇) $Se_{90}Te_{10}$; (☆) $Se_{80}Te_{20}$; (□) $Se_{90}S_{8}Br_{2}$ and (✡) $Se_{90}Te_{18}Br_{2}$.

it is noticeable that there is a slight curvature in the log ρ vs $1/T$ curves, the activation energy decreasing when the temperature goes down. The effect is more marked in the tellurium containing glasses although the overall change in activation energy from high to low temperatures is small (~10%). Such a change cannot be attributed to a variation of the mobility gap with temperature even if a non-linear dependence such as

$$E_g(T) = E_o - \gamma T^n$$

is sought. In fact that sign is unquestionably negative as determined by Mulls (1970) and therefore the expected form of the log ρ vs. $1/T$ curve will be concave and not convex as experimentally observed. Besides, since γ coefficients are, in non-crystalline semi-conductors, typically 10^{-4} eV/degree one would not anticipate any significant effect except at temperatures much higher than those encountered here.

To explain the curvature, a fit was tried to the formula

$$\rho \propto T^r \exp\left(\frac{E_\sigma}{kT}\right)$$

but without success. Experimental error may be disregarded since the results were consistently reproduced whereas for previous glass systems, and with the exception of two iodine containing samples, good fitting to the Arrhenius relation was obtained.

It is therefore probable that the curvature is due to a change in the conduction regime with an increasing role played by localized states at low temperatures. This may originate from an enlargement of the localized tails triggered by an increase in disorder or from a decrease in the mobility gap (which occurs in the Te alloys). This will make the difference $E_F - E_A$ relatively (to $E_F - E_V$) small enough so that localized conduction becomes competitive. An increase of the localized states

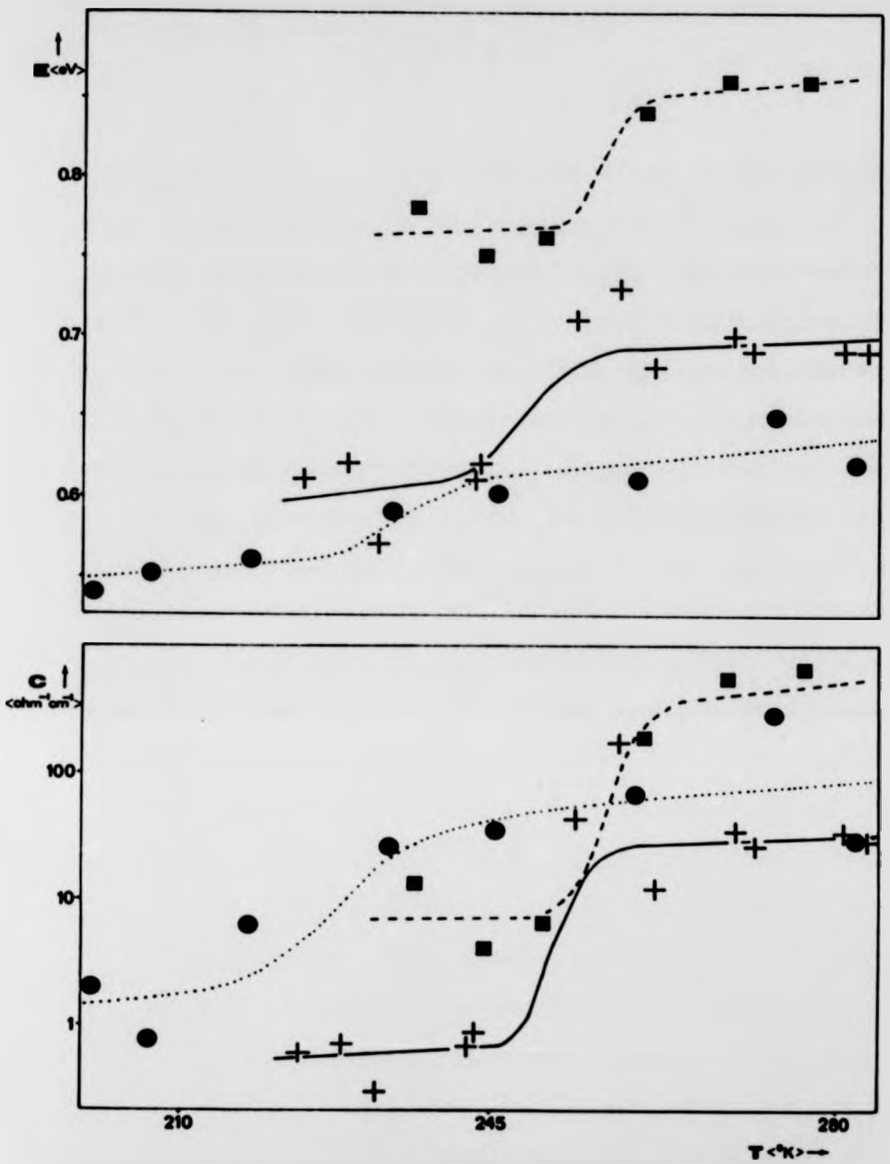

Fig. 4S - Plots of the activation energy and C factor as a function of the absolute temperature for the Se-Te glasses: (■) $Se_{90}Te_{10}$; (+) $Se_{80}Te_{20}$ and (●) $Se_{80}Te_{18}Br_2$.

density will account also for that occurrence. In fact the glasses seem to be characterised by two distinct sets of values regarding activation energy and pre-exponential factor which may describe two different conduction mechanisms, one at relatively high temperature and another at lower temperatures. To illustrate that the data may be adequately fitted by two different activation energies and two different C values, these parameters were plotted as a function of T. That is shown in fig. 48 . The conclusion is nevertheless limited by the relatively small variation observed. For the sulphur alloys the variation is even less. The spread of C values for Se-Te glasses found in literature (Hulls 1970; El-Mously and El-Zaidia 1973; Mehra et al.1977; Nagels et al. 1983), may constitute proof that a delocalised-localised transition takes place at temperatures close to room-temperature.

With regard to the Se-Te glasses it was observed that addition of tellurium progressively reduces the resistivity. This is a well known fact. Such a decrease appears to be related mainly to a diminution of the activation energy. This lowering in the activation energy was expected and it accompanies the decrease of the optical gap due to the introduction of tellurium as observed by optical absorption and photo-conductivity measurements (see sections 4.4.3 and 4.4.4). It is also known that the electrical gap of a-Te is smaller than that of a-Se even though a comparison between materials prepared by different methods should always be carefully considered. The values for the activation energy and pre-exponential factor as determined by the least squares method (that is considered as parameters of the "imposed" Arrhenius formula) are shown in table C. Activation energies compare reasonably well with others found in the literature referred to earlier.

The values for the pre-exponential factor C are contained in the interval (15, 125) that is similar to the values obtained for the other glass systems. A decrease of C caused by Te addition seems to occur but it is small and so difficult to assess. Mehra et al. (1977) reported such a decrease but this was not verified by others (Nagels et al.1983). Drift mobility experiments are also inconclusive. Kolomiets and Lebedev (1966) reported that addition of Te up to 3 at % does not alter hole drift mobility (Se-Te glasses are p-type as verified by Nagels et al. 1983). Schottmiller et al. (1970) found however a decrease of that parameter by more than an order of magnitude when 1% of Tellurium was added. Larger concentrations further lower the hole mobility, which means an increase in the density of localised states. This may justify the apparent observed augmented role played by localised conduction below $\sim 240^{\circ}K$.

The incorporation of 2 at % Br lowers the resistivity of both $Se_{90}Te_{10}$ and $Se_{80}Te_{20}$ to similar values which are also close to that observed for the equivalent Br doped selenium glasses. In addition, the activation energy determined for the $Se_{80}Te_{18}Br_2$ glass was ~ 0.6 eV, close to that obtained for the higher Br concentrations of the Br-Se system, although this result is an average value since the glass cannot be characterized by a single activation energy. Therefore in the Se-Te alloy case

$$E_{\sigma \text{ doped}} \neq \frac{2}{3} E_{\sigma \text{ nondoped}}$$

which does not support the hypothesis of halogen atoms going at D^- centres.

The activation energy change seems again to be the determining factor in the increase of the conductivity since the pre-exponential factor remains at a value around 50 $\Omega^{-1}cm^{-1}$.

These results are difficult to interpret. Incorporation of tellurium which is isoelectronic with selenium supposedly increases the chain fraction as indicated by a reduction of the viscosity (Lanyon 1969) and by the existence of only hexagonal Te (isomorphous with hexagonal Se) in crystalline form. Tellurium might therefore be expected to substitute for Se in the chains. As the electronegativity difference Te-Br (0.7 eV) is larger than that of Se-Br (0.5 eV) it is expected that Br will "attack" tellurium atoms preferentially. Then the expected C_2^+ acceptor centres may correspond to a different energy level than in the Se-Br glasses. However, since the mobility gap changes due to the presence of tellurium the estimate of the acceptor level location is not easy. More results in the series $Se_{100-x}Te_{x-2}Br_2$ are needed before clarification of the problem is possible.

In the case of the selenium-sulphur glasses it was observed that addition of 10 at % of sulphur had no marked effect with the values obtained for the room temperature resistivity and activation energy being very close to those measured for pure vitreous Se. The factor C was reduced by a factor of 6 which, due to the narrow temperature range, is not very significant. Reports on drift mobility (hole) experiments show no (Kolomiets and Lebedev 1966) or little decrease (Schottmiller et al. 1970) when sulphur concentrations of a similar kind ($\sim$ 7%) are introduced.

The results obtained may be compared with those described by El-Mously and El-Zaidia (1973) who found similar activation energy but values of σ and C about two orders of magnitude greater.

When bromine is added there is also a large increase in conductivity. The value of C is of the same order than in the Se-Br and Se-Cl systems, and the activation energy as well as the room temperature resistivity are just slightly higher. No great difference was expected since the S and Se

electronegativities are very similar and no significant difference in the optical gaps were observed (see 4.4.4). The small difference may be related to an enrichment of the ring fraction caused by the addition of sulphur (Ward and Myers 1969; Schottmiller et al. 1970). Sulphur in fact forms, by itself, a zero dimensional network glass (eight fold rings). Infrared transmission also seems to indicate the presence of S_8 rings.

The results for the Se-S glasses are presented in table C.

4.4.3 Infrared data

The plot of the absorption coefficient at the optical edge as a function of the photon energy for the $Se_{90}Te_{10}$ glass is shown in fig. 4C. The $Se_{88}Te_{10}Br_2$ sample is also characterized by a similar curve. The expected exponential behaviour was observed with the curve showing a slope greater than that observed for pure selenium. The value for E_t of 14.9 eV^{-1} determined is well inside the range of values observed in non-crystalline semiconductors (Tauc 1974). The curves were shifted towards lower energies due to the addition of tellurium which is a well known fact (e.g. Kamprath 1962). An estimation of Eg, the mobility gap, taken once more as the energy for which the absorption coefficient equals $10^3 cm^{-1}$ gave 1.76 eV. This result is compatible with the measured activation energy for conductivity. Comparing both values the Fermi level location is fixed at 0.06 eV below the middle of the gap.

Introduction of 10 at % of sulphur did not contribute to any significant modification of the parameters characterizing the optical absorption edge of pure selenium. This is consistent with the observed electrical behaviour.

Infrared transmission spectra of all samples were taken in the range 2 to 55.5 μm. Once more, transmission around 65% was observed. The results are shown in fig. 4T. Incorporation of Te leads to two additional bands at $415cm^{-1}$ and $635cm^{-1}$. The latter has already been described by

electronegativities are very similar and no significant difference in the optical gaps were observed (see 4.4.4). The small difference may be related to an enrichment of the ring fraction caused by the addition of sulphur (Ward and Myers 1969; Schottmiller et al. 1970). Sulphur in fact forms, by itself, a zero dimensional network glass (eight fold rings). Infrared transmission also seems to indicate the presence of S_8 rings.

The results for the Se–S glasses are presented in table C.

4.4.3 Infrared data

The plot of the absorption coefficient at the optical edge as a function of the photon energy for the $Se_{90}Te_{10}$ glass is shown in fig. 4C. The $Se_{88}Te_{10}Br_2$ sample is also characterized by a similar curve. The expected exponential behaviour was observed with the curve showing a slope greater than that observed for pure selenium. The value for E_t of 14.9 eV^{-1} determined is well inside the range of values observed in non-crystalline semiconductors (Tauc 1974). The curves were shifted towards lower energies due to the addition of tellurium which is a well known fact (e.g. Kamprath 1962). An estimation of Eg, the mobility gap, taken once more as the energy for which the absorption coefficient equals $10^3 cm^{-1}$ gave 1.76 eV. This result is compatible with the measured activation energy for conductivity. Comparing both values the Fermi level location is fixed at 0.06 eV below the middle of the gap.

Introduction of 10 at % of sulphur did not contribute to any significant modification of the parameters characterizing the optical absorption edge of pure selenium. This is consistent with the observed electrical behaviour.

Infrared transmission spectra of all samples were taken in the range 2 to 55.5 μm. Once more, transmission around 65% was observed. The results are shown in fig. 4T. Incorporation of Te leads to two additional bands at $415 cm^{-1}$ and $635 cm^{-1}$. The latter has already been described by

TABLE C

Composition	Se_9Te_1	Se_8Te_2	Se_9S_1	Se_5S_5	$Se_{8.8}Te_1Br_{0.2}$	$Se_{8.8}S_1Br_{0.2}$
σ_{RT} ($ohm^{-1}.cm^{-1}$)	$8.2\ 10^{-13}$	$3.6\ 10^{-11}$	$3.6\ 10^{-15}$		$2.7\ 10^{-9}$	$1.2\ 10^{-9}$
E_σ (eV)	0.82	0.67	0.84		0.60	0.63
C ($ohm^{-1}.cm^{-1}$)	125	15	2		50	72
E_t (eV^{-1})	14.9		9.5			
E_g (eV)	1.76		2.12			
I.R. bands(cm^{-1})	415; 635 (~200)	415; 635 (~200)	457; 606 803; 887	457;606;803 887; 1300		
E_{Ph} (eV)	1.56	1.45	1.68	1.94		
D.S.C. (°K)						
- endothermic	327		313;441,463	434; 457		314;~467
- exothermic	398		391	399		356; 391
E.S.R.			No extra signal			no extra signal

Summary of results for the Se-Te and Se-S based glasses.

I.R. bands listed do not include those for pure-selenium.

Mehra et al (1977) on samples prepared in evacuated ampoules. Vasko (1969) also reports a band at $\sim$ 650 cm^{-1} which he attributes to TeO_2 impurity. This band may however have a different origin since in the preparation method used by the former author it is thought that the presence of oxygen was unlikely. SeO_2 is removed from the melt by out-gassing (Vasko 1969) - as confirmed by the difficulties in obtaining SeO_2 bands, see 3.1.4 - and the same should happen with TeO_2 since the melting temperature used was higher. Tellurium leads to a cut-off at $\sim$ 270cm^{-1} which might be due to a further band at $\sim$200cm^{-1}.

Introduction of sulphur leads to additional bands at 457, 606, 803 and 887 cm^{-1}. A band at 1300 cm^{-1} only appears in the $Se_{50}S_{50}$ glass. All the bands except the 803cm^{-1} occur, relative to each other, at the same places as those reported by Vasko (1969) for pure vitreous sulphur, although this author did find slightly higher wave numbers. The 803cm^{-1} band was not apparent in that report. The 457cm^{-1} band is probably associated with a stretching mode of the S_8 molecules (Lucovsky 1979) with the corresponding bending mode not being visible as it coincides with a selenium band.

The spectrum, due to sulphur, of the Se-S alloy agrees fairly well with that of rhombic sulphur. In addition, it is equivalent to that of non-crystalline selenium if the correspondence:

Wave number of S band $\simeq$ 1.8 wave number of Se band,

is considered. This wave number ratio is similar to the

$$\left[\frac{m_{Se} \cdot r_{Se}^3}{m_S \cdot r_S^3}\right]^{\frac{1}{2}}$$

ratio which Lucovsky et al.(1967) had already verified for the Raman frequencies of the A_1 mode of the Se_8 and S_8 molecules. Lucovsky suggested

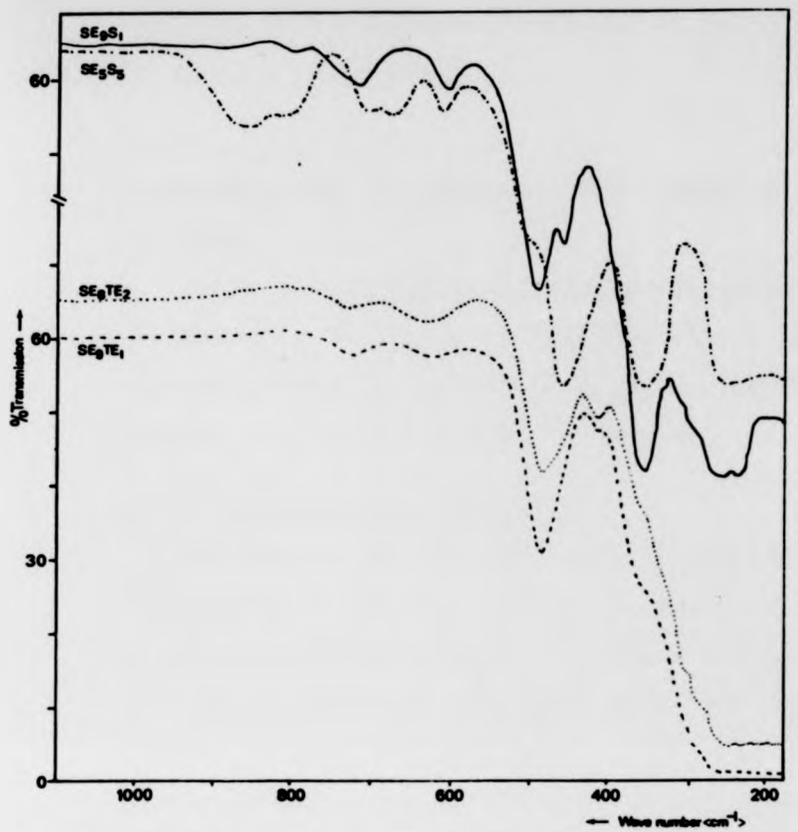

Fig. 4T - I.R. spectra for Se-S and Se-Te glasses.

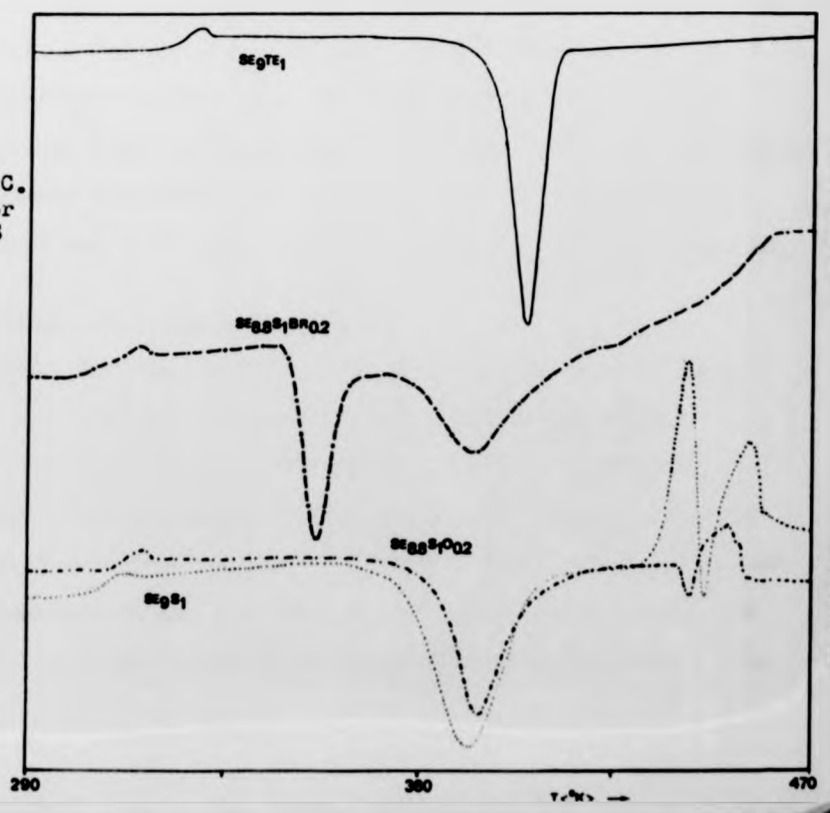

Fig. 4U - D.S.C. thermograms for Se-Te and Se-S glasses.

consequently that the short-range forces should be similar in the two molecules.

In the case of doping with bromine the additional incorporation of the element in the Se-S or Se-Te glasses did not cause the appearance of any further band. In particular the 531cm^{-1} band observed in S_2Br_2 by Ketelaar et al.(1956) could not be detected.

4.4.4 Photoconductivity measurements

The photoresponses of the glasses are shown in fig. 4V . It is obvious from the normalized curves that addition of Te shifts the photoconduction peak towards lower energies which is in accordance with both optical absorption and electrical data that indicated a decrease in the mobility gap. Tellurium addition leads to an increase whereas incorporation of sulphur does not contribute to any appreciable change in the photocurrent. Sulphur nevertheless seems to shift the peak towards higher energies as clearly visible in the $Se_{50}S_{50}$ sample. However, due to the reasons discussed before, the sample response showed some instability and thus the result needs confirmation. In the case of the non-normalized photocurrent curves the noticeable feature is that the low energy peak present in the Se and Se-S glasses is flattened out in the Se-Te samples.

4.4.5 Differential scanning calorimetry.

Fig. 4U shows the DSC thermograms obtained for the Se-S and Se-Te glasses. The softening point appears to be shifted toward higher temperatures by addition of Te whereas addition of S has apparently the opposite effect. The crystallization peak in the $Se_{90}T_{10}$ glass was shifted towards higher temperatures ($\sim 398^{\circ}K$), that is, about $25^{\circ}K$ higher than the crystallization peak for pure Se. The differences between the pure alloy and the bromine doped alloy thermograms were negligible. The

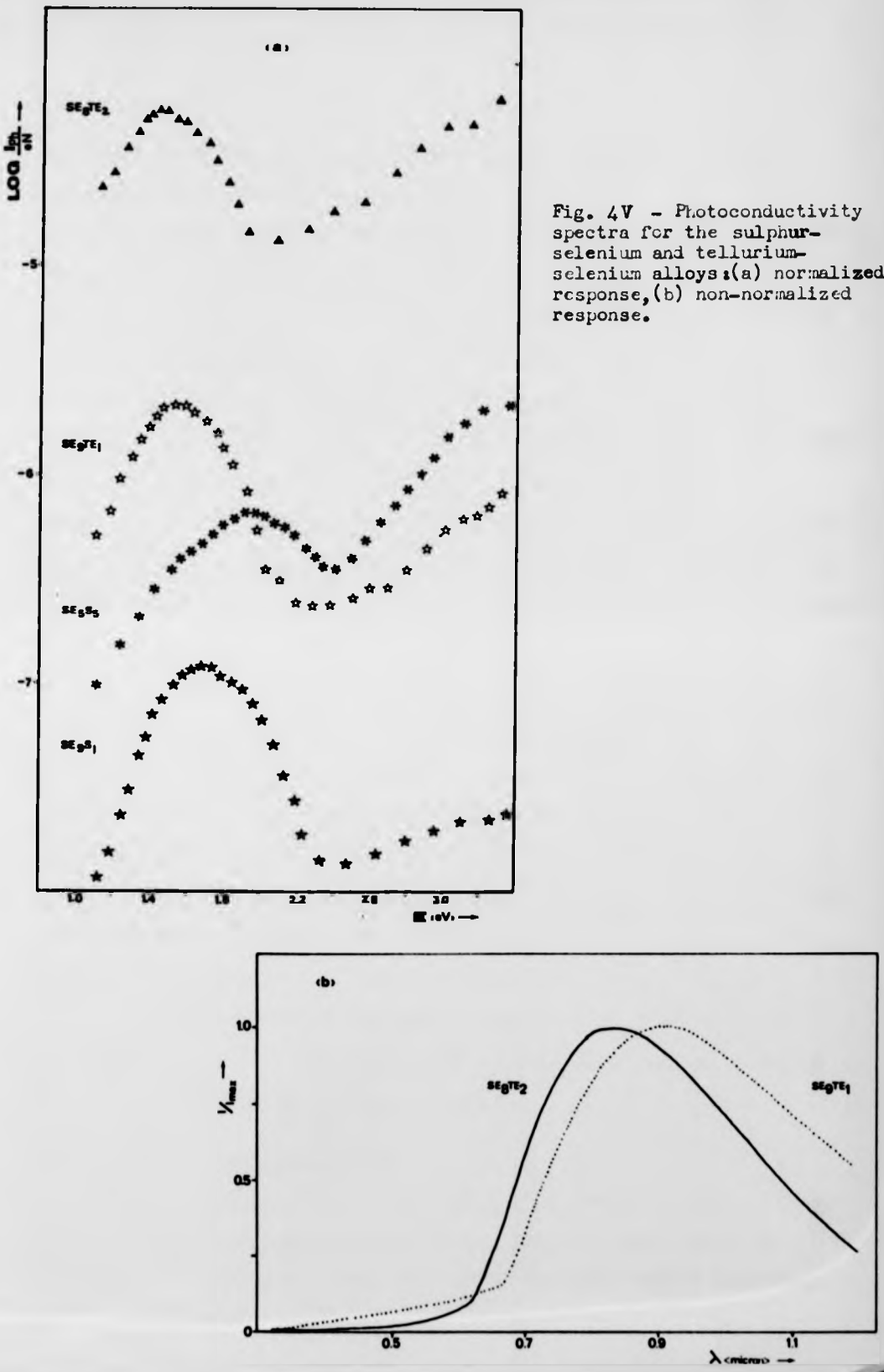

Fig. 4V - Photoconductivity spectra for the sulphur-selenium and tellurium-selenium alloys:(a) normalized response,(b) non-normalized response.

tendency of the DSC parameters to increase on addition of Te has been reported recently by Nagels et al. (1983).

The results concerning the selenium-sulphur glasses are more interesting. The endothermic peak temperature appears in the $Se_{90}S_{10}$ alloy at 313°K showing a slight decrease in the glass transition temperature. This was expected since sulphur forms a glass by itself of very low softening point (-27°C) (Rawson 1967), which explains the rubbery consistence at room temperature of the $Se_{50}S_{50}$ glass. The crystallization peak is very broad taking place at 391°K, that is at higher temperature than in pure Se. The melting process is characterized by two peaks at 440-442 and 456-470 °K. That is very different from what happens in pure Se where a single peak occurs. Such a fact can be interpreted as indicating that crystallization leads to two phases of different compositions.

The addition of Br has no apparent effect upon the softening point peak but strongly influences both the crystallization and the melting parts of the thermograms. Addition of Br leads to an additional narrow crystallization peak at a much lower temperature (356°K) but keeps the broad peak at 391°K with a reduction in its area. On melting, the first peak disappears probably as a shoulder of the second (which is maintained) as the melting starts at similar temperatures. This is similar to the observation by Nagels et al. (1983) on addition of iodine to $Se_{65}Te_{35}$ glass. It was also noticed that oxygen doping led to a third distinct thermogram (fig. 4V). The $Se_{50}S_{50}$ glass did not show any qualitatively new fact in relation to the $Se_{90}S_{10}$ alloy.

4.4.6 Field effect measurements

The I-V characteristic for a $Se_{90}Te_{10}$ glass sample is shown in fig. 4W(a). The curve presents three distinct parts: an ohmic region is followed by regions governed by a quadratic law and a higher power law

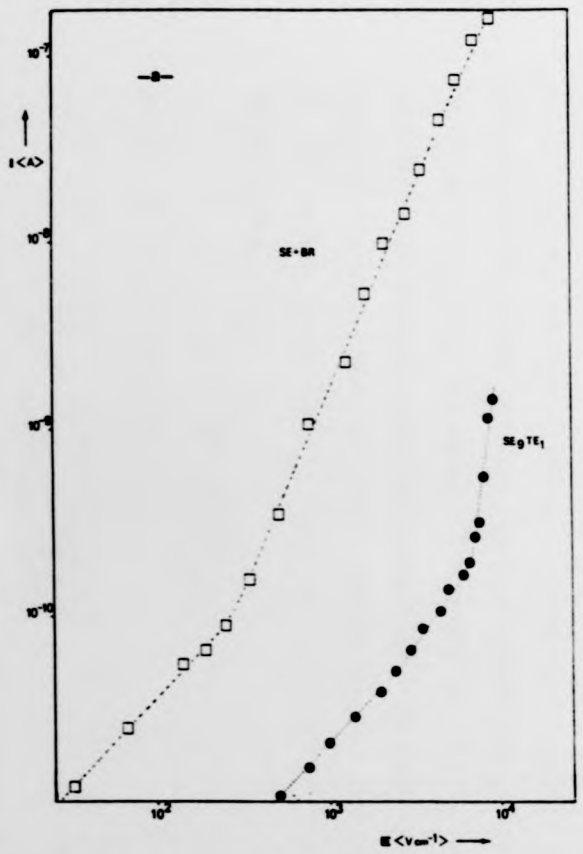

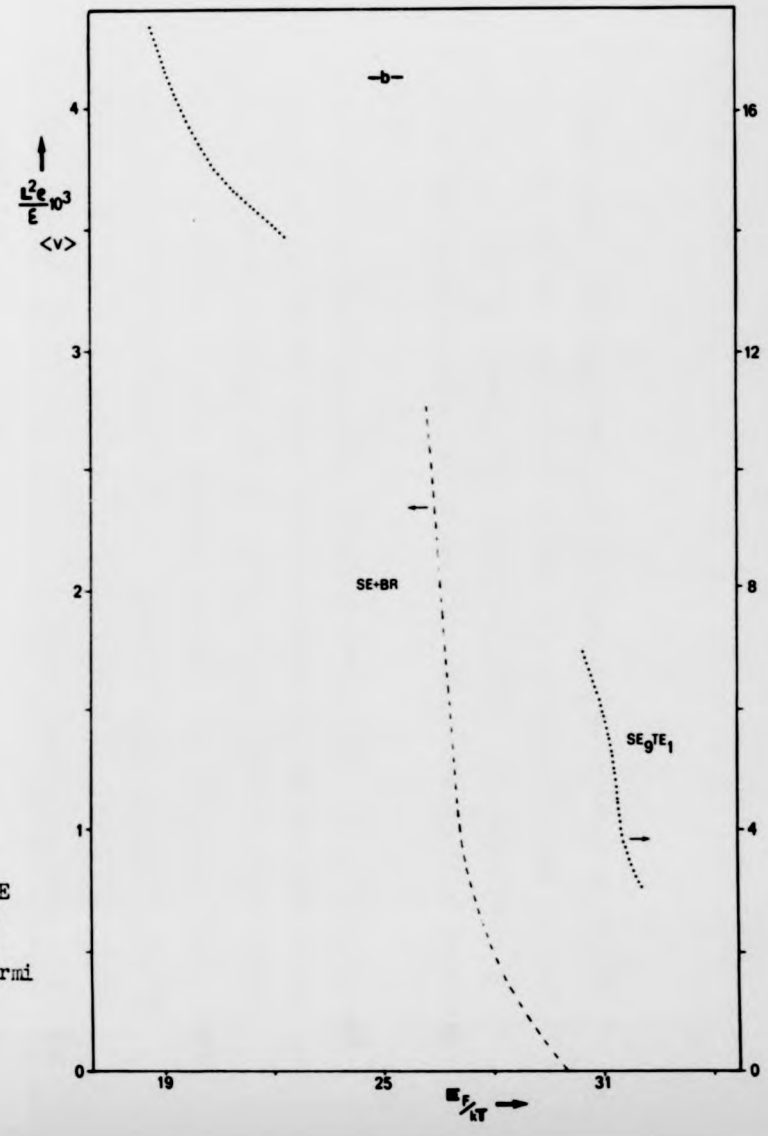

Fig 4W - (a) Log-log plots of the steady-state current vs. E for two different Se based glasses. The Br doping level of the upper sample was estimated at 60 ppm.
(b) The plot of $L^2\rho/\varepsilon$ as a function of the quasi-Fermi level for the same glasses is shown.

respectively. The departure from linearity occurs at about 3000Vcm^{-1}. As a time constant larger than one hour was found, the voltage was kept constant for a day before each reading was taken. The observation of large decay times in this kind of material is not unique (e.g. Fritzsche 1974).

Since seemingly no proper fitting could be made with a Poole-Frenkel type of effect the form of the I-V curve suggests that the increase in conductivity with the electric field may be attributed to "space charge limited currents". Similar interpretation has been given for field effect experiments on chalcogenides by, for example, Lanyon (1962), on Se, and Hulls (1970) on Se-Te glasses. However Adler (1981) argues that field effect in these kind of materials is unlikely. Fig. 4W(a) shows also data obtained for a Br containing Se glass.

The analysis of the experimental curves was made using the technique proposed by Pfister (1974). Such a technique allows a direct determination of the trapping centres distribution, whatever it may be, instead of assuming an "a priori" specific charge distribution, an assumption on which previous models are based. The method is valid provided that the conditions of constant mobility, homogeneous trap distribution and independence of the electric sample length from the voltage are satisfied. In this case it is possible to establish equations for the carrier density at the anode,

$$n = \frac{L}{e\mu} \cdot \frac{d\,(1/J)}{d\,(V/J^2)} \qquad (4.5)$$

and for the space charge density ρ ,

$$\frac{L^2\rho}{\epsilon} = \frac{d}{d(1/J)}\left[\frac{d\,(V/J^2)}{d\,(1/J)}\right] \qquad (4.6)$$

Together the two equations yield a relationship between ρ and n.

If the expression

$$E_F = kT \ln \left(\frac{N}{n}\right)$$

is then considered - N being the band density of states - it is possible, recurring to (4.5),

$$E_F = kT \ln(N\mu) + kT \ln \left[\frac{d(E/J^2)}{d(1/J)}\right]$$

Taking the energy reference level at $kT \ln(N\mu)$ an equation relating the quasi-Fermi energy to the directly available data, whatever the analysed region, can be obtained:

$$E_F = kT \ln \left[(2 - 1/\alpha) \frac{\Delta}{A} E^{1-\alpha} \right] \qquad (4.7)$$

A and α are the parameters which appear in the I-E characteristic. ($I = AE^{\alpha}$) and Δ stands for the sample area.

Eq. (4.7) together with e.g. (4.6) allow the plotting of ρ as a function of E_F. The curve of $\frac{L^2\rho}{\epsilon}$ versus E_F/kT for the $Se_{90}Te_{10}$ sample is shown in fig. 4W(b) where it is compared with a similar curve for the Se glass doped with 60 p.p.m. of Br. For the latter two samples of different thicknesses were measured. The dependence on L observed is of the form $J \propto 1/L^a$, with $4.5 < a < 3$ which is compatible with S.C.L.C. However, given the number of samples analysed, the result cannot be conclusive. From fig. 4W(b) it seems that Te contributes to an increase in the density of localized states which is qualitatively in accordance with a decrease in the value of the pre-exponential constant C (see 4.4.2).

Further speculation on these results seems inappropriate since the data for current dependence on sample thickness is so limited. In addition, the check on whether the trap density varies with temperature or not (Pfister 1974) could not be made and the quadratic part after the trap filled limit region was not reached and so electrical breakdown could not be ruled out.

4.5 Other selenium doped glasses

4.5.1 Introduction

The role of several other additives, besides halogens, on the electrical conductivity of vitreous selenium was also investigated. This included univalent (Ag, Cu, Tl and Na) and trivalent (Al, Bi and Sb) elements. All the foreign atoms were added to the host selenium in the elemental form. Once again EDAX measurements were made whenever possible (Cu, Tl, Sb) to check the presence of the impurity. Other than the determination of the resistivity, infrared and photoconductivity data were also taken. The results are summarized in table D.

4.5.2 Atomic doping with univalent elements

Silver, copper and thallium were added in percentages up to 1.5 at % approximately. All these elements seem to have a strong effect upon crystallization of Se into hexagonal form. Addition of univalent elements reduces viscosity, and also the complexity of the Se melt and therefore the crystallization kinetics are improved (Keezer 1969). For that reason glasses containing one of those elements could be prepared only by faster quenching upon a metal plate instead of the silica plate previously used. The problem in preparing sodium doped glasses was exacerbated by the limited solubility of Na in the selenium melt. 300 p.p.m. was in this case the maximum concentration possible.

All the dopants have a significant effect on the transmission infrared spectra of glassy selenium (fig. 4Y). Sodium causes new bands at 12.2 and 13.0 microns which have been already described by Tausend (1969). The bands at ~ 9 and ~16 microns also reported there were not observed in this work although similar sodium concentrations are concerned. Thallium leads to a new strong band at 14.5 μm and to two others at 13.1 and 24.0 μm

TABLE D

Doping level (at %)	1.5 Ag	1.5 Cu	1.5 Tl	0.03 Na	0.05 Bi	3.0 Sb	0.5 Al
σ_{RT} ($ohm^{-1}.cm^{-1}$)	$5.1\ 10^{-15}$	$2.7\ 10^{-16}$	$3.5\ 10^{-15}$	$3.1\ 10^{-15}$	$1.1\ 10^{-16}$	$2.6\ 10^{-15}$	$6.6\ 10^{-14}$
E_σ (eV)	0.99		1.07	1.05			0.86
C ($ohm^{-1}cm^{-1}$)	3400		6000	2500			36
I.R. bands (cm^{-1})	350		417; 690 763	770; 803	575;657;667 700;763;813	605	415
E_{Ph}(eV)	1.85	1.82	—	1.74			

Summary of results for vitreous Se doped with small amounts of various elements. I.R. bands listed are additional only.

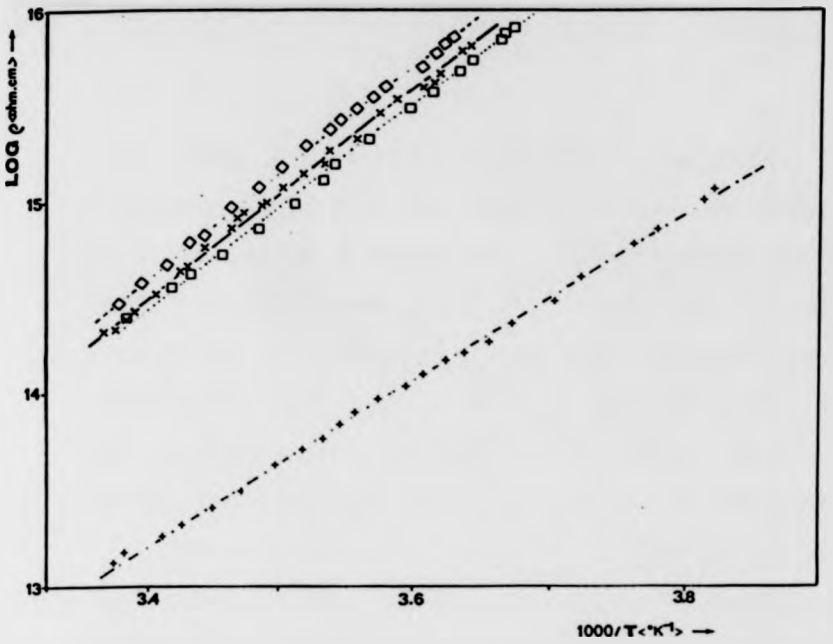

Fig. 4X - Log of the resistivity as a function of the reciprocal absolute temperature for Se glasses doped with small amounts of several elements: (◇) 300 ppm of Na; (×) 1 at % of Ag; (□) 1 at % of Tl and (+) 300 ppm of Al.

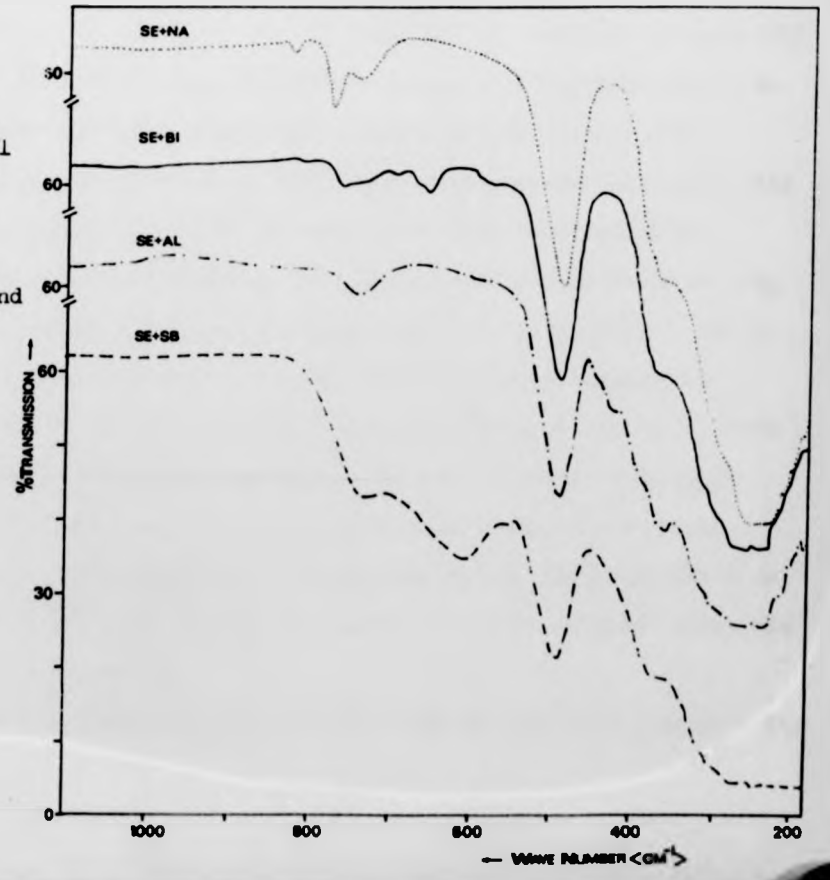

Fig. 4Y(a) - I.R. spectra for glassy Se doped with small amounts of the following elements: 300 ppm (Na); 500 ppm (Bi); 0.5 at % (Al) and 3 at % (Sb).

only visible for the higher Tl content (~1.5 at %). This is a completely different picture from that observed by the same author (Tausend 1969). Silver causes the disappearance of the Se shoulder at ~ 28 μm and also diminishes the transmission for wave numbers greater than 800 cm^{-1}. Copper does not contribute any new band but has a larger effect on the transmission leading to a "cut-off" beyond 500 cm^{-1}. A decrease in the optical gap is not consistent with the electrical and photoconductivity data, which might mean that some metal is not chemically bound to selenium.

The effect of all the univalent elements on the D.C. conductivity of vitreous Se is very similar (fig. 4X). No significant change was observed with the resistivity staying high ($> 10^{14}$ ohm cm) and close to that of "pure" selenium. However, both the activation energy E_σ and the pre-exponential constant C increased substantially being similar in all the glasses measured ($E_\sigma \sim$ 1.00 eV; $C > 10^3$ $ohm^{-1}cm^{-1}$). Twaddell et al.(1972) also reported 1.00 eV for the activation energy of K doped glasses. In addition, it seems now well established (Kolomiets and Lebedev 1966; Takasaki et al.1983; Pfister et al.1978) that univalent metals drastically reduce hole drift mobilities. At the same time there are indications that such elements do cause a change to n-type behaviour in Se containing glasses (Khan and Adler 1984) and selenium melt (Yao et al.1983). These facts might be due to the donor character of the elements considered leading to conversion of D^+ centres to negatively charged ones (D^-) which will account for the increased trapping of holes. If those monovalent elements lead to conductivity to change to n-type, an increase of the activation energy is possible since, in pure selenium, the Fermi level is located below mid gap. The optical gap width (> 2 eV) is also compatible with the E_σ value observed.

Nevertheless, the striking fact is the apparent relative insensitivity

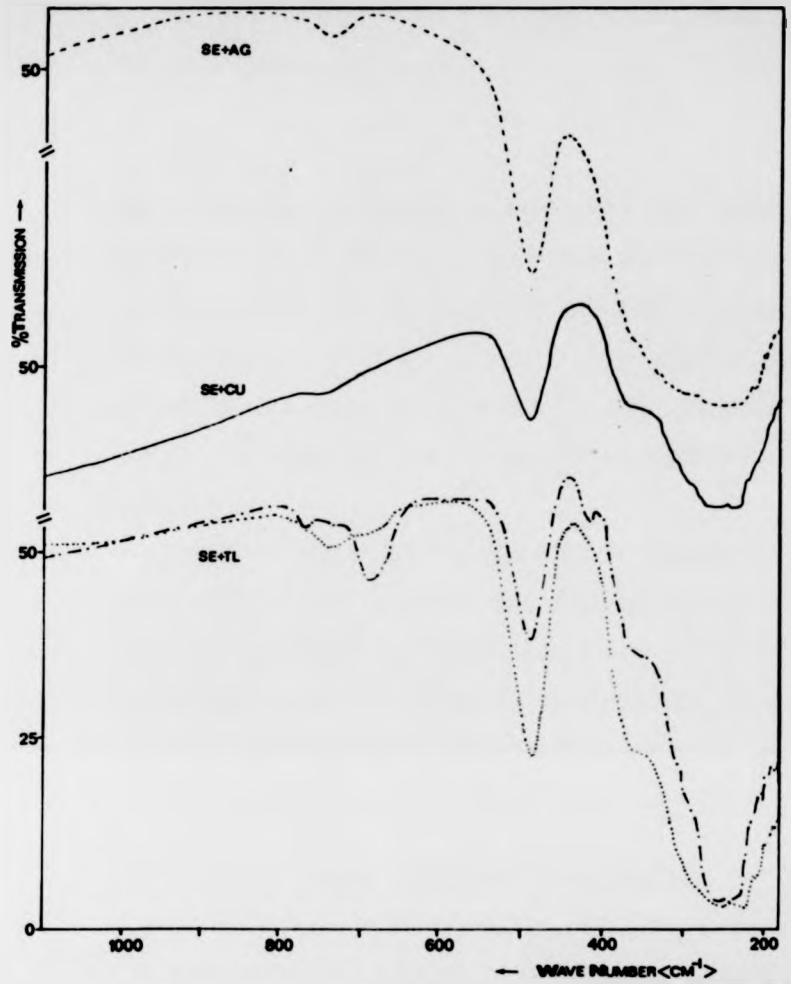

Fig. 4Y(b) -
I.R. spectra for glassy Se doped with small amounts of the following elements:
(---) 1 at % of Ag;
(—) 1 at % of Cu;
(-·-) and (···) 300 ppm and 1 at % of Tl respectively.

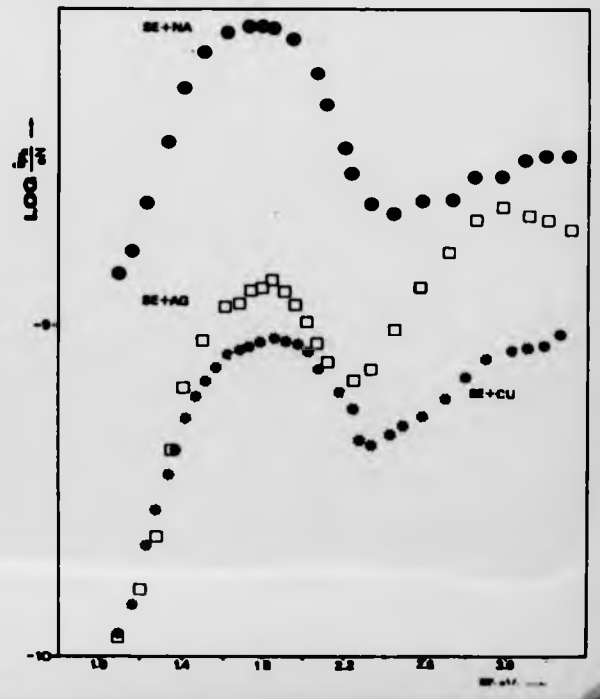

Fig. 4Z - Photoconductivity spectral responses for vitreous Se containing respectively 300 ppm of Na; 1 at % of Ag and 1 at % of Cu are shown.

of the electrical parameters towards the additive concentration. Pfister et al.(1978) observed as well that in Tl doped a-Se some properties, for example luminiscence, were independent of the thallium concentration. That was interpreted by considering that Tl atoms adopt a positive charge with the resulting Tl^+ centres being paired with D^- centres and therefore the density of charged defect centres remained undisturbed.

The photoconductivity responses of Ag, Cu and Na doped glasses is shown in fig. 4Z. They are very similar to that of "pure" selenium although the transition metals seem to cause a shift of the peak towards higher energies. Tl completely disrupts the structure of the photocurrent response. This might indicate dissimilarities between the thallium role and the role of the other metals in the glasses.

4.5.3 Atomic doping with trivalent elements

Glasses doped with aluminium, bismuth or antimony were also prepared. All three additives enhance crystallization. This has already been observed for Sb by Haisty and Krebs (1969). Silica plate quenching allowed the introduction of Sb only up to $\sim$ 3 at % which is between the maxima reported for air quenching (Patterson and Brau 1966) and water quenching (Haisty and Krebs 1969). Contrary to all the other elements which induced crystallization of hexagonal Se, antimony enhanced the formation of a different phase (Se_2Se_3).

Bismuth has the strongest crystallization effect which limits maximum Bi content possible to approximately 500 p.p.m. even if quenching onto a metal plate was used. The addition of aluminium is restricted by the formation of Al_2Se_3 which does not seem to dissolve well in the melt. Excess of Al_2Se_3 was easily noticed as it decomposes spontaneously in

moisture to give H_2Se gas. The maximum Al concentration introduced in the glass was ~0,5 at %.

Infrared spectra of all the glasses show modifications due to the foreign elements (fig. 4Y(b)). Sb contributes to a strong band at 16.5 μm. Al leads to a new band at ~ 24 microns, which might therefore be due to Al_2Se_3. Bi causes the appearance of several bands at 12.3, 13.1, 14.3, 15.0, 15.2 and 17.4 microns.

Addition of antimony shows no significant effect upon the resistivity at room temperature whereas aluminium causes some decrease (fig. 4X) which could be due to the presence of a second phase (Al_2Se_3). Neither the activation energy nor the factor C were altered. As these elements possibly cause chain branching in small amounts they would not be expected to produce a significant effect. It is interesting that Sb eliminates the effect of bromine exhibiting a compensation-like role. The result probably means that Br prefers to bind chemically with antimony where the electronegativity difference is larger.

Bismuth appears to cause a decrease of the conductivity although, due to the errors discussed in section 4.1.2, a definite conclusion cannot be asserted. In glass, Bi is probably 6-fold coordinated as in crystalline Bi_2Se_3 though doubts exist as to the existence of Bi^- (Tohge et al.1980b) or Bi^+ centres (Takahashi 1981). Introduction of new defect centres causing disturbance of D^+, D^- equilibrium will account for the n-type behaviour observed in Bi doped chalcogenide glasses (Tohge et al. 1979/80a). It was not obviously possible to check the thermoelectric power sign of the glasses prepared. The apparently diminished conductivity observed is in accordance with the reported decrease of both hole and electron drift mobilities in glassy selenium, originated by the introduction of bismuth (Takahashi 1981).

CHAPTER V - CONCLUSIONS

In this chapter the main conclusions of this work are presented.

5.1 Halogen doped glasses

As a first conclusion it is pointed out that selenium glasses can effectively be doped with halogen atoms in a controlled way. The resistivity and the activation energy are, to a certain extent, progressively lowered by the incorporation of the additive and in the cases of bromine or chlorine "truly" semiconducting glasses, in respect of the magnitude of the resistivity, could be prepared. The minimum resistivity obtained was nevertheless still two to three decades greater than that observed for single-crystal trigonal selenium (Murphy et al.1982). The effect of iodine although rather smaller was also well marked. In addition results were obtained indicating that vitreous selenium containing tellurium or sulphur can also be doped with bromine. The quantitative effect observed was however not substantially different.

The dopant quantities necessary to obtain the maximum effect, although minor, were nevertheless large by crystal doping standards. The effects of oxygen and halogens upon selenium glasses are, in that respect, also dissimilar.

Generally speaking electrical and optical results can be considered within the framework of the Mott-CFO model. Experimental absorption edges do agree with the exponential behaviour commonly observed in chalcogenide glasses. Also, typical of chalcogenides is the observation of a single activation energy for electric conduction. The results agree with this in most cases, the exception being the tellurium containing glasses. The existence of departures from the Arrehenius type behaviour is however not unknown in this group of glasses (see e.g. Hulls 1970).

The increase in conductivity with dopant was essentially attributed to the observed decrease in activation energy as neither the mobility of the main carriers nor the density of states at the band edges could be assumed to change significantly. Values of the pre-exponential factor for all glasses were, in fact, reasonably similar. Together with activation energy and optical gap estimations those values were interpreted for all glasses as indicating band conduction with reduction of mobility due to trapping and release interactions with localized states.

A second main conclusion is that all halogen doped glasses did show positive Seebeck coefficient, thus indicating p-type conductivity. The aim of obtaining n-type materials, envisaged at the commencement of the project, could not therefore be achieved. Interpretation of that fact in contest with the activation energy decrease is not easy. The possibilities of destruction of the D^- centres as in the charge dangling model of Street and Mott (1975) or creation of impurity acceptor levels caused by the addition of the halogen were considered. The observed facts for the Se-Te glasses do not favour the former. Analysis of the latter in the light of ideas put forward by Adler and Ioffa (1976) and Khan and Adler (1984) led to determination of an impurity (Br or Cl) energy level at $\sim$ 0,70 eV above the valence band. However, positive identification of these acceptor centres is not possible. Yao et.al. (1983) in the interpretation of related experiments suggest C_2^+ states. It is interesting to notice that polycrystalline trigonal selenium can also show a conductivity increase of several decades by doping with halogen (Murphy et al.1982).

Photoconductivity results showed a great dependance of the photocurrent on impurities - a phenomenon very common in crystalline solids. In contrast the position of the low energy peak remains visibly unchanged

although located at an energy significantly lower than the estimated optical gap. That might be considered as evidence for recombination processes involving defect centres. The shift of the photoconductivity peak towards lower energies with the addition of tellurium supports the observed optical absorption edge behaviour, indicative of the well documented diminution of the mobility gap.

The supporting experiments were disappointing in the sense that mostly negative, rather than positive, information was acquired. That was particularly the case for infrared spectroscopy. Transmission curves were devoid of new bands except for the chlorine case. Electron spin resonance also did not present any features attributable to dopants. Field effect experiments due to the large time constants involved could not be fully exploited. Differential scanning calorimetry gave evidence for some structural effects of the impurities, but due to irreparable equipment breakdown the experiments could not be pursued further.

5.2 Other glasses

The aim of obtaining significant impurity effects with other additives than halogens could not be fulfilled. This was particularly the case for the monovalent elements, thallium sodium, silver and copper. All of them were introduced in concentrations larger than the estimated number of network defects per unity of volume and thus "a priori" capable of altering the Fermi level location. Interpretation of this "failure" was not possible and it may differ from one dopant to another; it can be speculated based on drift mobility data, that the apparent increase in activation energy observed might be related to a change to n-type conduction.

5.3 Suggestions of further work

The range of materials studied comprised doping with three halogens. A fourth, fluorine, should obviously have been considered and could have made the interpretation of results more conclusive. The lack of commercial availability of any fluorine selenide and the lack of time to prepare one in the laboratory prevented this. The materials which should be studied as a natural extension of this work include primarily the detailed analysis of doped Se-S and Se-Te alloys; certainly, in the tellurium case, the improved conductivity would allow the determination of σ and S much further down in the temperature scale. However this will require substantial changes in the glass producing equipment. With regard to additional experimental techniques other than the already implicit in section 5.1, the following suggestions are made:- Since IR measurements provide very little structural information, the undertaking of Raman vibrational spectroscopy, not possible at Warwick, could be useful. Induced ESR is another possible source of further information as well as luminiscence. The measurement of the conductivity as a function of the electrical field should be carried out to its limit and, in addition, the dependence on the sample thickness should be object of careful examination; this would possibly show if space charge limited currents take place or not. Another obvious experiment to be continued in more detail is photoconductivity, as a function of the temperature and of the electrical field. Thermoelectric power measurements could only be taken, in stabilized conditions, in a very short temperature range; its determination in a much improved apparatus would therefore be welcome.

5.4 Review of later data on chalcogenide glasses

Since the commencement of this work a number of reports on impurity effects and chemical modifications in chalcogenides have been published.

Some of these have already been referred throughout the discusaion and are now, with others, summarised.

The effect of iodine upon some properties of a Se-Te alloy was studied by Nagels et al.(1983). They also verified the glasses to be p-type. Yao et al.(1983) observed the effect of several additives on liquid selenium. Once more it was noticed that halogens do not change the type of conduction whereas sodium and thallium doped melts behave as n-type. The result of various additives in both elemental and compound form on the carrier range in amorphous Se was investigated by Takasaki et al.(1983). Once again halogens seem to affect only electron range leaving the hole parameter intact, whereas other monovalent atoms have the opposite effect.

An important result, at least from the technological point of view, was achieved by Tohge et al (1979; 1980 a). By preparing Ge-Se and Ge-Se-Te alloys containing bismuth the first n-type chalcogenide glasses were, finally, obtained. Since then Khan and Adler (1984) also claim to have produced an n-type material by doping a Se-Te-As glass with lithium.

Selenium arsenide has also been the object of several works involving the alloying with metals, namely copper (Averyanov et al.(1984); Sawan et al.(1983); Frazer and Owen (1983)). The last paper is particularly interesting as data seems to be fitted only by a relation for small polarons.

More results are needed to clarify the overall picture. Nevertheless it seems very appropriate to chalcogenides, in general, and selenium, in particular. In fact the defect characterization of non-crystalline selenium remains uncertain as Vanderbilt and Joannopoulos (1983) recently published calculations that put in question the existence of a negative

U in this material. If that is so then the problem of introducing a large concentration of defects without any spins being present becomes a puzzling challenge. As far as the present trend indicates, it seems nevertheless that the key to the understanding of chalcogenide behaviour is still related to the possibility of variable coordination together with the availability of lone pair electrons, properties that are at the origin of the intrinsic defects that characterize this group of glasses.

REFERENCES

Abdullayev G.B., Asadov Y.G. and Mamedov K.P. 1969a in "The Physics of Selenium and Tellurium" (W. Cooper, Editor) Pergamon Press, Oxford.

Abdullayev G.B., Ibragimov N.I. and Mamedov Sh. V. 1969b in "The Physics of Selenium and Tellurium (W. Cooper, Editor) Pergamon Press, Oxford.

Abkowitz M. 1967, J. Chem. Phys. 46, 4537.

Adler D. 1981, Journal de Physique, Colloque C4, Supplément au No.10, 42, 3.

Adler D. and Yoffa E. 1976, Phys. Rev. Lett. 36, 1197.

Agarwal S.C. 1973, Phys. Rev. 7, 685.

Anderson P.W. 1958, Phys. Rev. 109, 1492.

Anderson P.W. 1975, Phys. Rev. Lett. 34, 953.

Averyanov V.L., Gelmont B.L. et al. 1984 J. Non-Crystalline Solids 64, 279.

Bagley B.G. 1974 in "Amorphous and Liquid Semiconductors" (J. Tauc, Editor) Plenum Press, London and New York.

Blumenthal R.N. and Seitz M.A. 1974 in "Electrical Conductivity in Ceramics and Glass" (N. Tallan, Editor) Marcel Dekker, New York.

Born M. and Wolf E. 1959 "Principles of Optics" Pergamon Press, Oxford.

Bube R.H. 1959 in "Methods of Experimental Physics" (K.L. Horowitz and V.A. Johnson, Editors) Academic Press, London.

Burley R.A. 1968, Phys. Stat. Sol. 29, 551.

Cohen M.H. 1970a, J. Non-Crystalline Solids 2, 432.

Cohen M.H. 1970b, J. Non-Crystalline Solids 4, 391.

Cohen M.H., Fritzsche H. and Ovshinsky S.R. 1969, Phy. Rev. Lett. 22, 1065.

Connell G.A.N. 1979 in "Amorphous Semiconductors" (M.B. Brodsky, Editor) Springer Verlag, Berlin.

Danilov A.V. 1965 cited by Owen A.E. (1967).

Davis E.A. and Mott N.F. 1970, Phil. Mag. 22, 903.

Davis E.A. 1979 in "Amorphous Semiconductors" (M.H. Brodsky, Editor) Springer Verlag, Berlin.

De Vos J.C. 1954, Physica 20, 690.

Donald I.W. and McMillan P.W. 1978, J. of Materials Science 13, 1151.

Dunlap Jr. W.C. 1959 in "Methods of Experimental Physics" (K.L. Horowitz and V.A. Johnson, Editors) Academic Press, London.

Eisenberg A. and Tobolsky A.V. 1960, J. Polymer Sci. 46, 19.

Elliott S.R. 1984 "Physics of Amorphous Materials", Longman, London.

El-Mously M.K. and El-Zaidia M.M. 1973, J. Non-Crystalline Solids 11, 519.

Emin D. 1972, J. Non Crystalline Solids 8-10, 511.

Emin D., Seager C.H. and Quinn R.K. 1972, Phys. Rev. Lett. 28, 813.

Fraser M.I. and Owen A.E. 1983, J. Non-Crystalline Solids 59-60 pt.2, 1031.

Frederikse H.P.R., Johnson V.A. and Scanlon W.W. 1959 in "Methods of Experimental Physics" (K.L. Horowitz and V.A. Johnson, Editors) Academic Press, London.

Fritzsche H. 1974 in "Amorphous and Liquid Semiconductors" (J. Tauc, Editor), Plenum Press, Oxford.

Fritzsche H. 1983, J. Non-Cryst. Solids, 59 & 60, 1289.

Gerding H. and Houtgraaf H. 1959, Rev. Trav. Chim. 73, 737.

Gobrecht H. 1969, in "The Physics of Selenium and Tellurium". (W.C. Cooper, Editor) Pergamon Press, Oxford.

Goldschmidt V.M. 1926 in "Geochemical Distribution Laws No. 8", Skiffer Norske Videnskaps. Akad. Mat. Naturv. K1.

Goodman C.H.L. 1975, Nature 257, 370.

Grochowski E.G. and Brenner W. 1971, J. Non-Crystalline Solids 6, 83.

Hagen S.H. and Derks P.J.A. 1984, J. Non-Crystalline Solids 65, 241.

Haisty R.W. and Krebs H. 1969 in "The Physics of Selenium and Tellurium" (W.C. Cooper, Editor), Pergamon Press, Oxford.

Hartke J.L. and Regensburger P.G. 1965, Phys. Rev. 139, A970.

Hulls K. 1970, Thesis, University of Warwick.

Ioffe A.F. and Regel A.R. 1960, Progr. Semicond. 4, 237.

Juska G., Mataliones A., Sakalas A. and Viscakas J. 1969, Phys. Stat. Sol. 36K, 121.

Kamprath V.W. 1962, Annalen der Physik, 7, 382.

Kastner M., Adler D. and Fritzsche H. 1976, Phys. Rev. Lett. 37, 1504.

Keem J. 1975, Chemical Instrumentation 6(2), 133.

Keezer R.C. 1969 in "The Physics of Selenium and Tellurium" (W.C. Cooper, Editor) Pergamon Press, Oxford.

Keezer R.C. and Bailey M.W. 1967, Mat. Res. Bull 2, 185.

Ketelaar J.A.A., Hooge F.N. and Blasse G. 1956 cited by Stammreich and Forneris (1956).

Khan B.A. and Adler D. 1984, J. Non-Crystalline Solids 64, 35.

Klug H.P. and Alexander L.E. 1974 "X-Ray Diffraction Procedures", John Wiley, New York.

Knight J.C. and Davis E.A. 1974, J. Phys. Chem. Solids 35, 543.

Kolomiets B.T. 1964, Phys. Stat. Sol. 7, 359.

Kolomiets B.T. and Lebedev E.A. 1966, Soviet Physics-Solid State 8, 905.

Kosyrev P.T. 1959, Soviet Phys-Solid State 1, 102.

Kreidl N.J. 1977, J. Non-Crystalline Solids 26, 605.

Kumeda M., Jinno Y., Susaki M. and Shimizu T. 1976, Japan J. Appl. Phys. 15, 201.

Lacourse W.C., Twaddell V.A. and MacKenzie J.D. 1970, J. Non-Crystalline Solids 3, 234.

Lakatos, A.I. and Abkowitz M. 1971, Phys. Rev. B3, 1791.

Lampert M.A. and Mark, P. 1970, "Current Injection in Solids". Acad Press N.Y.

Lanyon H.P.D. 1963, Phys. Rev 130(1), 134.

Larabee R.D. 1959, J. Opt. Soc. Amer. 49, 619.

Lucovsky G.V. 1969 in "The Physics of Selenium and Tellurium" (W. Cooper Editor) Pergamon Press, Oxford.

Lucovsky G.V. 1979 in "The Physics of Selenium and Tellurium" (E. Gerlach and P. Grosse, Editors) Springer Verlag, Heidelberg.

Lucovsky G., Mooradian A., Taylor W., Wright C.B. and Keezer R.C. 1967, Solid State Commun. 5, 113.

MacKenzie J.D. 1970, J. Non-Crystalline Solids 2, 16.

MacKenzie J.D. 1977, J. Non-Crystalline Solids 26, 458.

Marshall J.M. and Owen A.E. 1972, Phys. Stat. Sol. 9(12), 181.

McMillan P.W. and Shutov S.D. 1977, J. Non-Crystalline Solids 24, 307.

Mehra R.M., Mathur P.C., Kathuria A.K. and Snyam R. 1977, Phys. Stat. Sol.(a) 41, K189.

Mehra R.M., Mathur P.C., Kathuria A.K. and Shyam R. 1978, J. Phys. Chem. Solids, 39, 295

Moeller T. 1961 "Quimica Inorganica" Editorial Reverte, Barcelona.

Mort J. 1973 in "Electrical and Optical Properties of Amorphous Semiconductors" (Aberdeen Summer School).

Mott N.F. 1969, Phil. Mag. 19, 835.

Mott N.F. 1970, Phil. Mag. 22, 7.

Mott N.F. 1976, Phil. Mag 34, 1101.

Mott N.F. 1978, J. Non-Cryst. Solids 28, 147.

Mott N.F. and Davis E.A. 1979 "Electronic Processes in Non-crystalline Materials", Clarendon Press, Oxford.

Murphy K.E., Wunderlich B.B. and Wunderlich B. 1982, J. Phys. Chem. 86, 2827.

Nagels P. 1979 in "Amorphous Semiconductors" (M.H. Brodsky, Editor) Springer Verlag, Berlin.

Nagels P., Ali M. and Rotti M. 1983, Physica 117B & 118B, 989.

Ovshinsky S.R. 1968 Phys. Rev. Lett 21, 1450.

Owen A.E. 1967 Glass Ind. 48, 637, 695.

Owen A.E. and Robertson J.M. 1970, J. Non-Crystalline Solids 2, 40.

Patterson R.J. and Brau M.J. 1966, presented at the Electrochemical Society Meeting, Cleveland, Ohio (cited by Haisty and Krebs 1969).

Pfister J.C. 1979, Phys. Stat. Sol. (a) 24, K15.

Pfister et. al. 1978, Phys. Rev. Letters, 41, 1318.

Popov A.I. 1978, Inorg. Mater. (U.S.A.) 14, 178.

Rawson H. 1967 "Inorganic Glass Forming Systems" Academic Press, London.

Roberts G.G. 1973 in Electronic and Structural Properties of Amorphous Semiconductors" (P.G. LeComber and J. Mort, Editors) Academic Press, London.

Robertson J. 1982, Phys. Chem. Glass 23(1), 1.

Rose A. 1955, Phys. Rev. 97, 1538.

Rutgers G.A.W. 1958 in "Handbuch der Physick" (S. Flugge, Editor), Springer-Verlag, Berlin Gottingen Heidelberg.

Sampath P.I. 1966, J. Chem. Phys. 45, 3519.

Savage J.A. 1982, J. Non-Crystalline Solids 47(1), 101.

Sawan Y., El-Gabaly M. and Kollias N. 1983 Physica 117B & 118B, 995.

Schottmiller J., Tabak M. et al. 1970, J. Non-Crystalline Solids 4, 80.

Shirai T., Hamada S. and Kobayoski 1963, J. Chem. Soc. Japan 84, 968.

Spear W.E. and Le Comber P.G. 1975, Solid State Commun. 17, 1193.

Stammreich H. and Forneris R. 1956, Spectrochim. Acta 8, 46.

Street R.S. and Mott N.F. 1975, Phys. Rev. Lett. 35, 1293.

Takahashi T. 1981, J. Non-Crystalline Solids, 44, 239.

Takasaki Y., Maruyama E., Uda T. and Hirai T., 1983,
J. Non-Crystalline Solids, 59 & 60. 949.

Tauc J. 1974 in "Amorphous and Liquid Semiconductors" (J. Tauc Editor),
Pergamon Press, Oxford.

Tauc J. Grigorovici R. and Vancu A., 1966, Phys. Stat. Solidi
15, 627.

Tausend A. 1969 in "The Physics of Selenium and Tellurium"
(W.C. Cooper, Editor) Pergamon Press, Oxford.

Tohge N., Yamamoto Y., Minami T. and Tanaka M. 1979, Appl. Phys. Lett.
34, 640.

Tohge N., Minami T. and Tanaka M., 1980a, J. Non-Crystalline Solids
37, 23.

Tohge N., Minami T. and Tanaka M. 1980b, J. Non-Crystalline Solids
38 & 39. 283.

Tohge N., Minami T. and Tanaka M. 1983, J. Non-Crystalline Solids
59 & 60, 999.

Topping J. 1962 "Errors of observation and their treatment"
Chapman and Hall, London.

Turnbull D. 1969, Contemp. Phys. 10, 473.

Twaddell V.A., Lacourse W.C. and MacKenzie J.D. 1972,
J. Non-Crystalline Solids 8-10, 831.

Vanderbilt D. and Joannopoulos J.D. 1983, J. Non-Crystalline Solids
59 & 60. 937.

Vaško A. 1969 in "The Physics of Selenium and Tellurium" (W.C. Cooper,
Editor) Pergamon Press, Oxford.

Vaško A., Ležal D. and Srb I. 1970, J. Non-Crystalline Solids 4, 311.

Yao M., Hosokawa S. and Endo H. 1983, J. Non-Crystalline Solids, 59 & 60, 1083.

Wang R. and Merz M.D. 1976, Nature 260, 35.

Ward A.T. and Myers M.B. 1969, J. Phys. Chem. 73, 1374.

Weaire D. and Thorpe M.F. 1971, Phys. Rev. B4, 2508.

Wimmer J.M. and Bransky I 1974 "Electrical Conductivity in Ceramics and Glass" (N. Tallan, Editor) Marcel Dekker, Inc. New York.

Zachariasen W.H. 1932, J. Am. Chem. Soc. 54, 3841.

Zallen R. 1983 "The Physics of Amorphous Solids", Wiley, New York.